Summer 8-2012

Adult Neurogenesis in the Spiny Lobster, Panulirus Argus: Molecular, Cellular, and Physiological Changes of Olfactory Receptor Neurons

Tizeta Tadesse
Georgia State University

ADULT NEUROGENESIS IN THE SPINY LOBSTER, *PANULIRUS ARGUS*: MOLECULAR, CELLULAR, AND PHYSIOLOGICAL CHANGES OF OLFACTORY RECEPTOR NEURONS

by

TIZETA TADESSE

Under the Direction of Charles D Derby

ABSTRACT

Adult neurogenesis of olfactory receptor neurons (ORNs) occurs in diverse organisms including in decapod crustaceans. This dissertation describes the molecular, cellular, and physiological changes that occur during adult neurogenesis of ORNs in the antennular lateral flagellum (LF) of the spiny lobster *Panulirus argus*. Examination of the role of *splash* (spiny lobster achaete scute homolog) in adult neurogenesis and regeneration using *in situ* hybridization showed *splash* was not closely associated with the formation of sensory neurons under normal physiological conditions. Damage to the LF, which induces regeneration, enhanced *splash* expression, suggesting an association between *splash* with regeneration and repair. This study suggests that *splas*h plays multiple roles in the olfactory organ of adult spiny lobsters. Examination of extracellular and intracellular Ca^{2+} in mediating spontaneous and odor-induced responses of ORNs, using calcium imaging showed that odor-induced Ca^{2+} transient responses and spontaneous Ca^{2+} oscillations in ORN somata are primarily mediated by an influx of extracellular Ca^{2+} through Co^{2+} -sensitive Ca^{2+} channels, but that intracellular Ca^{2+}stores also have some contribution.

These responses are independent of TTX-sensitive Na^+ channels, suggesting that these Ca^{2+} responses may reflect receptor potentials. Examination of changes in odor specificity, sensitivity, and temporal responses in adult-born ORNs showed an increase in the percentage of odorant-responsive ORNs as they age from newly-born cells to mature, and a decrease in odorant-responsive ORNs as they senesce. As adult-born ORNs age, there was a decrease in the percentage of ORNs that undergo spontaneous Ca^{2+} oscillations and an increase in the amplitude of oscillation. ORNs became more broadly tuned as they senesce, and their response profile, defined by the most effective odorant, changed. Odor sensitivity changed with age. This study demonstrated that the physiological response properties of adult-born ORNs changed with functional maturation. Taken together, this dissertation reveals molecular, cellular and physiological changes in adult born ORNs and elucidates mechanisms of adult neurogenesis.

INDEX WORDS: Sensory neuron, Olfactory system, Neurogenesis, Regeneration, *In situ* hybridization, Calcium imaging, Odorant, Chemical senses, *Panulirus argus*

ADULT NEUROGENESIS IN THE SPINY LOBSTER, *PANULIRUS ARGUS*: MOLECULAR, CELLULAR, AND PHYSIOLOGICAL CHANGES OF OLFACTORY RECEPTOR NEURONS

by

TIZETA TADESSE

A Dissertation Submitted in Partial Fulfillment of the Requirements for the Degree of

Doctor of Philosophy

in the College of Arts and Sciences

Georgia State University

2012

ADULT NEUROGENESIS IN THE SPINY LOBSTER, *PANULIRUS ARGUS*: MOLECULAR, CELLULAR, AND PHYSIOLOGICAL CHANGES OF OLFACTORY RECEPTOR NEURONS

by

TIZETA TADESSE

Committee Chair: Charles D Derby

Committee: Timothy S McClintock

Manfred Schmidt

Phang C Tai

William W Walthall

Electronic Version Approved:

Office of Graduate Studies

College of Arts and Sciences

Georgia State University

August 2012

DEDICATION

In memory of my mother ‘Mami’

ACKNOWLEDGMENTS

First and foremost, my deepest gratitude goes to my advisor Dr. Charles Derby without whom; this dissertation would not be possible. I am extremely grateful to have received an amazing scientific training from Chuck. Irrespective of his busy schedule, he was always available for discussion, for editing/ commenting on manuscripts, and many more. I thank him for being patient, for challenging me and most of all for believing in me. It's a bitter sweet moment as I close this chapter of my life due to my unforgettable experience in the 'Derby Lab'. "Chuck, you are one of a kind!!! You are the best!!!"

I thank my committee members, Dr. Manfred Schmidt, Dr. Timothy McClintock, Dr. Phang Tai, and Dr. Bill Walthall for their expertise, comments and support. Especial thanks to Manfred for technical training, constructive criticism of this dissertation and for always being available to help in lab work.

I thank current and former Derby Lab members, especially Vivian Vu-Ngo, Drs. Juan Aggio, Zeni Shabani, Michiya Kamio, Ko-Chun Ko for their expertise and friendship. I thank Omar Haque and Jessica Haulk for assistantship. I thank the Neuroscience Institute, Brains and Behavior program and Department of Biology for financial and technical support.

My heart-felt gratitude goes to my dear parents, Tade and and to my late mother Mami. Thank-you for instilling in me at a younger age the value of education, and the will to achieve whatever I set my mind on. To my dearest family Dagem, Helina, Fikre, Heiwote, Mieraf, Algi and Betty: thank-you for your unconditional love, care, patience and support. Finally, I thank my friends Mahin, Amy, Karine, Iselle, Rahwa, and others for their support.

TABLE OF CONTENTS

LIST OF TABLES

LIST OF FIGURES

CHAPTER 1: GENERAL INTRODUCTION

Overview

Chemoreception, defined by the ability of organisms to detect chemicals in their environment, is the most primitive of all senses. Chemical detection and identification is mediated by the peripheral sensory neurons in both vertebrates and invertebrates. The olfactory and gustatory systems in some adult animals have the ability to regenerate sensory cells (Lindsey and Tropepe, 2006; Miura and Barlow, 2010). Some adult animals also have continuous addition and turnover of peripheral sensory neurons and central neurons throughout adulthood (Lindsey and Tropepe, 2006; Ming and Song, 2011). Adult neurogenesis of olfactory receptor neurons (ORNs) occurs in diverse organisms (Calof et al., 1996; Steullet et al., 2000a; Harrison et al., 2001; Mackay-Sim, 2010; Lazarini and Lledo, 2010). However, the mechanisms and functions of adult neurogenesis are not fully known. The focus of this dissertation is to describe the molecular, cellular, and physiological changes that occur during adult neurogenesis of ORNs in the spiny lobster *Panulirus argus* and propose mechanisms that underlie proliferation, maturation, and aging of adult-born ORNs.

Clinical and biological perspective on studying adult neurogenesis

The discovery that adult animals have the capacity to produce new neurons from an adult neural stem or progenitor cell was a tremendous break-through for biologists and clinicians. According to the Centers for Disease Control and Prevention, millions of people are affected by neurodegenerative diseases such as Parkinson's and Alzheimer's, and brain and spinal cord injuries. These conditions are caused by damage to the nervous system where the potential for self-repair is low because of its very limited regenerative ability. Normal aging related sensory deficits and cognitive decline also impact millions of people worldwide. There is a huge potential for using adult neural stem cells as a therapeutic intervention

for neurodegenerative and aging related conditions. Therefore, understanding the mechanisms of adult neurogenesis is likely to contribute significantly to the advancement of therapeutics.

Until the early 1990s, the dogma was that in adult animals or humans, new neurons cannot be produced, the number of neurons does not increase in adults, and a neuron that dies cannot be replaced. From a biologist's perspective, the discovery of adult neurogenesis (Altman, 1962; Reynolds and Weiss, 1992) meant that the nervous systems of some species across the animal kingdom are more plastic than previously thought. Some important questions in the field are: what controls the survival and activity of neural stem cells? Why are stem cells present or active in some parts of the nervous system and not others? What modulates their activity? To begin to elucidate the mechanisms of adult neurogenesis, it is imperative to understand neuronal development.

Organization and function of the chemosensory organ in spiny lobsters

The paired antennules are major chemosensory organs in decapod crustaceans (Derby, 2000; Cate and Derby, 2001). Each antennule has a lateral flagellum (LF) and a medial flagellum (MF). The LF has two major classes of specialized sensilla: unimodal (chemoreceptive) aesthetasc sensilla, and bimodal (chemo-mechanoreceptive) non-aesthetasc sensilla of various types that project to the olfactory lobes and the lateral antennular neuropils, respectively, in the brain (Schmidt and Ache, 1992, Schmidt et al., 1992). The aesthetasc and non-aesthetasc sensilla are components of the two main antennular chemosensory pathways in decapod crustaceans. Selective ablation and behavioral studies showed that the aesthetasc pathway is used for odor associative learning and odor discrimination, for mediating food-related cues (Steullet et al., 2001, 2002; Horner et al., 2004), and conspecific social and sexual chemical cues and signals (Gleeson, 1982; Atema, 1995; Horner et al., 2008; Shabani et al., 2008, 2009).

In the Caribbean spiny lobster, *Panulirus argus*, aesthetasc sensilla are exclusively located on the ventral-distal region of the LF, where specific types of non-aesthetasc sensilla are also located, collectively forming a 'tuft'. The LF is organized as repeating cuticular units called annuli, containing ca.

100 aesthetasc-bearing annuli per LF, ca. 20 aesthetascs per annulus, and ca. 300 ORNs per aesthetasc, making a total of ca. 1,200,000 ORNs per spiny lobster. Each aesthetasc sensilla is innervated by the dendrites of the 300 ORNs that are assembled beneath the cuticular shaft as a dense package of cell bodies. Each aesthetasc sensilla also has auxiliary cells surrounding the ORN inner dendrites (Grünert and Ache, 1988; Steullet et al., 2000a, 2000b) and aesthetasc tegumental glands containing secretory cells that are arranged in a rosette (Schmidt et al., 2006). Aesthetasc sensilla have a thin cuticle that allows odorant molecules to move inside the sensillum (Grünert and Ache, 1988; Derby et al., 1997).

Adult neurogenesis of olfactory receptor neurons

Neurogenesis is a process that generates new functional neurons from either stem cells or neural precursor cells. Neural stem cells undergo asymmetric cell division giving rise to a neural precursor cell and a stem cell (self-renewal). Neural precursor cells further proliferate, and the daughter cells differentiate, mature, integrate into existing neural circuits, and eventually senesce. Adult neurogenesis of ORNs occurs in humans (Mackay-Sim, 2010), mammals (Calof et al., 1996), and crustaceans (Steullet et al., 2000a; Harrison et al., 2001). Many adult crustaceans have indeterminate growth, thereby increasing in size throughout their life. Spiny lobsters have continuous proliferation and turnover of aesthetasc and non-aesthetasc sensilla, which house sensory neurons (Steullet et al., 2000a; Harrison et al., 2001, 2003). Aesthetascs and non-aesthetasc sensilla and their associated sensory neurons are added in the proximal proliferation zone (PZ) of the LF (Steullet et al., 2000a). They mature to become responsive to chemicals in the mature zone, which is located distal to the PZ. Aesthetasc sensilla become old and gradually shed with each molt in the senescence zone, distal to the mature zone.

Two factors are known to affect rates of adult proliferation of ORNs in *P. argus*. One is molt stage. As part of their normal growth, crustaceans molt by shedding their old cuticle and growing a new one. There are four molting stages for crustaceans: premolt (pre-ecdysis), molt (ecdysis), postmolt (post-ecdysis), and intermolt (Lyle and MacDonald, 1983). The process of molting is under the control of the

major circulating steroid molting hormone, 20-hydroxyecdysone (20-HE), secreted from the Y-organ. Ecdysteroid titers in the hemolymph of the American lobster, *Homarus americanus*, show a surge of 20-HE during premolt (Synder and Chang, 1991). Addition of ORNs is highest in premolt compared to postmolt or intermolt animals (Harrison et al., 2001).

A second factor controlling the rate of adult neurogenesis is damage to the LF, which is a common occurrence for lobsters. Damage-induced loss of aesthetasc sensilla in adult spiny lobsters increases the number of proliferating cells within the PZ, resulting in addition of new aesthetasc sensilla and complete morphological regeneration (Harrison et al., 2003, 2004; Stoss et al., 2004).

Molecular and cellular factors associated with adult-born ORNs in *P. argus*

During early olfactory development, the spatial and temporal expression of different classes of transcription factors regulates cell proliferation, differentiation, and determination (Ledent and Vervoort, 2001; Bertrand et al., 2002). One key family of transcription factors are the *achaete-scute complex* (*ASC*) genes known for their role in development of cuticular sensilla of insects and other arthropods. In the embryonic ectoderm of *Drosophila melanogaster*, the expression of proneural *ASC* genes *achaete*, *scute*, and *lethal of scute* forms proneural clusters (Skeath and Carroll, 1994; Bertrand et al., 2002). One cell of a proneural cluster up-regulates the expression of *achaete* and *scute*, which induces the expression of *Notch* receptor in that cell. Notch receptor interaction with *Delta* ligand in neighboring cells inhibits *achaete* and *scute* expression through activation *hairy enhancer of split*. This results in delamination of one sensillum progenitor cell and the maintenance of ectodermal fate in the remaining cells of the proneural cluster.

Based on this knowledge, we identified one crustacean ASC homolog named *splash* (*spiny lobster achaete scute* homolog) cloned from the LF of adult *P. argus* (Chien et al., 2009). Using semi-quantitative RT-PCR, we showed that *splash* is expressed in neural, non-neural, and non-proliferating tissues. Due to the fact that semi-quantitative PCR requires that the tissue is homogenized, the cellular localization of *splash* was not known. Thus, the experiments in Chapter 2 address the role of *splash* in

adult neurogenesis and regeneration by examining the gene expression using *in situ* hybridization (ISH). Using adult spiny lobsters, *splash* expression was correlated with the following variables: (1) cell type, (2) developmental zone (proliferation, maturation and mature zones), (3) molt stage (intermolt and premolt LF), and (4) LF damage.

Physiological changes during functional maturation of adult-born ORNs in *P. argus*

During embryonic development of mammals, sequential expression of odor transduction genes in ORNs coincides with changes in the ORNs' physiological response properties; whether a similar pattern of changes occurs in the functional maturation of adult-born ORNs is not known. Functional maturation of ORNs during embryogenesis results from molecular, physiological, biochemical, and structural changes (Mair, 1986). For example in rats, the sequence of odor transduction gene expression coincides with functional maturation of ORNs. The half maximal gene expression shows at embryonic day E16 GTP binding protein (G_{olf}) expression, at E19 olfactory cation channel, at E19 ~E-20 odorant receptors (ORs), and at ~E22 olfactory marker protein (OMP) is the sequential expression (Margalit and Lancet, 1993). The physiological responses of ORNs also change, i.e. they become more selective as they develop (Gesteland et al., 1982).

To propose mechanisms underlying the changes in physiological response during functional maturation of adult-born ORNs, and given that Ca^{2+} is a major contributor for odor activation, modulation, and adaptation (Schild and Restrepo, 1998; Menini, 1999; Matthews and Reisert, 2003) in mature ORNs of diverse organisms, it was necessary to understand the role of Ca^{2+} in lobster ORNs. In odor transduction of mature ORNs of vertebrates, odors bind to G-protein (G_{olf}) coupled receptors, which activate adenylyl cyclase, leading to formation cyclic AMP or IP_3. These second messengers activate cyclic-nucleotide-gated (CNG) channels, causing an influx of Ca^{2+} and activation of somatic voltage-gated channels. Ca^{2+} is also involved in neuronal development, including proliferation and differentiation (Leclerc et al., 2011), and in mature cells in aging and dying (Gleichmann and Mattson, 2011; Toescu and

Vreugdhenhil, 2010). Ca^{2+} channels in the plasma membrane and in the endoplasmic reticulum maintain Ca^{2+} homeostasis (Clapham, 2007).

Thus, the experiments in Chapter 3 address the mechanisms underlying odor-induced Ca^{2+} transients and spontaneous oscillations in Ca^{2+} in ORNs from intermolt spiny lobsters and the establishment of Ca^{2+} imaging of spiny lobster ORNs in an *in vitro* 'LF slice' preparation developed in parallel with Ukhanov et al. (2011). Four different experiments were conducted that addressed the role of (1) extracellular Ca^{2+} concentration, (2) Co^{2+} sensitive Ca^{2+} channels, (3) intracellular Ca^{2+} concentration, and (4) tetrodotoxin (TTX) sensitive Na^{+} channels. Odor-activated Ca^{2+} response and spontaneous oscillations in Ca^{2+} were quantified and compared with saline controls.

Lastly, the goal of Chapter 4 is to describe the changes in the physiological response properties of adult-born ORNs with maturation in the spiny lobster. Using the 'LF slice' preparation for Ca^{2+} imaging established for MZ (Chapter 3; Tadesse et al., 2011), we used LF slices from all three developmental zones. We analyzed spontaneous Ca^{2+} oscillations and odor-induced Ca^{2+} transients across these zones and examined as variables developmental zone (three zones representing the age of ORNs), odorant type (five compounds tested), and odorant concentration (three concentrations tested).

1.1 References

Altman J. 1962. Are new neurons formed in the brains of adult mammals? Science. 135:1127-1128.

Atema J. 1995. Chemical signals in the marine environment: dispersal, detection, and temporal signal analysis. PNAS USA. 92:62-66.

Bertrand N, Castro DS, Guillemot F. 2002. Proneural genes and the specification of neural cell types. Nat Rev Neurosci. 3:517-530.

Calof AL, Hagiwara N, Holcomb JD, Mumm JS, Shou J. 1996. Neurogenesis and cell death in olfactory epithelium. J Neurobiol. 30:67-81.

Cate HS, Derby CD. 2001. Morphology and distribution of setae on the antennules of the Caribbean spiny lobster *Panulirus argus* reveal new types of bimodal chemo-mechanosensilla. Cell Tiss Res. 304:439-454.

Chien H, Tadesse T, Liu H, Schmidt M, Walthall WW, Tai PC, Derby CD. 2009. Molecular cloning and characterization of homologs of *achaete–scute* and *hairy–enhancer of split* in the olfactory organ of the spiny lobster *Panulirus argus*. J Molec Neurosci. 39:294-307.

Clapham DE. 2007. Calcium signaling. Cell. 131:1047-1058.

Derby CD, Cate HS, Gentilcore LR. 1997. Perireception in olfaction: molecular weight sieving by aesthetasc sensillar cuticle determines odorant access to receptor sites in the Caribbean spiny lobster *Panulirus argus*. J. Exp. Biol. 200: 2073-2081.

Derby CD. 2000. Learning from spiny lobsters about chemosensory coding of mixtures. Physiol Behav. 69:203-209.

Gesteland RC, Yancey RA, Farbman AI. 1982. Development of olfactory receptor neuron selectivity in the rat fetus. Neuroscience. 7:3127-3136.

Gleeson RA. 1982. Morphological and behavioral identification of the sensory structures mediating pheromone reception in the blue crab *Callinectes sapidus*. Biol Bull. 163:126-171.

Gleichmann M, Mattson MP. 2011. Neuronal calcium homeostasis and dysregulation. Antioxid Redox Signal. 14:1261-1273.

Grünert U, Ache BW. 1988. Ultrastructure of the aesthetasc (olfactory) sensilla of the spiny lobster *Panulirus argus.* Cell Tiss Res 251:95-103.

Harrison PJH, Cate HS, Swanson ES, Derby CD. 2001. Postembryonic proliferation in the spiny lobster antennular epithelium: rate of genesis of olfactory receptor neurons is dependent on molt stage. J Neurobiol 47:51-66.

Harrison PJH, Cate HS, Steullet P, Derby CD. 2003. Amputation-induced activity of progenitor cells leads to rapid regeneration of olfactory tissue in lobsters. J Neurobiol 55:97-114.

Harrison PJH, Cate HS, Derby CD. 2004. Localized ablation of olfactory receptor neurons induces both localized regeneration and widespread replacement of neurons in spiny lobsters. J Comp Neurol 471:72-84.

Horner AJ, Weissburg MJ, Derby CD. 2004. Dual antennular chemosensory pathways can mediate orientation by Caribbean spiny lobsters in naturalistic flow conditions. J Exp Biol 207:3785-3796.

Horner AJ, Weissburg MJ, Derby CD. 2008. The olfactory pathway mediates sheltering behavior of Caribbean spiny lobsters, *Panulirus argus*, to conspecific urine signals. J Comp Physiol A 194:243-253.

Lazarini F, Lledo PM. 2011. Is adult neurogenesis essential for olfaction? Trends Neurosci. 34: 20-30.

Leclerc C, Néant I, Moreau M. 2011. Early neural development in vertebrates is also a matter of calcium. Biochimie. 93:2102-2111.

Ledent V, Vervoort M. 2001. The basic helix-loop-helix protein family: comparative genomics and phylogenetic analysis. Genome Res 11:754-770.

Lindsey BW, Tropepe V. 2006. A comparative framework for understanding the biological principles of adult neurogenesis. Prog Neurobiol. 80:281-307.

Lyle WG, MacDonald CD. 1983. Molt stage determination in the Hawaiian spiny lobster *Panulirus marginatus*. J Crust Biol 3:208-216.

Mackay-Sim A. 2010. Stem cells and their niche in the adult olfactory mucosa. Arch Ital Biol. 148:47-58.

Mair RG. 1986. Ontogeny of the olfactory placode. Experientia. 42:213-223.

Margalit T, Lancet D.1993. Expression of olfactory receptor and transduction genes during rat development. Brain Res Dev Brain Res. 73:7-16.

Matthews HR, Reisert J. 2003. Calcium, the two-faced messenger of olfactory transduction and adaptation. Curr Opin Neurobiol. 13:469-475.

Menini A.1999. Calcium signaling and regulation in olfactory neurons. Curr Opin Neurobiol. 9:419-426.

Ming GL, Song H. 2011. Adult neurogenesis in the mammalian brain: significant answers and significant questions. Neuron. 70:687-702.

Miura H, Barlow LA. 2010. Taste bud regeneration and the search for taste progenitor cells. Arch Ital Biol. 148:107-118.

Reynolds BA, Weiss S. 1992. Generation of neurons and astrocytes from isolated cells of the adult mammalian central nervous system. Science. 255:1707-1710.

Schild D, Restrepo D. 1998. Transduction mechanisms in vertebrate olfactory receptor cells. Physiol Rev. 78:429-466.

Schmidt, M, Van Ekeris L, Ache BW. 1992. Antennular projections to the midbrain of the spiny lobster. I. Sensory innervation of the lateral and medial antennular neuropils. J Comp Neurol 318:277-290.

Schmidt M, Chien H, Tadesse T, Johns ME, Derby CD. 2006. Rosette-type tegumental glands associated with aesthetasc sensilla in the olfactory organ of the Caribbean spiny lobster, *Panulirus argus*. Cell Tiss Res 325:369-395.

Shabani S, Kamio M, Derby CD. 2008. Spiny lobsters detect conspecific blood-borne alarm cues exclusively through olfactory sensilla. J Exp Biol 211:2600-2608.

Shabani S, Kamio M, Derby CD. 2009. Spiny lobsters use urine-borne olfactory signaling and physical aggressive behaviors to influence social status of conspecifics. J Exp Biol 212:2464-2474.

Skeath JB, Carroll SB. 1994. The *achaete-scute* complex: generation of cellular pattern and fate within the *Drosophila* nervous system. FASEB J 8:714-721.

Snyder MJ, Chang ES. 1991. Ecdysteroids in relation to the molt cycle of the American lobster, *Homarus americanus*. I. Hemolymph titers and metabolites. Gen Comp Endocrinol. 81:133-145.

Steullet P, Cate HS, Derby CD. 2000a. A spatiotemporal wave of turnover and functional maturation of olfactory receptor neurons in the spiny lobster *Panulirus argus*. J Neurosci 20:3282-3294.

Steullet P, Cate HS, Michel WC, Derby CD. 2000b. Functional units of a compound nose: aesthetasc sensilla house similar populations of olfactory receptor neurons on the crustacean antennule. J Comp Neurol 418:270-280.

Stoss TD, Nickell MD, Hardin D, Derby CD, McClintock TS. 2004. Inducible transcript expressed by reactive epithelial cells at sites of olfactory sensory neuron proliferation. J Neurobiol 58:355-368.

Tadesse T, Schmidt M, Derby CD. 2011. Calcium imaging of olfactory receptor neurons in the spiny lobster, *Panulirus argus*. 573.01/CC5. Neuroscience Meeting Planner. Washington, DC: Society for Neuroscience. Online.

Toescu EC, Vreugdenhil M. 2010. Calcium and normal brain ageing. Cell Calcium. 47:158-164.

Ukhanov K, Bobkov Y, Ache BW. 2011. Imaging ensemble activity in arthropod olfactory receptor neurons *in situ*. Cell Calcium. 49:100-107.

CHAPTER 2: DISTRIBUTION AND FUNCTION OF *SPLASH*, AN *ACHAETE-SCUTE* HOMOLOG IN THE ADULT OLFACTORY ORGAN OF THE CARIBBEAN SPINY LOBSTER *PANULIRUS ARGUS*.

Authors: Tizeta Tadesse*, Manfred Schmidt, William W. Walthall, Phang C. Tai, and Charles D. Derby

Published: (2011) Developmental Neurobiology, 71(4): 316-335.

Affiliation: Neuroscience Institute and Department of Biology, Georgia State University, Atlanta, GA

Author contribution: Tadesse T designed experiments, collected and analyzed all the data and wrote the paper. Derby CD and Schmidt M contributed to the experimental design, the data analysis and editing of the manuscript. Tai PC and Walthall WW contributed to the experimental design and technical input.

Acknowledgements We thank the Keys Marine Laboratory for supplying spiny lobsters, Dr. Hsin Chien for *splash* and *GluR1* clones, Vivian Ngo-Vu for outstanding technical assistance, Omar Haque for assisting with ISH processing, Birgit Neuhaus for assisting with confocal microscopy, and Dr. Timothy McClintock for his generous gift of GluR1 antibody and valuable discussions. This work was supported by NIH DC00312 (CDD), GSU Dissertation Grant and a Brains & Behavior fellowship (TT).

2.1 Abstract

achaete-scute complex (*ASC*) genes, which encode basic helix-loop-helix transcription factors, regulate embryonic and adult neurogenesis in many animals. In adult arthropods, including crustaceans, *ASC* homologs have been identified but rarely functionally characterized. We took advantage of the recently identified crustacean homolog, *splash* (*spiny lobster achaete scute* homolog), in the olfactory organ of the Caribbean spiny lobster *Panulirus argus* to examine its role in adult neurogenesis. We tested the hypothesis that *splash* is associated with but not restricted to sensory neuron formation in the olfactory organ, the antennular lateral flagellum (LF), of adult spiny lobsters. We demonstrated *splash* labeling in epithelial cells across LF developmental zones (i.e., proliferation and mature zones), in auxiliary cells surrounding dendrites of olfactory receptor neurons (ORNs), and in immature and mature ORNs, but not in granulocytes or chromatophores. Since ORN proliferation varies with molt stage, we examined *splash* expression across molt stages and found that molt stage affected *splash* expression in the ORN mature zone but not in the proliferation zone. *In vivo* incorporation of bromodeoxyuridine (BrdU) showed no correlation in the cellular pattern of *splash* expression and BrdU labeling. *splash* labeling was dramatically enhanced in the proliferation zones following LF damage, demonstrating an enhanced expression during repair and/or regeneration. We conclude that *splash* is not closely associated with the formation of sensory neurons under normal physiological conditions but may be involved in repair and regeneration. We also propose that *splash* has additional roles other than neurogenesis in adult crustaceans.

Key words: *ASC* homolog, sensory neuron, olfactory system, regeneration, *in situ* hybridization

2.2 List of Abbreviations

AE	aesthetasc sensilla
ASC	achaete-scute complex
ATG	aesthetasc tegumental glands
bHLH	basic-helix-loop-helix
BrdU	5-bromo-2'-deoxyuridine
D-Ep	dorsal epithelium
dPZ	distal proliferation zone
GluR1	ionotropic glutamate receptor
ICC	immunocytochemistry
ISH	*in situ* hybridization
LF	lateral flagellum
mPZ	middle proliferation zone
MZ	mature zone
NAE	non-aesthetasc sensilla
ORN	olfactory receptor neuron
PA-5/7/9	post-ablation days 5/7/9
pH3	phosphorylated histone 3
pPZ	proximal proliferation zone
PZ	proliferation zone
splash	*spiny lobster achaete-scute homolog*
V-Ep	ventral epithelium

2.3 Introduction

Transcription factors are essential for regulating gene expression in multicellular organisms. Spatial and temporal expression of different classes of transcription factors regulate neural development, such as cell proliferation, differentiation, and determination (Ledent and Vervoort, 2001; Bertrand et al., 2002). In recent studies, alternative functions for transcription factors classically defined in their role in development were documented. Functions include sensory maintenance (Ohkawara et al., 2004; Millimaki et al., 2010), intercellular signaling (Prochiantz and Joliot, 2003), and even interacting with AMPA/kainate receptors to regulate neuronal physiology (Chao et al., 2005).

One of the best-studied examples of transcription factors are the *achaete-scute complex* (*ASC*) genes known for their role in development of cuticular sensilla of insects. *ASC* homologs have been identified in various animals besides insects, and their roles in neurogenesis, oligodendrogenesis (Gordonet al., 1995; Cau et al., 1997, 2002; Murrayet al., 2003; Manglapus et al., 2004; Kim et al., 2008), and formation of various cancers (Rapa et al., 2008; Kitamura et al., 2009) have been elucidated. *ASC* are basic helix-loop-helix (bHLH) genes consisting of four related types: *achaete* (*ac*), *scute* (*sc*), *lethal of scute* (*l'sc*), and *asense* (*as*). In the embryonic ectoderm of *Drosophila melanogaster*, the expression of proneural *ASC* genes *achaete*, *scute*, and *lethal of scute* form proneural clusters that are competent to form sensillum progenitor cells (Skeath and Carroll, 1994; Bertrand et al., 2002). Up-regulation of *achaete* and *scute* in one cell of a proneural cluster induces the expression of *Notch* and *Delta*, which in turn inhibit *achaete* and *scute* expression in neighboring cells by activating *hairy enhancer of split*. This results in delamination of one sensillum progenitor cell and maintenance of ectodermal fate in the remaining cells of the proneural cluster. Sensillum progenitor cells also activate the expression of *asense*, which instructs sensillar formation (Brand et al., 1993). *asense* is expressed in all neural precursor cells (Sunet al., 1998; Wheeler et al., 2003) and thus mutations in *asense* result in broader phenotypes, suggesting that *asense* encodes a multifunctional protein (Domínguez and Campuzano, 1993).

Investigations into the identity and function of *ASC* homologs in crustaceans have only recently begun. Two *ASC* homologs have been identified in the branchiopod *Triops longicaudatus* (Wheeler and Skeath, 2005). We recently identified *splash* (*spiny lobster achaete scute* homolog) from the antennular lateral flagellum of the Caribbean spiny lobster *Panulirus argus* (Chien et al., 2009). *splash* has the conserved bHLH and C-terminal domains typical of a bHLH transcription factor, and it has higher identity with the general class of *ASC* homologs rather than with any one of the specific members, *achaete*, *scute*, *lethal of scute*, or *asense* (Chien et al., 2009).

The focus of our study is to elucidate the role of *splash* in the antennular lateral flagellum of adult spiny lobsters. Chemosensilla are distributed across most of the body surface of crustaceans, with the paired antennules being the most prominent chemosensory organs (Derby, 2000; Cate and Derby, 2001). Each antennule has two flagella: the lateral flagellum (LF) and a medial flagellum (MF) (Fig. 2-1A). The LF has two major classes of specialized sensilla: unimodal (chemoreceptive) aesthetasc sensilla, and bimodal (chemo-mechanoreceptive) non-aesthetasc sensilla of various types (Fig. 2-1B). Aesthetasc sensilla are limited to the ventral and distal region of the LF where they co-occur with specific types of non-aesthetasc sensilla, collectively forming a 'tuft'. The LF is comprised of pseudosegments called annuli, each containing about 20 aesthetasc sensilla. Each aesthetasc sensilla is innervated by the dendrites of approximately 300 bipolar ORNs. Associated with each aesthetasc sensilla are auxiliary cells surrounding the ORN inner dendrites (Fig. 2-1C) (Grünert and Ache, 1988; Steullet et al., 2000a, 2000b) and aesthetasc tegumental glands containing secretory cells arranged in a rosette (Schmidtet al., 2006). Out of the ten types of non-aesthetasc sensilla on the LF (Cate and Derby, 2001), the organization of only a few has been described (Cate and Derby, 2002; Schmidt and Derby, 2005). Axons of sensory neurons of aesthetasc and non-aesthetasc sensilla innervate the olfactory lobes and lateral antennular neuropils, respectively (Schmidt and Ache, 1992, Schmidt et al., 1992).

Adult crustaceans such as spiny lobsters which have indeterminate growth experience continuous addition and turnover of sensory systems (Schmidt, 2007). This includes continuous proliferation of aesthetasc and non-aesthetasc sensilla and turnover (Steullet et al., 2000a; Harrison et al., 2001, 2003). In

addition, damage-induced loss of aesthetasc sensilla in adult spiny lobsters results in the addition of new aesthetasc sensilla, and loss of the entire LF results in its regeneration (Harrison et al., 2003, 2004). As part of normal maintenance and growth, aesthetascs are added in the proximal proliferation zone (PZ) (Fig. 2-1D) of the LF (Steullet et al., 2000a). Distal to the PZ are the maturation and mature zones where ORNs mature and respond to chemical stimuli. Distal to the mature zone is the senescence zone, where aesthetascs are shed with each molt. ORN precursor cells arise as 'epithelial patches' in the ventral epithelium of the PZ, which then due to cellular proliferation form clusters of ORNs, and each cluster eventually is associated with an aesthetasc sensillum (Harrison et al., 2004). Non-aesthetasc sensilla are also added in the PZ. The rate of addition of ORN precursor cells is dependent on molt stage and degree of damage. Addition of cells is highest in premolt compared to postmolt or intermolt animals (Harrison et al., 2001). Damage to the LF increases the number of proliferating cells within the PZ, resulting in complete morphological and functional regeneration (Harrison et al., 2003, 2004; Stoss et al., 2004).

As part of our effort to understand the role of *splash* in adult spiny lobsters, we used semi-quantitative RT-PCR to examine *splash* expression in different tissues and to determine if expression levels change with molt stage (Chien et al., 2009). Our finding that *splash* expression in the LF is highest in premolt animals, when formation of new sensilla peaks in PZ (Harrison et al., 2001), is consistent with a role of *splash* in this process. However, we also found that *splash* expression levels are similar across all developmental zones of the LF, from the proliferation to senescence zones. Furthermore, *splash* is expressed not only in the LF but also in other neural and non-neural tissues. Together, these results lead to the hypothesis that *splash* may have multiple functions in the LF of adult spiny lobster, including but not limited to participation in cellular proliferation.

Our current study aimed to test this hypothesis, using *in situ* hybridization to correlate cellular patterns of *splash* expression and adult neurogenesis in the LF, using cell type, molt stage, and LF developmental zones as variables. We found that *splash* is expressed not only in ORN precursors and immature ORNs but also in mature and non-proliferating cells of different types. We also found that molt stage had no effect on intensity of *splash* labeling in the proliferation zone. However, the mature zone of

intermolt lobsters had an increase in *splash* labeling compared to premolt lobsters. The increase in *splash* labeling following damage to the LF suggests an association with repair and regeneration. This leads us to conclude that *splash* has a variety of functions, including novel roles, in the LF of adult spiny lobsters.

2.4 Methods

Animals

Young adult Caribbean spiny lobsters (*Panulirus argus*) of 50-75 mm carapace length were collected near the Florida Keys Marine Laboratory and shipped to Georgia State University where they were held in 400-liter aquaria with re-circulated, filtered, and aerated artificial seawater (Instant Ocean™, Aquarium Systems Inc., Mentor, OH, USA) at 20-25ºC. Animals were maintained in a 12 hr: 12 hr light: dark cycle and fed shrimp or squid three times per week. Molt stage of the animals was determined by microscopic examination of the pleopods, as described by Lyle and MacDonald (1983), and of LF after processing for *in situ* hybridization (ISH) or immunocytochemistry (ICC).

In situ Hybridization

Our protocol was a modification from those of Ishii et al. (2004), McClintock et al. (2008), and McIntyre et al. (2008).

Riboprobe preparation We used three sets of plasmid DNA containing *splash*: a 832-nucleotide sequence for the open reading frame, a 437-nucleotide sequence for the bHLH domain of 5'*splash*, and a 387-nucleotide sequence for the C' terminal of 3'*splash* (Accession # DQ489559; Chienet al., 2009). We also cloned the binding domain of an ionotropic glutamate receptor subunit, GluR1 (Accession # GQ252689), from adult spiny lobsters and used a 433-nucleotide sequence from it (139-572 bp) for ISH. We cloned this GluR1 in *P. argus* and used it for ISH because it, like its homolog in *H. americanus* (Hollins et al., 2003; Stepanyan et al., 2004, 2006), reliably labels ORNs. Plasmid DNA sequences were digested with restriction enzymes. GluR1 and *splash* digoxigenin (DIG) labeled antisense and sense (negative controls) RNA probes were synthesized from linearized plasmid DNA using *in vitro*

transcription with DIG RNA Labeling Kit (T7/Sp6) according to the manufacturer's protocol (Roche Applied Science, Indianapolis, IN). RNA probes were precipitated by adding 4 M LiCl + 100% ethanol and placed in -80°C for 60-90 min. Probes were centrifuged at 20,800 x g for 15 min at 4°C, supernatant was discarded, and the pellet was washed with ice cold 70% ethanol and centrifuged at 20,800 x g for 15 min at 4°C. Supernatant was discarded and pellets were air dried and brought into solution with 25 µl diethylpyrocarbonate (DEPC)-treated distilled H_2O (dH_2O) (Invitrogen, Carlsbad, CA). Diluted RNA probes were verified using 1.5-2% agarose gels.

Tissue collection LF were removed from animals by cutting proximal to the aesthetasc tuft region and dissected into 5-8 annuli long pieces in *P. argus* saline (460 mM NaCl, 13 mM KCl, 13.6 mM $CaCl_2$, 10 mM $MgCl_2$, 14 mM Na_2SO_4, 3 mM HEPES, 1.7 mM glucose, pH 7.4, adjusted with NaOH). The annuli were numbered according to Schmidt et al. (2006), as represented in Figure 2-1D, with '1' representing the most proximal aesthetasc-bearing annulus, annuli proximal to '1' having progressively larger negative numbers, and annuli distal to '1' having progressively larger positive numbers. Thus, the PZ is represented by annuli -10 to 12, with the proximal PZ being annuli -10 to -5, the middle PZ being annuli -4 to 4, and the distal PZ being 5 to 12. The mature zone is represented by annuli 13 to 52, and the senescence zone is represented by annuli 53 and greater. Dissected annuli were typically hemisectioned, thus maintaining intact the ventral aesthetasc-bearing areas. All annuli were placed in 2-ml Eppendorf tubes and fixed overnight in 4% paraformaldehyde (PFA) in 0.1 M Sörensen phosphate buffer (SPB), pH 7.4, followed by daily incubation for 5-7 days in 0.5 M EDTA pH 8.0 for decalcification. Tissues were rinsed overnight in 0.1 M SPB and stored in fresh 0.1 M SPB at 4°C until used. Twenty-four hr before hybridization or immunodetection, annuli were embedded in 15% gelatin porcine type A 300 bloom diluted in dH_2O and fixed overnight in 4% PFA in 0.1 M phosphate buffer solution (PBS) pH 7.4 (for ISH) or 4% PFA in SPB (for ICC). Tissues were rinsed in PBS or SPB and sectioned at 50 µm using a vibratome and either placed on Superfrost Plus microscope slides (VWR, West Chester, PA) and dried on a low heat plate for ISH or placed in wells for free floating immunodetection.

Hybridization Tissues were processed as follows: 4% PFA in PBS for 15 min, PBS (pH 7.4) for 3 min, proteinase K in Tris-EDTA (TE buffer) at 37˚C for 12 min, 4% PFA for 10 min, PBS for 3 min, 0.2 M HCl for 10 min, PBS for 3 min, 0.1 M triethanol amine-HCl (pH 8.0) for 1 min with stirring, 0.25% of acetic anhydrate + 0.1 M triethanol amine-HCl (pH 8.0) for 10 min with stirring, PBS at RT for 3 min, and 60%, 80%, 95%, 100%, 100% ethanol each for 90 sec. Sections were air dried, circled using a PAP pen (Electron Microscopy Sciences, Hatfield, PA), and placed horizontally in a hybridization chamber kept moist with 50% formamide in dH_2O. Fresh hybridization solution (50% formamide in dH_2O, 10 mM Tris-Cl of pH 8.0, 200 µg/ml yeast tRNA, 10% dextran sulfate, 1x Denhardt's solution, 600 mM NaCl, 0.25% SDS, 1 mM EDTA of pH 8.0, and DEPC H_2O) was heated to 85˚C for 10 min. One µl of DIG-RNA probe was added to 200 µl heated hybridization solution, mixed, and incubated at 85˚C for an additional 5-10 min before being added to each slide. Parafilm was used to spread the solution and remove air bubbles before covering individual slides and incubating overnight at 55˚C.

Post-hybridization Parafilm was removed and slides were washed on a shaker as follows: 2 x sodium chloride sodium citrate (SSC), 50% formamide at 65˚C for 30 min, TNE (10 mM Tris-Cl at pH 7.5, 0.5 M NaCl, 1 mM EDTA) at 37˚C for 10 min, TNE + RNase A at 37˚C for 30 min, TNE at 37˚C for 10 min, 2 x SSC at 65˚C for 20 min, 0.2 x SSC at 65˚C for 20 min, and 0.1 x SSC at 65˚C for 20 min.

NBT/BCIP detection Sections were processed by treatment with DIG1 buffer (150 mM NaCl, 100 mM Tris-Cl, pH 7.5, and 1% blocking reagent from Roche Applied Sciences) at RT for 5 min, DIG1 buffer at RT for 60 min (~500 µl/slide) in a water-only moist chamber, 1:1000 anti-DIG-alkaline phosphatase (AP) (Roche Applied Sciences) in DIG1 buffer at RT for 60 min (~400 µl/slide), DIG1 buffer for 2 times in 0.01% Tween 20 at RT for 15 min each covered with foil, DIG3 buffer (100 mM NaCl, 100 mM Tris-Cl at pH 9.5, 50 mM $MgCl_2$) for 3 min, then in NBT/BCIP (Roche Applied Sciences) overnight in the dark at RT. The color reaction was terminated with 10 mM Tris-Cl (pH 7.5), 1 mM EDTA for 10 min and rinsed in dH_2O for 5 min. Slides were incubated in Hoechst 33258 or Sytox green (Invitrogen) for 30 min, rinsed in dH_2O, and cover slipped using Fluoromount G (Electron Microscopy

Sciences). For double labeling with BrdU, tissues were transferred from slides to free-floating wells using a paint brush and continued for BrdU detection.

5-bromo-2-deoxyuridine (BrdU) Labeling

Administration BrdU (5 mg/100 g body weight in *P. argus* saline) was injected into the hemolymph at the base of walking legs. Animals were returned to their holding tanks for 17-24-hours before tissues were collected and stored as described above.

Immunocytochemistry BrdU detection was as follows. Sections were rinsed three times for 10 min in 0.1 M SPB and twice in 1:1 DNase I (50 mM Tris HCl pH 7.5, 10mM $MgCl_2$, 50 µg/ml BSA, 0.3% Triton-X-100): 0.1 M TSPB buffer (0.02% sodium azide, 0.3% Triton X-100, 0.1 M SPB) for 20 min. Sections were then incubated in 1:150 anti-BrdU antibody (mouse monoclonal, Becton Dickinson BioSciences, Franklin Lakes, NJ) diluted with antibody incubation medium (1:1 DNase I buffer and 0.1 M TSPB, 1:100 Protease Inhibitor Cocktail, 100 U/ml DNase) overnight at RT. For sections that were double labeled with BrdU, 1:200 anti-phosphorylated histone 3 (pH3) (Santa Cruz Biotechnology, Santa CruzCA) was added. In other ICC procedures, we used 1:500 anti-GluR1 rabbit polyclonal antiserum raised against *Homarus americanus* Accession # GQ252689 (Hollins et al., 2003; Stepanyan et al., 2004, 2006) to label mature ORNs and 1:10,000 anti-acetylated tubulin mouse monoclonal antibody to label non-aesthetasc sensory neurons (Schmidt and Derby, 2005). Primary antibodies were diluted in 0.1 M SPB and left overnight at RT. All sections were rinsed in 0.1 M TSPB four times for 30 min each then incubated for 4-12 h in a secondary antibody goat anti-rabbit (1:200 CY3 goat anti-rabbit or Alexa 488 goat anti-mouse: Jackson ImmunoResearch, West Grove, PA) and on some sections the F-actin marker phalloidin Alexa 488 1:50 (Molecular Probes, Eugene OR) (data not shown) was added at 1:100 dilution. Sections were rinsed three times for 30 min each in 0.1 M SPB followed by either 0.007mg/ml Hoechst 33258 or 10^{-4} mM Sytox green (Invitrogen) for 30 min, then rinsed in 0.1 M SPB. Sections were mounted on slides and coverslipped using Fluoromount G (for double labeling with *splash* RNA probe) or 1:1 glycerol/0.1 M SPB containing 5% diazabicyclol [2.2.2]octane (DABCO) and 0.01% sodium azide.

Image Analysis

NBT/BCIP-labeled tissues were analyzed using a light microscope (Axioplan2: Zeiss, Jena, Germany) and images captured using a digital camera Leica DC 500 and images were processed in Paint Shop Pro 5 (Jasc Software, Eden Prairie, MN). For fluorescently labeled tissues, a multi-photon microscope was used (LSM 510: Zeiss, Jena, Germany). An argon laser was used to visualize AlexaFluor-488 labeled secondary antibodies, a helium-neon laser to visualize CY3-labeled secondary antibodies, and a titanium-sapphire 2-photon laser was used to visualize Hoechst 33258. All digital images were arranged into figures using Adobe Illustrator CS 11.0 .0 (San Jose, CA).

Ablation Experiments

Ablations were performed as described by Harrison et al. (2003). Intermolt animals of 56–73 mm carapace length with no visible damage were taken from their aquarium and the right LF was ablated with scissors, removing ca. 80% of the aesthetasc-bearing annuli. Animals were observed for 10-15 min and returned to their holding aquarium. The remainder of the right LF containing the proliferation zone and some transition zone, and the left LF (unablated side), were collected 5, 7, or 9 days after ablation. Tissues were fixed and processed for ISH, and images were captured as described above.

Data Analysis

The effect of molt stage on *splash* expression in the LF was evaluated by examining tissue sections from three premolt animals and three intermolt animals and rating the intensity of *splash* labeling in the proliferation zone and mature zone. ORN precursor cells in the epithelium and ORN clusters were identified as previously described (Harrison et al., 2001, 2003). Intensity of labeling was rated by an observer who was blind to the condition of the antennule. These data are presented in two ways. One

presentation is a comparison of the percentage of ORN precursor cells or ORN clusters in the proliferation zone or the number of ORNs in the mature zone that are *splash*+ vs. *splash*– for premolt and intermolt animals. The mean values ± SEM are presented in stacked bar graphs in Figure 2- 4. The second method was a comparison of the intensity of *splash* labeling in ventral epithelium and ORNs in the proliferation zone and mature zone of premolt vs. intermolt animals. Intensity of splash labeling was determined using the following scale: no labeling (-), faint labeling (+), intense labeling (++), and very intense labeling (+++). Median values from the three animals in each molt condition were determined and shown for the three regions of the proliferation zone (pPZ, mPZ, dPZ) and mature zone (MZ) in Table 2-1.

The effect of antennular ablation on *splash* expression was examined for three groups of animals (three animals per group): five-, seven-, or nine-days after ablation (P5, P7, P9, respectively. Intensity of splash labeling was quantified as described in the second method of the preceding paragraph and presented as the median intensity for two regions of the proliferation zone (pPZ, dPZ) and at the site of injury of the ablation (results shown in Table 2-2).

The degree to which *splash* expression is coincident with proliferating cells was examined by comparing the % of BrdU+ cells that are also *splash*+ in the proliferation zone of three intermolt animals. The numbers of BrdU+/*splash*+ and BrdU+/ *splash*– cells were counted for each animal and mean percentage values were calculated and shown in Figure 2-5.

Chemicals

All chemicals were obtained from Sigma Aldrich (St. Louis, MO) unless otherwise noted.

2.5 Results

Cellular Localization of *splash*, an *ASC* Homolog, in the Antennular Lateral Flagellum

Towards understanding the role of *ASC* homologs in adult crustaceans, we examined the cellular expression pattern of *splash*, a spiny lobster *achaete-scute complex* (*ASC*) homolog. We tested the hypothesis that *splash* is associated with but not restricted to the formation of ORNs and other sensory neurons in the antennular lateral flagellum (LF) of adult animals. We localized *splash* labeling using digoxigenin RNA probes for *in situ* hybridization in adult lobsters. We first established the pattern of labeling in adult intermolt animals to compare it with premolt animals and for regenerating LF (where proliferation is highest), and also examined the correlation between *splash* expression and cellular proliferation in the LF. Adult neurogenesis associated with sensilla in the tuft region of the LF originates from proliferation in the ventral epithelium in the proximal part of the proliferation zone (= proximal PZ) (Harrison et al., 2003, 2004). If *splash* functions in sensilla formation as do other proneural ASC homologs, then we expected to detect patches of *splash* labeling in the ventral epithelium of the proximal proliferation zone, or one very intense *splash*+ cell within each epithelial patch.

We began by examining *splash* labeling in intermolt LF. The cellular morphology of the tuft region of unlabeled intermolt LF is shown in sagittal section in Figure 2-2A (also see Fig. 2-1C). The aesthetasc sensilla are on the ventral surface of the LF where ventral epithelial cells and clusters of ORNs, with their dendrites extending into the aesthetascs, are located. Dorsal to the aesthetasc-bearing cuticle is a layer of dorsal epithelial cells. We tested three digoxigenin labeled *splash* RNA probes that targeted the open reading frame, the bHLH domain, and the C' terminal (data not shown). In intermolt PZ, we found intense *splash* open reading frame RNA labeling in the cytoplasm of epithelial cells in the ventral epithelium of the proximal PZ where new ORN clusters had not yet formed (Fig. 2-2B). However, *splash* labeling in the epithelium was uniform and not organized as patches. In the middle PZ, most newly formed ORN clusters showed very intense *splash* labeling (Fig. 2-2C), but these were interspersed with ORN clusters devoid of *splash* labeling. In most of the labeled clusters, a few ORNs and some neighboring epithelial cells were unlabeled (Fig. 2-2D). Using *splash* 5' bHLH probe (Fig. 2-2E) and C' terminal probe (data not shown), labeling had a similar pattern but of faint intensity compared to the ORF probe (Fig. 2-2C & D). We did not detect *splash* labeling in the numerous chromatophores (Fig. 2-2F),

which are multipolar pigmented cells that provide coloration (Noël and Chassard-Bouchaud, 2004). We also did not detect *splash* labeling in granulocytes that are located throughout the LF (Battison et al., 2003; Schmidt and Derby, 2006) (Fig. 2-2G).

As a positive control for our DIG labeled RNA *in situ* hybridization, we used RNA probes based on clone of a partial sequence of a *P. argus* ionotropic glutamate receptor, GluR1 subunit. Our *P. argus* GluR1 clone (Accession # GQ252689) was of the binding domain subunit, and this domain has 97% sequence identity to OET07, the GluR1 in *H. americanus* (Hollins et al., 2003). Our GluR1 probe labeled ORNs in *P. argus* (Fig. 2-2H), as expected since the *H. americanus* GluR1 homolog also labeled ORNs (Hollins et al., 2003; Stepanyan et al., 2004, 2006). The GluR1 probe labeled all ORNs in the PZ, including immature cells, and all ORNs in mature zone of LF but did not label any other types of cells in the LF. Immunocytochemical double labeling using anti-GluR1 antiserum and the nuclear marker Hoechst 33258 confirmed and extended results of RNA labeling, by showing labeling in the somata and dendrites of ORNs in the PZ and mature zone (Fig. 2-2J).

For negative controls of *in situ* hybridization, we used a GluR1 sense probe (Fig. 2-2I), hybridization buffer omitting *splash* RNA probe (Fig. 2-2K), an RNase control in which tissue was exposed to RNase A prior to adding *splash* RNA probes (Fig. 2-2L), and a control lacking primary antibody but having anti-DIG alkaline phosphatase (Fig. 2-2M). In these negative controls, we saw no labeling of cellular structures other than aesthetasc tegumental glands (Schmidt and Derby, 2005). Most controls showed non-specific binding in the acellular cuticle. Our prior success using a similar *in situ* hybridization procedure to localize a CUB-serine protease in the olfactory organ (Schmidt et al., 2006) also served as a positive control for our current study of *splash* labeling. One of our negative controls, *splash* sense probes, occasionally labeled epithelial cells and ORNs. We speculate that labeling with the *splash* sense probes may occur due to a *splash* natural antisense transcript, as identified for many genes (Alfano et al., 2005; Katayama et al., 2005; Mercer et al., 2008, 2010; Smalheiser et al., 2008) including one in prawn (Yin et al., 2007).

Effect of Molt Stage on *splash* Labeling

Molt stage affects the number of ORN precursor cells in that premolt animals have more BrdU+ cells compared to postmolt or intermolt animals (Harrison et al., 2001). If *splash* expression is correlated with neural proliferation, then we expect to observe lower levels of *splash* labeling in the epithelium of the PZ of intermolt animals, where the lowest numbers of BrdU+ cells are observed. To begin to test our hypothesis, we performed *in vivo* BrdU incorporation followed by ICC. We found many isolated BrdU+ cells in the proximal ventral epithelial. In the middle and distal PZ, we found BrdU+ cells in clusters (Fig. 2-3B). Triple-labeling of tissue with anti-BrdU, anti-phosphorylated histone 3, and Hoechst 33258 showed several M-phase (i.e. phosphorylated histone 3 +) cells within ORN clusters containing S-phase (i.e. BrdU+) cells (Fig. 2-3C). This suggests that neural proliferation occurs in intermolt LF, as previously described (Harrison et al., 2001).

We examined *splash* labeling pattern throughout the LF of intermolt lobsters and compared it to the LF of premolt lobsters. In proximal PZ of intermolt animals, which lack immature ORN clusters, we found intense *splash* labeling in the cytoplasm of ventral epithelial cells (Fig. 2-3D, Table 2-1). In middle PZ, we also observed *splash* labeling in epithelial cells as well as in many cells of newly formed ORN clusters, most likely representing immature neurons (Fig. 2-3E) (N= 4). Interestingly, some immature ORN clusters adjacent to intensely labeled clusters were not labeled (Fig. 2-4). We observed labeled clusters that contained some unlabeled cells (Fig. 2-4). Our observation of numerous *splash*+ cells in the PZ and our semi-quantitative PCR data showing that non-proliferating tissues have *splash*+ cells (Chienet al., 2009) led us to examine the distal PZ where ORNs differentiate and the mature zone where chemical-responsive ORNs are located. We found abundant and heterogeneous *splash* labeling in somata of cells in the ventral epithelial and ORNs in the distal PZ (Fig. 2-3F) and mature zone (Fig. 2-3G, Table 2-1). Each ORN cluster also contained unlabeled cells (Fig. 2-4). Aesthetasc tegumental glands, which are abundant in the aesthetasc-bearing zone, were non-specifically labeled. The mature zone of intermolt lobsters had *splash* labeling of similar intensity to that in the distal PZ (Table 2-1), including very intense *splash*+ cells in the ORN clusters (Fig. 2-4, Table 2-1). Our method of determining molt stage verified that our

intermolt animals, as expected, did not have new cuticle and setae formed beneath the old cuticle (Fig. 2-3H). To determine the effect of molt stage on *splash* labeling, we examined premolt LF. Unlike intermolt LF, premolt proximal PZ contained many newly formed ORN clusters and auxiliary cells (Fig. 2-3I) that will become associated with aesthetasc sensilla that emerge after the animal molts. Not as many epithelial cells in the ventral epithelium of premolt animals were intensely labeled for *splash* compared with intermolt animals (Table 2-1). Similar to intermolt, we found some unlabeled ORN clusters interspersed with many clusters that had *splash* labeling (Fig. 2-4). In distal PZ (Fig. 2-3J) and mature zone (Fig. 2-3K) of premolt animals, we observed patches with intense *splash* labeling (Table 2-1) in the ventral epithelial proximal to each sensillum. In addition, most ORN clusters contained both *splash*+ and *splash*– cells (Fig. 2-4). Contrary to our prediction, we found no molt stage related differences in the degree of *splash* labeling in the ventral epithelium. In premolt animals, new cuticle and setae formed beneath the old cuticle and setae (Fig. 2-3L). Thus, our lack of correlation between molt stage and intensity of *splash* expression was not due to the technique of molt staging. Interestingly, we observed that *splash* labeling in immature and mature ORN clusters was more intense in intermolt animals compared to premolt animals (Table 2-1). The majority of ventral epithelial cells in the distal PZ and mature zones of intermolt animals also showed more intense labeling compared to premolt animals.

Because *splash* labeling was not specific to proliferating areas of the LF, we wanted to determine if it is a general feature of all cell types in the LF. We observed *splash* specific labeling in auxiliary cells surrounding the dendrites of ORNs (Grünert and Ache, 1988) (Fig. 2-3F, I, J) and non-specific labeling in aesthetasc tegumental glands, which are abundant in the aesthetasc region of the LF. Furthermore, we found *splash* labeling in dorsal epithelial (Fig. 2-3M) and in mesial and lateral regions of the LF (data not shown) where proliferation is not known to occur. Unlike in the ventral epithelium, most if not all dorsal epithelial cells contained *splash* labeling. In distal regions of the LF in regions proximal to the mature zone, there was a decrease in the intensity of *splash* labeling in dorsal epithelial cells (Fig. 2-3N). Granulocytes and chromatophores in LFs of intermolt (see Fig 2-2) and premolt (data not shown) animals did not have *splash* labeling. These data suggest that *splash* is not tightly correlated with molt stage

dependent neural proliferation but is clearly involved in other functions, as indicated by labeling in mature ORNs, auxiliary cells, and dorsal epithelial cells, all of which do not normally show cell proliferation in adult animals.

splash is Not Exclusively Expressed in BrdU+ Cells

To determine whether there is a relationship between *splash* expression and adult cell proliferation, we harvested LF 24-h after BrdU injection and examined this tissue for BrdU and *splash* labeling in the ventral epithelium of the PZ. If *splash* is involved with the generation of ORNs, then we expect that proliferating (i.e. BrdU+) cells will be *splash*+. As previously described (Harrisonet al., 2001), we observed BrdU+ cells in several regions of the PZ, including the ventral epithelium, newly formed ORN clusters, and other areas. We also observed BrdU+ cells with different nuclear shapes within the PZ. The majority of BrdU+ cells in clusters were located in the lateral LF. We found numerous BrdU+ cells (Fig. 2-5A) and numerous *splash*+ cells (Fig. 2-5B), but very few double-labeled cells (i.e. *splash*+ and BrdU+) (Fig. 2-5D) in the ventral epithelium and ORN clusters of the PZ (Fig. 2-5B, D). The few double-labeled cells were clearly distinct from other epithelial cells based on the shape of the nucleus, which appeared more circular compared to surrounding epithelial cells that were either *splash*+ or BrdU+ (Fig. 2-5C). There were very few cells that had the same morphology but were *splash*+ and BrdU- (Fig. 2-5C). These data do not provide direct evidence for *splash* expression with cell proliferation.

splash Labels Non-Aesthetasc Sensory Neurons in the Lateral Flagellum

The LF has unimodal (chemo) aesthetasc sensilla and bimodal (chemo-mechano) non-aesthetasc sensilla (Fig. 2-1B). We already showed *splash* labeling in aesthetasc ORNs (see Fig. 2-3). To determine whether *splash* is associated with non-aesthetasc sensilla, we examined the regions of the LF containing non-aesthetasc but not aesthetasc sensilla – the lateral and mesial regions of LF – for *splash*+ cells. We found large *splash*+ cells (approximately 30 µm x 20 µm L x W) of various morphologies that were not aesthetasc ORNs (5 µm) (Fig. 2-6A-H). These cells were found as singlets (Fig. 2-6C, D), pairs (Fig. 2-6A, B), or groups of four to six (Fig. 2-6E- H). The somata of these cells had bipolar extensions and a

spherical nucleus containing a large central nucleolus typical of sensory neurons. Their nucleus lacked *splash* labeling and was larger than the nucleus of ORNs. The nucleolus was often *splash*+ (Fig. 2-6A, D, F). All identified large bipolar cells, unlike ORNs, were *splash*+ (> 200 cells, N = 6 LF). A subset of the bipolar *splash*+ cells appeared to send processes ventrally towards the cuticle (Fig. 2-6E-H). We also observed small *splash*– cells among the large bipolar *splash*+ cells (Fig. 2-6H). Some of the large bipolar cells were located more closely to either the lateral, mesial, or dorsal region of PZ of the LF but hardly ever in medial region where ORNs were located. These cells were found in all areas of LF, from the PZ to the mature zone and in animals of any molt stage.

Based on their bipolar morphology and position on the LF, we hypothesized that some of these cells innervate non-aesthetasc sensilla. To test this, we examined the mature zone labeled with three markers: anti-acetylated tubulin and the F-actin marker phalloidin (data not shown) to visualize non-aesthetasc sensory neurons and their processes (Schmidt and Derby, 2005); and Hoechst 33258 to visualize nuclei (N=6). We found that numerous large bipolar cells (nucleus diameter, 15 µm) were located in approximately the same anatomical position on LF as observed with *splash* labeling. Many of the bipolar cells innervated non-aesthetasc sensilla (Fig. 2-6I), though some in this plane of section were not clear (Fig. 2-6J). Unlike ORNs (nucleus diameter, 8 µm), these cells did not express GluR1 (ISH, N=10; ICC, N=2) (Fig. 2-6K, L). These data demonstrate that *splash* is associated with unimodal (chemo) and bimodal (chemo-mechano) sensilla in the adult olfactory organ.

Damage to the Olfactory Organ Increases *splash* Labeling

The LF exhibits remarkable plasticity. Partial or complete ablation of the LF in an intermolt animal causes a large increase in addition of aesthetascs and related sensory tissue in the proliferation zone, resulting in regeneration of the LF to the length and shape of its pre-amputated size (Harrison et al., 2003, 2004) over the course of a few months. Regeneration is fueled by a gradual increase in the number of BrdU+ cells in epithelial cells in the PZ that begins as early as 3 days after ablation, peaks at 9 days after ablation, and is over by 19 days post-ablation. Ablation also causes an increase in formation of

BrdU+ ORN clusters, with one peak occurring at 7 days after ablation and with another peak just before the next molt (Harrison et al., 2003). We hypothesized that if *splash* is involved in damage-induced proliferation, then we would expect an increase in *splash* labeling on the same time course as BrdU labeling following damage. We unilaterally damaged the LF by partially ablating its distal end and examined its PZ at 5-, 7-, and 9-days post-ablation. In the proximal and middle PZ 5 days after ablation, *splash* labeling was present in some epithelial cells but not in ORN clusters, and the intensity of labeling was low (Fig. 2-7A, C, respectively, Table 2-2). At 7 (data not shown) and 9 (Fig. 2-7B, D) after ablation, *splash* labeling in epithelial cells and ORN precursor cells was intense. In the distal PZ at 5 days post ablation, *splash* labeling was more intense compared to the proximal PZ (Fig. 2-7A) but not as intense as at 7 or 9 days post-ablation (Fig. 2-7 B-F, Table 2-2). Thus, following LF damage, *splash* expression increased in areas of the LF where cellular proliferation also occurred, and had a similar time course as the increase in cell proliferation.

To determine the role of *splash* in damage-induced repair that leads to regeneration, we examined the areas next to the site of damage (i.e., immediately proximal to the blastema), which includes the mature zone. *splash* labeling was present in the ventral epithelium at post-ablation days 5 (Fig. 2-7G), 7, and 9 (Fig. 2-7H), but the labeling was more intense and widespread at later times, including in lateral and mesial epithelial cells (Fig. 2-7I, Table 2-2). The increase in *splash* labeling compared to intermolt mature zone (see Fig. 2-3) suggests that *splash* is involved in damage-induced proliferation and in damage-induced repair.

2.6 Discussion

This is the first description of the cellular distribution of an *ASC* homolog in an adult arthropod. *splash*, an *ASC* homolog in the Caribbean spiny lobster *Panulirus argus*, is expressed in the adult antennular lateral flagellum (LF), a major chemosensory organ in decapod crustaceans. *splash* is expressed in both immature and mature ORNs and also in other cell types. Molt stage, which affects the

extent of ORN proliferation, did not affect *splash* expression in proliferating ORNs but it did affect expression in mature ORNs. Damage to the LF, which induces regeneration, also enhanced *splash* expression, suggesting an association between *splash* with regeneration and repair. We conclude that *splash* plays multiple roles in the adult spiny lobster olfactory organ.

The Role of *splash* in Neurogenesis in the Olfactory Organ of Adult Spiny Lobsters

The function of *ASC* homologs in neurogenesis is best known from studies of the formation of sensilla in embryos of insects, especially *Drosophila*. In this model, *ASC* homologs are expressed in unspecified ectodermal cells that form a proneural cluster, from which one cell takes on a neural fate (Skeath and Carroll, 1994; Skeath and Doe, 1996) ultimately forming a sensory organ. According to this model, if *splash* is a proneural gene and functions in ORN neurogenesis of adult spiny lobsters as do *ASC* homologs of insects, then we would expect to observe one or a cluster of *splash*+ cells in the ventral epithelium of the proliferation zone where new ORNs originate. However, we found that *splash* is uniformly expressed in the ventral epithelium of the LF of intermolt animals (Fig. 2-2). *ASC1* homolog expression in crustacean larvae initially has a uniform expression pattern, but as development proceeds, selected cells within a cluster increase expression (Wheeler and Skeath, 2005) suggesting that insect and crustacean development is similar. Our results do not support the idea that *splash* functions as a proneural gene in the LF of adult spiny lobsters. Relevant to this idea are our data on the effect of molt stage on *splash* labeling. Because molt stage affects proliferation, with the number of BrdU+ cells in PZ being higher in premolt compared to intermolt animals, we examined the effect of molt stage on *splash* labeling. If *splash* were a proneural gene, then conditions in which cell proliferation in the PZ is enhanced, such as in the premolt stage, should also increase *splash* labeling. Counter to this expectation, we found no major difference in the intensity of *splash* labeling in the PZ of premolt and intermolt animals (Fig. 2-3 & Table 2-1). Our third evidence that *splash* does not function as a proneural gene in the PZ is the labeling of epithelial cells across all LF developmental zones including a higher expression in the dorsal epithelium (where aesthetascs and their ORNs do not reside) versus ventral epithelium of the PZ.

We determined whether there is a direct relationship between *splash* expression and cell proliferation using BrdU labeling. We previously showed that after a one-time injection of BrdU and a 24-h survival time, many epithelial cells formed patches and many cells within developing ORN clusters in the proliferation zone were BrdU+ (Harrison et al., 2001; 2003). Using the same labeling strategy, we also found many BrdU+ cells in both locations; however, only a small percentage (6% for epithelial cells, 18% for cells in ORN clusters) of these BrdU+ cells were also *splash* + (Fig. 2-5). To interpret this result, two aspects of BrdU labeling have to be considered. Firstly, BrdU is incorporated into DNA during the S-phase of the cell cycle and is then distributed into the two daughter cells generated by the cell division. Thus a BrdU+ cell can be either a proliferating cell (in S-phase) or a post-mitotic cell. Secondly, BrdU can be incorporated into the DNA of proliferating cells as long as it is available in the hemolymph, which is 12-24-h post injection in another crustacean, the crayfish *Pacifastacus leniusculus* (Söderhäll et al., 2003). Given the fact that there is no evidence for a synchronization of cell divisions in the proliferation zone (Harrison et al., 2001; 2003), the population of BrdU+ cells that we observed 24-h after BrdU injection should include a sizeable proportion of cells that were still in S-phase (proliferating) at the time of fixation. Thus, the finding that only a minor percentage of BrdU+ cells in both locations was also *splash* + suggests that expression of *splash* is not tightly correlated with cell proliferation. In conjunction with our other results, this leads us to conclude that *splash* does not play a major role in proliferation that gives rise to sensory neurons in adult spiny lobsters.

splash May Play a Role in Repair and Regeneration from Injury in the Olfactory Organ of Adult Spiny Lobsters

Support for our hypothesis comes from the positive correlation between *splash* expression and ablation-induced proliferation, suggesting a role for *splash* in regeneration of a damaged or ablated olfactory organ. Our data show that ablation of the distal end of the LF, which enhances the rate of cell proliferation resulting in regeneration (Harrison et al., 2003, 2004), also enhances *splash* expression in the LF proliferation zone (Fig. 2-7). We observed a dramatic increase of *splash* labeling in epithelial cells and

ORN precursor clusters in the proliferation zone at 7 and 9 days after ablation (Fig. 2-7B, D) compared with 5 days post-ablation (Fig. 2-7A, C).

Another animal model that is instructive to our understanding of neurogenesis associated with regeneration is limb regeneration in fiddler crabs. An expressed sequence tag library of the blastema four days after limb removal, and thus early in regeneration, failed to identify any *ASC* homologs but did identify an *enhancer of split* homolog (Durica et al., 2006). Interestingly, the spiny lobster olfactory organ also expresses a *hairy - enhancer of split* homolog (Chien et al., 2009), though its role in regeneration has yet to been examined. In lobsters, damage to or ablation of the LF also enhanced proliferation zone enriched transcript (*PET-15)*, which is thought to be a regulator of endogenous proteases in proliferating epithelia, in PZ (Stoss et al., 2004). Thus, we believe that the expression of two genes with possibly different functions, *splash* and *PET-15*, is regulated by diffusible signals from damaged tissue.

Regeneration of ORNs shares many similarities but also some differences with normal neurogenesis in the context of changes in gene expression (Gordon et al., 1995; Manglapus et al., 2004; Shetty et al., 2005). Our study demonstrates that *splash* is one of the genes that is not involved in normal ORN formation but is involved in regeneration (Fig. 2-7B, D). A recent study of zebrafish showed that *sox2* transcription factor is required for regeneration but not during initial development of hair cells (Millimaki et al., 2010). It would be interesting to determine whether inhibiting *splash* expression inhibits regeneration.

Multiple Roles of *splash* in Lobster Olfactory Organ

We propose that *splash* has multiple roles, based on its expression in a diversity of cell types in different parts of the LF and over different molt stages. *splash* is expressed in epithelial cells located in the ventral and dorsal PZ and MZ, in auxiliary cells, in immature and mature ORNs associated with aesthetasc sensilla, and in large bipolar sensory neurons innervating non-aesthetasc sensilla. *splash* is not expressed in some other cells types, including granulocytes and chromatophores. Thus, *splash* expression in the LF is not exclusively in tissue involved in the formation of ORNs, and it is consistently expressed

in mature sensory neurons of aesthetasc and non-aesthetasc sensilla. To our knowledge, *ASC* expression and function in adult arthropods have not been examined. Therefore this is the first demonstration of expression of an *ASC* homolog in mature neurons in arthropods.

There are multiple functional possibilities for *splash* expression in multiple cell types. Firstly, *splash* may function as a transcription factor whose primary role is in the maintenance of sensory neurons. For example, *NeuroAB*, a novel bHLH transcription factor, is expressed in mitotic cells; however, its predominate expression in bipolar and amacrine cells in the developing and mature chick retina suggests that it functions in the maintenance of neurons rather than in proliferation (Ohkawara et al., 2004). *sox2* encodes a transcription factor involved in maintenance of stem cells (Avilion et al., 2003) and formation of sensory epithelium in the inner ear of mice (Hume et al., 2007) and chicks (Neves et al., 2007), but it has other roles in developing zebrafish. Although progenitors of hair cells and support cellsexpress *sox2*, knockdown studies showed no effect on hair cell formation but an effect on maintenance of hair cells and support cells (Millimaki et al., 2010). In *Drosophila*, expression of *engrailed* (Blagburn, 2008) in mature olfactory sensory neurons suggests additional functions in maintenance rather than in early development. Taken together, transcription factors previously known for functions during early development are now known to have additional roles in later stages, and *splash* may be another example.

Secondly, *splash* may have dual functions: it may have transcriptional and non-transcriptional roles depending on the developmental stage (immature vs. mature cells, or larvae vs. adult) or cell type in which it is expressed. Eyes absent (Eya) has two functions: as a transcription factor and a tyrosine phosphatase during eye development (Tootle et al., 2003; Rebay et al., 2005). Other bHLH transcription factors have intercellular functions rather than as the more typical intracellular signals (Prochiantz and Joliot, 2003). *splash* maybe a transcription factor but have anti-proneural rather than proneural functions as shown for Daughterless (Da) in eye development of *Drosophila* (Lim et al., 2008).

Thirdly, *splash* may function as a transcription factor but regulate the expression of genes that regulate the physiology but not the development of cells. In adult *C. elegans*, within a few hours after

altering the expression of *lin-12* Notch receptor homolog using inducible RNAi and conditional gain of function, changes in locomotor behavior were observed suggesting an effect on the physiological properties of neurons and not in cell fate specification (Chao et al., 2005). *lin-12* genetically interacts with an AMPA/kainate receptor homolog *glr-1* expressed in command interneurons suggesting a physiological mechanism for a developmental gene. The novel finding that *lin-12* functions in the neuronal physiology via the canonical transcriptional activation in adults is further evidence that there may be more transcription factors that have developmental and additional unidentified functions. It is likely that similar to *lin-12, splash* may function in mature ORNs or bipolar cells by regulating the expression of various ion channels. In summary, although our results do not demonstrate *splash* as a transcription factor or a non-transcriptional function, based on it being an *ASC* homolog, it is likely that one of its function is as a transcription factor. Our data suggest that *splash* may be another example of transcription factors having multiple functions, although more work is necessary to elucidate the nature of these functions.

Expression of an Ionotropic Glutamate Receptor Specific to Mature ORNs of Spiny Lobsters

Our need for an ORN-specific label for *in situ* hybridization led us to clone a spiny lobster homolog of an ionotropic glutamate receptor subunit, GluR1. This was based on previous work on the clawed lobster *H. americanus* which identified a GluR1 homolog (OET07) that is specifically expressed in all aesthetasc ORNs and not in other cell types (Hollins et al., 2003; Stepanyan et al., 2004, 2006). Our partial sequence of *P. argus* GluR1 is highly similar to its *H. americanus* homolog and *P. argus* GluR1 is also expressed in all ORNs. The function of GluR1 is unknown. However, Corey et al. (2010) proposed that the olfactory organ of spiny lobsters has additional ionotropic receptors besides GluR1 and that they have sequence similarity to ionotropic receptors expressed in antennal olfactory neurons in *Drosophila* (Benton et al., 2009). This raises the intriguing hypothesis that the lobster's ionotropic receptors might be involved in olfactory transduction, and that GluR1, since it is expressed in all ORNs, is a co-receptor functionally related to the insect Or83b.

2.7 References

Alfano G, Vitiello C, Caccioppoli C, Caramico T, Carola A, Szego MJ, McInnes RR, Auricchio A, Banfi S. 2005. Natural antisense transcripts associated with genes involved in eye development. Hum Mol Genet 14:913-923.

Avilion AA, Nicolis SK, Pevny LH, Perez L, Vivian N, Lovell-Badge R. 2003. Multipotent cell lineages in early mouse development depend on SOX2 function. Genes Dev. 17:126-140.

Battison A, Cawthorn R, Horney B. 2003. Classification of *Homarus americanus* hemocytes and the use of differential hemocyte counts in lobsters infected with *Aerococcus viridans* var. *homari* (Gaffkemia). J Invert Pathol 84:177-197.

Benton R, Vannice KS, Gomez-Diaz C, Vosshall LB. 2009. Variant ionotropic glutamate receptors as chemosensory receptors in *Drosophila.* Cell 136:149-162.

Bertrand N, Castro DS, Guillemot F. 2002. Proneural genes and the specification of neural cell types. Nat Rev Neurosci 3:517-530.

Blagburn JM. 2008. Engrailed expression in subsets of adult *Drosophila* sensory neurons: an enhancer-trap study. Invert Neurosci. 8:133-146.

Brand, M, Jarman AP, Jan LY, Jan YN. 1993. *asense* is a *Drosophila* neural precursor gene and is capable of initiating sense organ formation. Development 119:1-17.

Cate HS, Derby CD. 2001. Morphology and distribution of setae on the antennules of the Caribbean spiny lobster *Panulirus argus* reveal new types of bimodal chemo-mechanosensilla. Cell Tiss Res 304:439-454.

Cate HS, Derby CD. 2002. Ultrastructure and physiology of the hooded sensillum, a bimodal chemo-mechanosensillum of lobsters. J Comp Neurol 442:293-307.

Cau E, Gradwohl G, Fode C, Guillemot F. 1997. *Mash1* activates a cascade of bHLH regulators in olfactory neuron progenitors. Development 124: 1611-1621.

Cau E, Casarosa S, Guillemot F. 2002. *Mash1* and *Ngn1* control distinct steps of determination and differentiation in the olfactory sensory neuron lineage. Development 129: 1871-1880.

Chao MY, Larkins-Ford J, Tucey TM, Hart AC. 2005. *lin-12* Notch functions in the adult nervous system of *C. elegans*. BMC Neurosci 12:45.

Chien H, Tadesse T, Liu H, Schmidt M, Walthall WW, Tai PC, Derby CD. 2009. Molecular cloning and characterization of homologs of *achaete–scute* and *hairy–enhancer of split* in the olfactory organ of the spiny lobster *Panulirus argus*. J Molec Neurosci 39:294-307.

Corey EA, Bobkov Y, Ache BW. 2010. Molecular characterization and localization of olfactory-specific ionotropic glutamate receptors in lobster olfactory receptor neurons. Chem Senses 35:A65.

Derby CD. 2000. Learning from spiny lobsters about chemosensory coding of mixtures. Physiol Behav 69:203-209.

Domínguez M, Campuzano S. 1993. *asense*, a member of the *Drosophilaachaete-scute* complex, is a proneural and neural differentiation gene. EMBO J 12:2049-2060.

Durica DS, Kupfer D, Najar F, Lai H, Tang Y, Griffin K, Hopkins PM, Roe B. 2006. EST library sequencing of genes expressed during early limb regeneration in the fiddler crab and transcriptional responses to ecdysteroid exposure in limb bud explants. Integr Comp. Biol 6:948-964

Gordon MK, Mumm JS, Davis RA, Holcomb JD, Calof AL. 1995. Dynamics of MASH1 expression *in vitro* and *in vivo* suggest a non-stem cell site of MASH1 action in the olfactory receptor neuron lineage. Molec Cell Neurosci 6:363-379.

Grünert U, Ache BW. 1988. Ultrastructure of the aesthetasc (olfactory) sensilla of the spiny lobster *Panulirus argus.* Cell Tiss Res 251:95-103.

Harrison PJH, Cate HS, Swanson ES, Derby CD. 2001. Postembryonic proliferation in the spiny lobster antennular epithelium: Rate of genesis of olfactory receptor neurons is dependent on molt stage. J Neurobiol 47:51-66.

Harrison PJH, Cate HS, Steullet P, Derby CD. 2003. Amputation-induced activity of progenitor cells leads to rapid regeneration of olfactory tissue in lobsters. J Neurobiol 55:97-114.

Harrison PJH, Cate HS, Derby CD. 2004. Localized ablation of olfactory receptor neurons induces both localized regeneration and widespread replacement of neurons in spiny lobsters. J Comp Neurol 471:72-84.

Hollins B, Hardin D, Gimelbrant AA, McClintock TS. 2003. Olfactory-enriched transcripts are cell-specific markers in the lobster olfactory organ. J Comp Neurol 455:125-138.

Hume CR, Bratt DL, Oesterle EC. 2007. Expression of LHX3 and SOX2 during mouse inner ear development. Gene Expr Patterns 7:798-807.

Ishii K, Mußmann M, MacGregor BJ, Amann R. 2004. An improved fluorescence in situ hybridization protocol for the identification of bacteria and archaea in marine sediments. FEMS Microbiol Ecol 50:203-213.

Katayama S, Tomaru Y, Kasukawa T, Waki K, Nakanishi M, Nakamura M, Nishida H, Yap CC, Suzuki M, Kawai J, Suzuki H, Carninci P, Hayashizaki Y, Wells C, Frith M, Ravasi T, Pang KC, Hallinan J, Mattick J, Hume DA, Lipovich L, Batalov S, Engström PG, Mizuno Y, Faghihi MA, Sandelin A, Chalk AM, Mottagui-Tabar S, Liang Z, Lenhard B, Wahlestedt C. 2005. Antisense transcription in the mammalian transcriptome. Science 309:1564-1566.

Kim EJ, Battiste J, Nakagawa Y, Johnson JE. 2008. Ascl1 (Mash1) lineage cells contribute to discrete cell populations in CNS architecture. Molec Cell Neurosci 38:595-606.

Kitamura H, Yazawa T, Sato H, Okudela K, Shimoyamada H. 2009. Small cell lung cancer: Significance of RB alterations and TTF-1 expression in its carcinogenesis, phenotype, and biology. Endocrine Pathol 20:101-107.

Ledent V, Vervoort M. 2001. The basic helix-loop-helix protein family: Comparative genomics and phylogenetic analysis. Genome Res 11:754-770.

Lim J, Jafar-Nejad H, Hsu Y-C, Choi K-W. 2008. Novel function of the class I bHLH protein Daughterless in the negative regulation of proneural gene expression in the *Drosophila* eye. EMBO Rep 9:1128-1133.

Lyle WG, MacDonald CD. 1983. Molt stage determination in the Hawaiian spiny lobster *Panulirus marginatus*. J Crust Biol 3:208-216.

Manglapus GL, Youngentob SL, Schwob JE. 2004. Expression patterns of basic helix-loop-helix transcription factors define subsets of olfactory progenitor cells. J Comp Neurol 479:216-233.

McClintock TS, Glasser CE, Bose SC, Bergman DA. 2008. Tissue expression patterns identify mouse cilia genes. Physiol Genom 32:198-206.

McIntyre JC, Bose SC, Stromberg AJ, McClintock TS. 2008. Emx2 stimulates odorant receptor gene expression. Chem Senses 33:825-837.

Mercer TR, Dinger ME, Sunkin SM, Mehler MF, Mattick JS. 2008. Specific expression of long noncoding RNAs in the mouse brain. 105: 716-721.

Mercer TR, Qureshi IA, Gokhan S, Dinger ME, Li G, Mattick JS, Mehler MF. 2010. Long noncoding RNAs in neuronal-glial fate specification and oligodendrocyte lineage maturation. BMC Neurosci 11:14.

Millimaki BB, Sweet EM, Riley BB. 2010. Sox2 is required for maintenance and regeneration, but not initial development, of hair cells in the zebrafish inner ear. Dev Biol. 338:262-269.

Murray RC, Navi D, Fesenko J, Lander AD, Calof AL. 2003. Widespread defects in the primary olfactory pathway caused by loss of *Mash1* function. J Neurosci 23:1769-1780.

Neves J, Kamaid A, Alsina B, Giraldez F. 2007. Differential expression of Sox2 and Sox3 in neuronal and sensory progenitors of the developing inner ear of the chick. J Comp Neurol. 503:487-500.

Noël PY, Chassard-Bouchaud C. 2004. Chromatophores and pigmentation. In: Forest J, von Vaupel Klein JC, editors. The CrustaceaI.Leiden: Brill, p 145-160.

Ohkawara T, Shintani T, Saegusa C, Yuasa-Kawada, Takahashi M, Noda M. 2004. A novel basic helix-loop-helix (bHLH) transcriptional repressor, NeuroAB, expressed in bipolar and amacrine cells in the chick retina. Brain Res Mol Brain Res 128:58-74.

Prochiantz A, Joliot A. 2003. Can transcription factors function as cell-cell signalling molecules? Nat Rev Mol Cell Biol 4:814-819.

Rapa I, Ceppi P, Bollito E, Rosas R, Cappia S, Bacillo E, Porpiglia F, Berruti A, Papotti M, Volante M. 2008. Human ASH1 expression in prostate cancer with neuroendocrine differentiation. Mod Pathol 21:700-707.

Rebay I, Silver SJ, Tootle TL. 2005. New vision from Eyes absent: transcription factors as enzymes. Trends Genet 21:163–171.

Schmidt M, Ache BW. 1992. Antennular projections to the midbrain of the spiny lobster. II Sensory innervation of the olfactory lobe. J Comp Neurol 318:291-303.

Schmidt M, Derby CD. 2005. Non-olfactory chemoreceptors in asymmetric setae activate antennular grooming behavior in the Caribbean spiny lobster *Panulirus argus*. J Exp Biol 208:233-248.

Schmidt M, Derby CD. 2006 Hemocyte infiltration of olfactory receptor neuron clusters after aesthetasc damage in the spiny lobster. Chem Senses 31:A139.

Schmidt, M, Van Ekeris L, Ache BW. 1992. Antennular projections to the midbrain of the spiny lobster. I. Sensory innervation of the lateral and medial antennular neuropils. J Comp Neurol 318:277-290.

Schmidt M, Chien H, Tadesse T, Johns ME, Derby CD. 2006. Rosette-type tegumental glands associated with aesthetasc sensilla in the olfactory organ of the Caribbean spiny lobster, *Panulirus argus*. Cell Tiss Res 325:369-395.

Shetty RS, Bose SC, Nickell MD, McIntyre JC, Hardin DH, Harris AM, McClintock TS. 2005. Transcriptional changes during neuronal death and replacement in the olfactory epithelium. Mol Cell Neurosci. 1: 90-107.

Skeath JB, Carroll SB. 1994. The *achaete-scute* complex: Generation of cellular pattern and fate within the *Drosophila* nervous system. FASEB J 8:714-721.

Skeath JB, Doe CQ. 1996. The *achaete-scute* complex proneural genes contribute to neural precursor specification in the *Drosophila* CNS. Curr Biol 6:1146-1152.

Smalheiser NH, Lugli G, Torvik VI, Mise N, Ikeda R, Abe K. 2008. Natural antisense transcripts are co-expressed with sense mRNAs in synaptoneurosomes of adult mouse forebrain. Neurosci Res 62:236-239.

Söderhäll I, Bangyeekhun E, Mayo S, Söderhäll K. 2003. Hemocyte production and maturation in an invertebrate animal; proliferation and gene expression in hematopoietic stem cells of *Pacifastacus leniusculus*. Dev Comp Immunol 27:661-672.

Stepanyan R, Hollins B, Brock SE, McClintock TS. 2004. Primary culture of lobster (*Homarus americanus*) olfactory sensory neurons. Chem Senses 29:179-187.

Stepanyan R, Day K, Urban J, Hardin DL, Shetty RS, Derby CD, Ache BW, McClintock TS. 2006. Gene expression and specificity in the mature zone of the lobster olfactory organ. Physiol Genom 25:224-233.

Steullet P, Cate HS, Derby CD. 2000a. A spatiotemporal wave of turnover and functional maturation of olfactory receptor neurons in the spiny lobster *Panulirus argus*. J Neurosci 20:3282-3294.

Steullet P, Cate HS, Michel WC, Derby CD. 2000b. Functional units of a compound nose: Aesthetasc sensilla house similar populations of olfactory receptor neurons on the crustacean antennule. J Comp Neurol 418:270-280.

Stoss TD, Nickell MD, Hardin D, Derby CD, McClintock TS. 2004. Inducible transcript expressed by reactive epithelial cells at sites of olfactory sensory neuron proliferation. J Neurobiol 58:355-368.

Sun Y, Jan LY, Jan YN. 1998. Transcriptional regulation of *atonal* during development of the *Drosophila* peripheral nervous system. Development 125:3731-3740.

Tootle TL, Silver SJ, Davies EL, Newman V, Latek RR, Mills IA, Selengut JD, Parlikar BE, Rebay I. 2003. The transcription factor Eyes absent is a protein tyrosine phosphatase. Nature 426:299-302.

Wheeler SR, Carrico ML, Wilson BA, Brown SJ, Skeath JB. 2003. The expression and function of the *achaete-scute* genes in *Tribolium castaneum* reveals conservation and variation in neural pattern formation and cell fate specification. Development 130:4373-4381.

Wheeler SR, Skeath JB. 2005. The identification and expression of *achaete-scute* genes in the branchiopod crustacean *Triops longicaudatus*. Gene Express Patt 5:695-700.

Yin GL, Qi C, Yang WJ. 2007. Naturally occurring antisense RNA of allostatin gene in the prawn, *Macrobrachium rosenbergii*. Comp Biochem Physiol 146B:20-25.

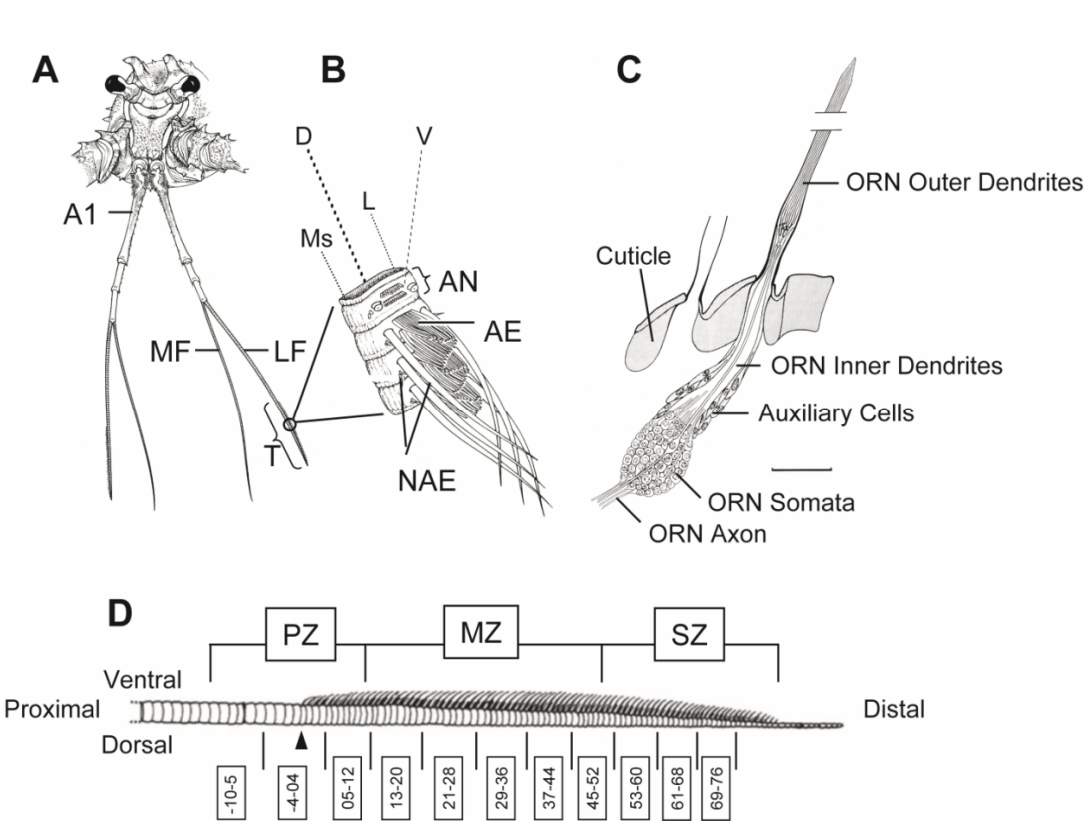

Figure 2-1 Schematic drawings of the antennular lateral flagellum (olfactory organ) of the adult spiny lobster *P. argus*.

A A pair of antennules (A1: first antennae) is located on the head of the animal. Each antennule has two flagella, a medial (MF) and a lateral (LF). **B** Each flagellum is comprised of repeated cuticular units called annuli (AN). Each annulus in the distal tuft (T) region of the LF bears ca. 20 olfactory sensilla called aesthetascs (AE). Non-aesthetasc sensilla (NAE) are located on mesial (Ms), lateral (L), dorsal (D), and ventral (V) sides of both flagella. **C** Sagittal section of LF showing aesthetasc ultrastructure. Each aesthetasc is innervated by the outer dendrites of about 300 bipolar olfactory receptor neurons (ORNs). The inner dendrites are surrounded by auxiliary cells. ORN axons project into the brain. **D** LF developmental zones are divided into regions of 6 annuli with proximal to the left and distal to the right. Throughout the animal's life, aesthetasc sensilla and their associated ORNs are added to the LF in the proliferation zone (PZ), mature and become chemoresponsive in the mature zone (MZ), and are then shed in the senescence zone (SZ). In this figure, each annulus is given a number, with '1' representing the most proximal aesthetasc-bearing annulus, annuli proximal to '1' having progressively larger negative numbers, and annuli distal to '1' having progressively larger positive numbers. According to this numbering scheme, the PZ is represented by annuli -10 to 12, with the proximal PZ being annuli -10 to -5, the middle PZ being annuli -4 to 4, and the distal PZ being annuli 5 to 12. The mature zone is represented by annuli 13 to 52, and the senescence zone is represented by annuli 53 and greater. Drawings are modified from Grünert and Ache (1998), Harrison et al. (2004), and Schmidt et al. (2006)

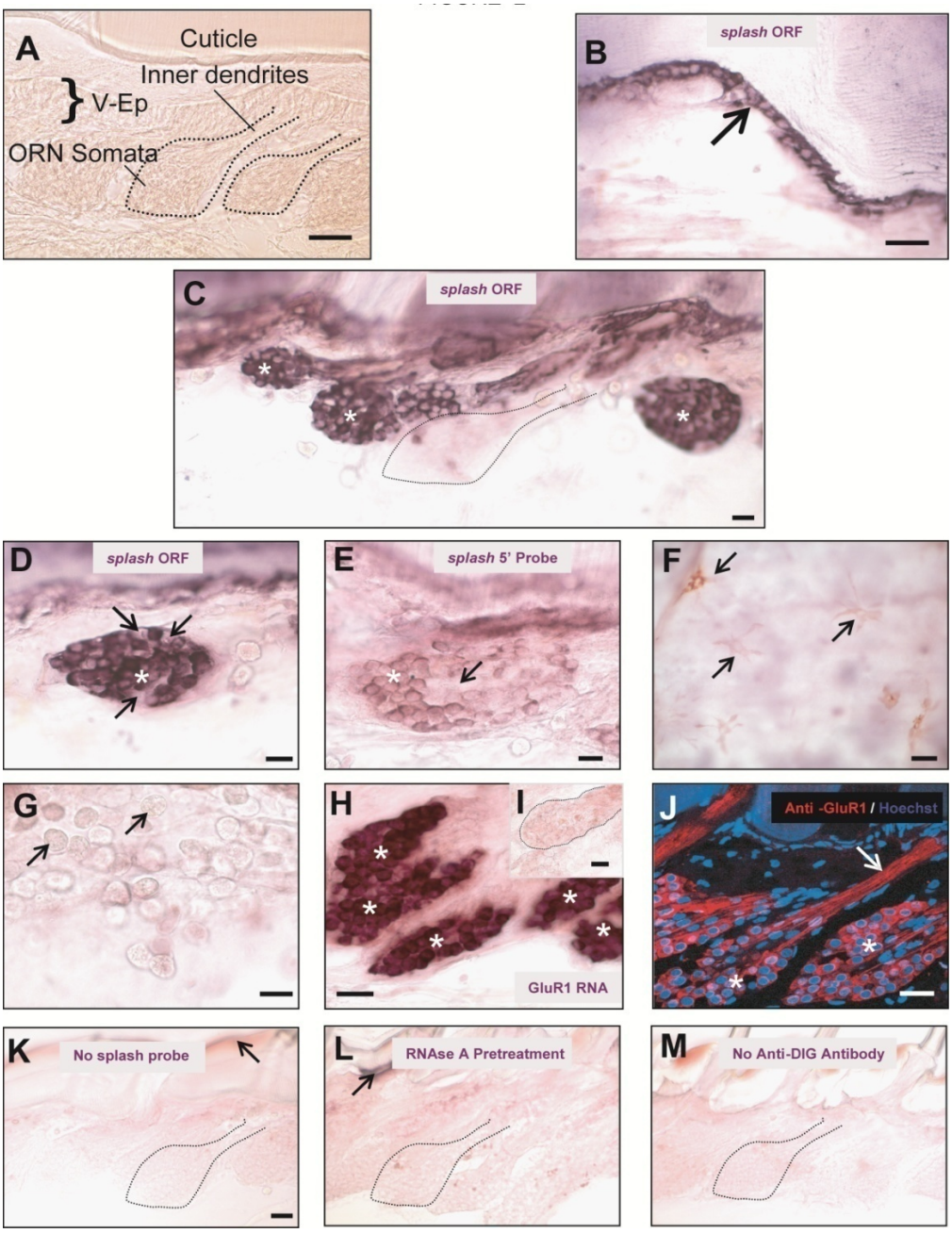

Figure 2-2 *In situ* hybridization with digoxigenin RNA probes for *splash* in the antennular lateral flagellum of an adult intermolt spiny lobster.

A Cellular morphology of the tuft region of the lateral flagellum (LF) in an unlabeled sagittal section. All subsequent sections are presented in this orientation. The epithelium on the ventral surface of the LF (V-Ep) is indicated by a bracket. Two of the four olfactory receptor neuron (ORN) clusters shown in this image are outlined in black. **B-G** Results using *splash* RNA open reading frame (ORF) probe or *splash* RNA bHLH 5' probe in the proliferation zone. **B** Ventral epithelium (arrow) in proximal PZ, which lacked ORN clusters, was uniformly labeled by *splash* ORF probe. **C, D** Newly formed ORN clusters in the middle PZ were intensely and abundantly labeled by *splash* ORF probe (asterisks), although some

ORN clusters were completely devoid of labeling (indicated by outline in **C**), andsome cells within an ORN cluster were also devoid of labeling (arrows in **D**). **E** *splash* bHLH 5' probe labeling of ORN clusters (asterisk) was qualitatively similar but less intense compared to *splash* ORF probe, including that some cells within a labeled ORN cluster were not labeled (arrow). **F** Multipolar chromatophores (arrows) and **G** granulocytes (arrows) did not label with either probe. **H-J** Positive control using RNA probes for an ionotropic glutamate receptor subunit (GluR1). **H** Antisense RNA probe for GluR1 labeled the majority of ORNs in the mature zone (asterisks). **I** Sense RNA probe for GluR1 showed no labeling of ORNs (outline) in the mature zone. **J** Double labeling using anti-GluR1 antibody (red) and the nuclear marker Hoechst 33258 (blue) showed labeling of ORN somata (asterisks) and inner dendrites (arrow) in the mature zone. **K-M** Negative controls for digoxigenin (DIG) labeled RNA *in situ* hybridization with NBT/BCIP (purple) using immature and mature zones. **K** Control using hybridization buffer without *splash* RNA probe. **L** Control treated with RNase A prior to the application of *splash* RNA probes. **M** Control lacking primary antibody. All three negative controls showed no *splash* specific labeling, but there was non-specific labeling of the cuticle (arrow) and aesthetasc tegumental glands (data not shown). *ScaleBars* 50 µm(**A-D**), 20 µm (**E-G**), 50 µm (**H-I**),20 µm (**J-M**)

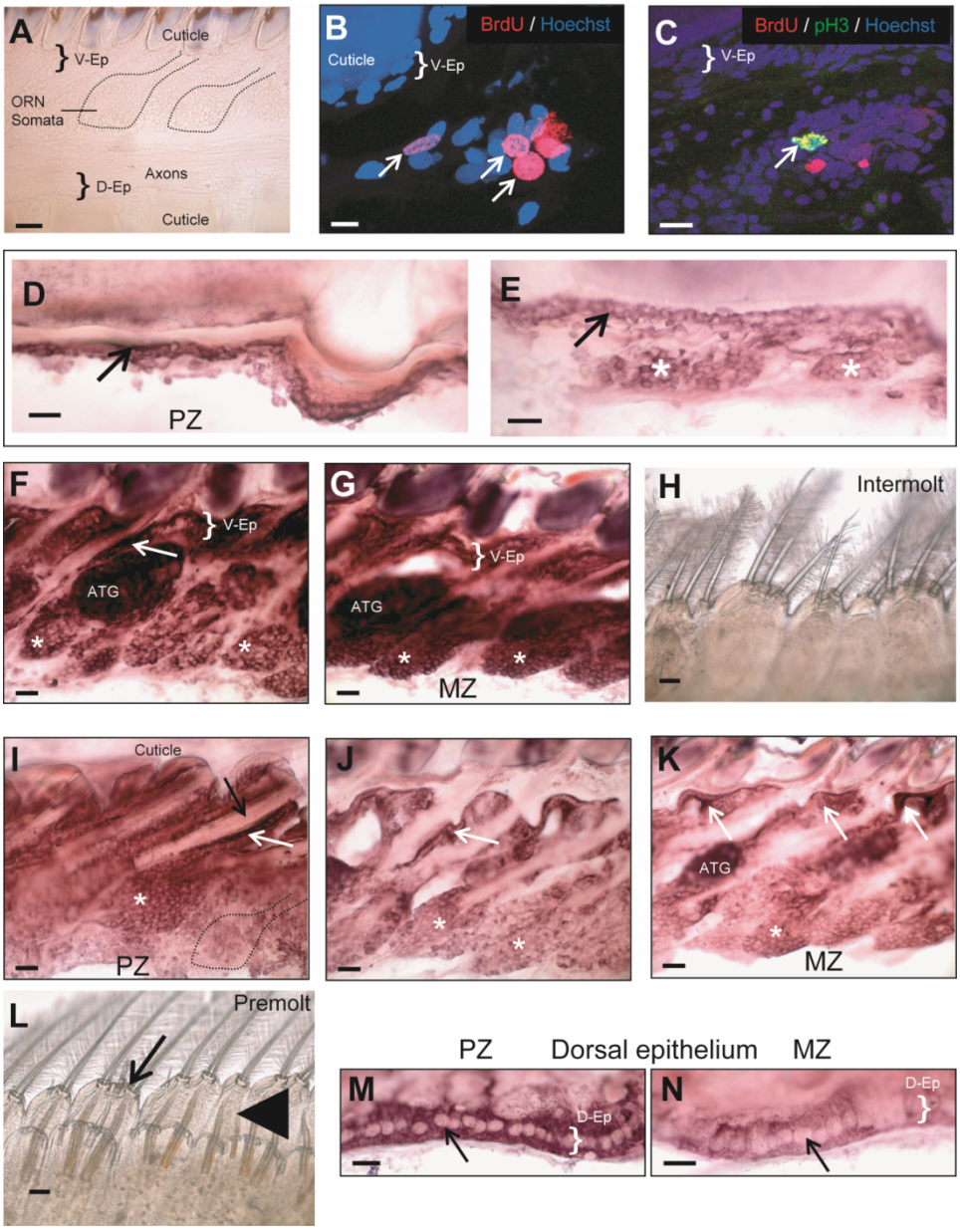

Figure 2-3 Effect of molt stage on *splash* labeling.

A Cellular morphology in the mature zone of an unlabeled antennular lateral flagellum, showing the ventral (V-Ep) and dorsal (D-Ep) epithelium in sagittal section. **B-C** Confocal micrographs showing proliferating cells in the proliferation zone (PZ) of an intermolt animal. **B** BrdU labeling (after a single injection of BrdU and 24-h survival) together with Hoechst 33258 staining showing BrdU+ (S-phase) cells (red) in a newly formed ORN cluster proximal to the V-Ep. BrdU+ cells had diverse nuclear shapes (arrows). **C** Triple labeling with anti-BrdU (red), anti-phosphorylated histone 3 (pH3) (green), and Hoechst 33258 (blue), showing a pH3+ (M-phase) cell (arrow) in an ORN cluster containing BrdU+ (S-phase) cells. **D-G** *splash* bHLH 5' probe labeling in a lateral flagellum of an intermolt animal. **D** Proximal proliferation zone (PZ), which lacked ORN clusters, had intense *splash* labeling in most of the V-Ep (arrow). **E** Middle PZ had *splash* labeling in epithelial cells and in most cells of newly formed ORN

clusters (asterisks). **F** Distal PZ had intense *splash* labeling in the V-Ep, and very intense labeling in many ORN somata (asterisks), and in auxiliary cells surrounding the ORN inner dendrites (white arrow). Each ORN cluster contained some unlabeled cells. Aesthetasc tegumental glands (ATGs), which are abundant in the aesthetasc bearing region of the LF, were non-specifically labeled (see also Fig. 2.2). **G** Mature zone had very intense *splash* labeling including *splash*+ cells in the ORN clusters (asterisks). **H** Determination of molt stage based on pleopod morphology showed that this intermolt animal did not have new setae beneath the cuticle. **I-L***splash* 5' bHLH probe labeling in the lateral flagellum of a premolt animal. **I** Proximal PZ contained newly formed aesthetasc sensillum (black arrow) that will emerge on the LF cuticular surface after the animal's next molt. Auxiliary cells (white arrow) and some cells in ORN clusters (asterisk) had intense *splash* labeling, but some ORN clusters were unlabeled. **J** Distal PZ had intense *splash* labeling in the V-Ep. The inner dendrites were surrounded by intensely labeled auxiliary cells (arrow). Most ORN clusters (asterisks) contained both *splash*+ and *splash*– cells. **K** Mature zone was similar in *splash* labeling in V-Ep compared to middle PZ. There were many ORNs in MZ with intense labeling (asterisk). **L** Premolt animal had new cuticle with new setae (arrowhead) beneath the old cuticle (arrow)that will be shed at the next molt. **M-N** Dorsal epithelial cells (D-Ep) in proximal PZ (**M**) showed very intense *splash* labeling in the cytoplasm compared to MZ (**N**). *splash* labeling in D-Ep of PZ is more intense than in V-Ep. *Scale Bars* 100 µm (**A**), 10 µm (**B**), 20 µm (**C**), 50 µm (**D-J**), 20 µm (**K-N**)

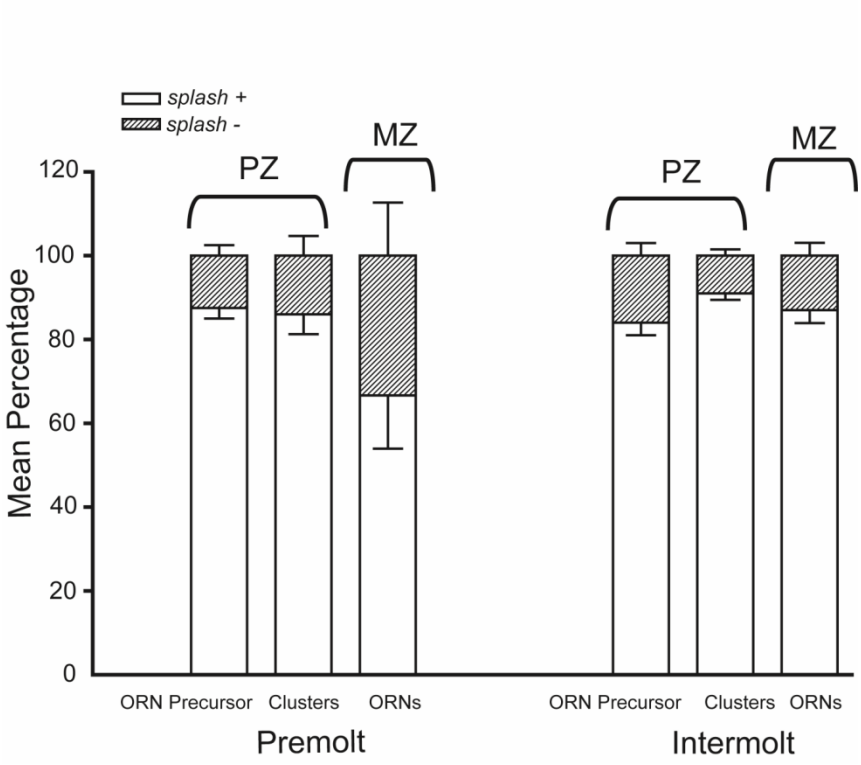

Figure 2-4 The mean percentage of *splash*+ and *splash*- cells in the antennular lateral flagellum.

Data are shown for the proliferation zone (PZ) and mature zone (MZ) of premolt animals (left figure) and intermolt animals (right figure). In the PZ, data are shown for ORN precursor cells and ORN clusters; in the MZ, data are shown for ORNs. Values are mean ± SEM for 3 animals per molt stage. The majority of cells in both regions (PZ, MZ) and for both molt stages (premolt, intermolt) were *splash*+. The only molt-stage difference was that compared to premolt animals, intermolt animals had an even higher percentage of *splash*+ ORNs in the MZ.

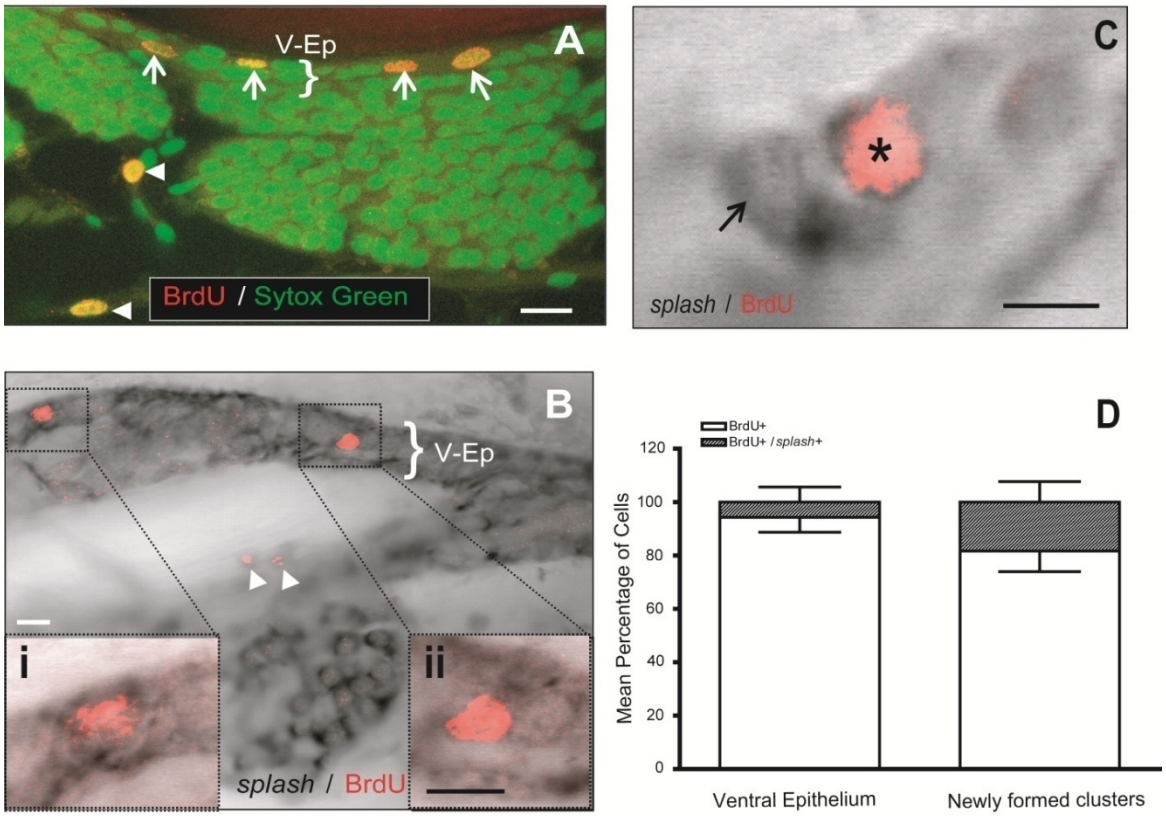

Figure 2-5 *splash* and BrdU labeling in intermolt proliferation zone (PZ) of the antennular lateral flagellum.

A After a single injection of BrdU followed by a 24-h survival period, numerous BrdU+ cells were located in the ventral epithelium (white arrows) and other areas (white arrowheads). Double labeling is with the nuclear marker, Sytox Green. **B** Confocal scan of *splash* RNA labeling (black) and anti-BrdU labeling (red) in the PZ of a premolt animal showed one BrdU+/*splash*+ cell (i) and one BrdU+/*splash*- cell (ii) in the ventral epithelium. Isolated BrdU+ cells (arrowheads) were BrdU+/*splash*-. **C** Two adjacent cells in the ventral epithelium were either BrdU+/*splash*+ (asterisk) or BrdU-/*splash*+ (black arrow). **D** The mean ± SEM values of the percentage of BrdU+/ *splash*+ (gray bars) and BrdU+ cells (white bars) in the PZ. Only a small percentage of BrdU+ cells were labeled with *splash* in both the ventral epithelium (6%, n = 15) and newly formed ORN clusters (18%, n = 58), compared with cells labeled with BrdU only (94 %, n = 126 and 82%, n= 230) (number of animals = 3). *Scale Bars* 20 µm (**A**), 50µm (**B**), 10µm (**B i, ii**), 10 µm (**C**)

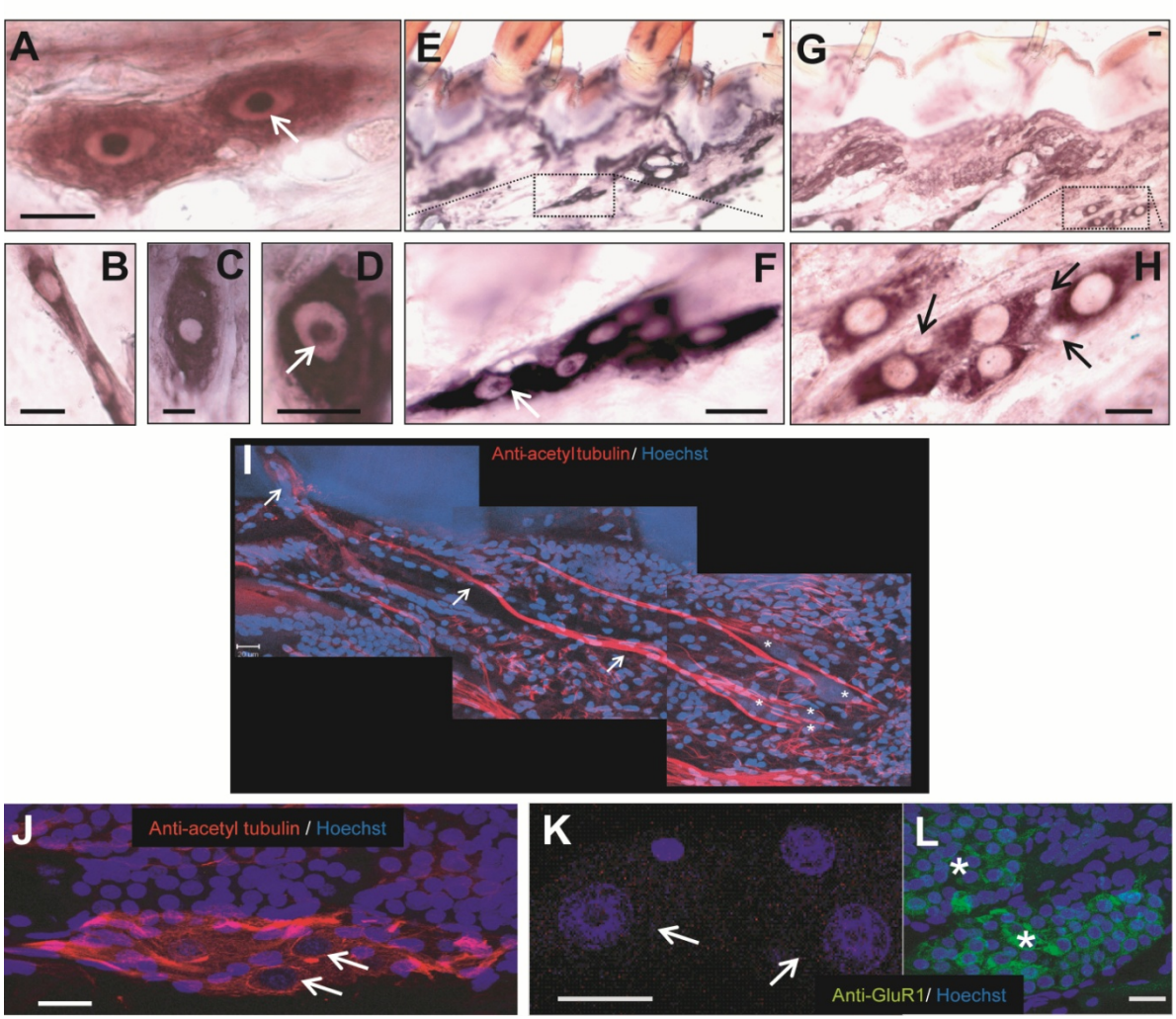

Figure 2-6 *splash* labeling of non-aesthetasc sensory neurons in the antennular lateral flagellum.

A-H Large somata of non-aesthetasc sensory neurons with typical bipolar morphology were *splash*+. Some had *splash* labeling in the nucleolus (white arrows) (**A**, **D, F**). These cells occurred in singlets (**C**, **D**), pairs (**A**, **B**), or groups of 4-6 (**E**-**H**) in the lateral, mesial, dorsal, and occasionally ventral regions of the LF. **I**-**L** Confocal images of immunostained sections of LF showing large bipolar cells sensory neurons. **I** Bipolar cells (asterisks) with thick dendrites (white arrows) innervating non-aesthetasc sensilla were labeled with anti-acetylated tubulin (red) and stained with Hoechst 33258 (blue). **J** Other types of bipolar cells (white arrows) double labeled with anti-acetylated tubulin (red) and Hoechst 33258 (blue) were located dorsally. **K** Large bipolar cells stained with nuclear marker Hoechst 33258 (blue) had a distinctive nuclear morphology and did not label with anti-GluR1 (green), unlike ORNs (**L**). *Scale Bars* 20 µm

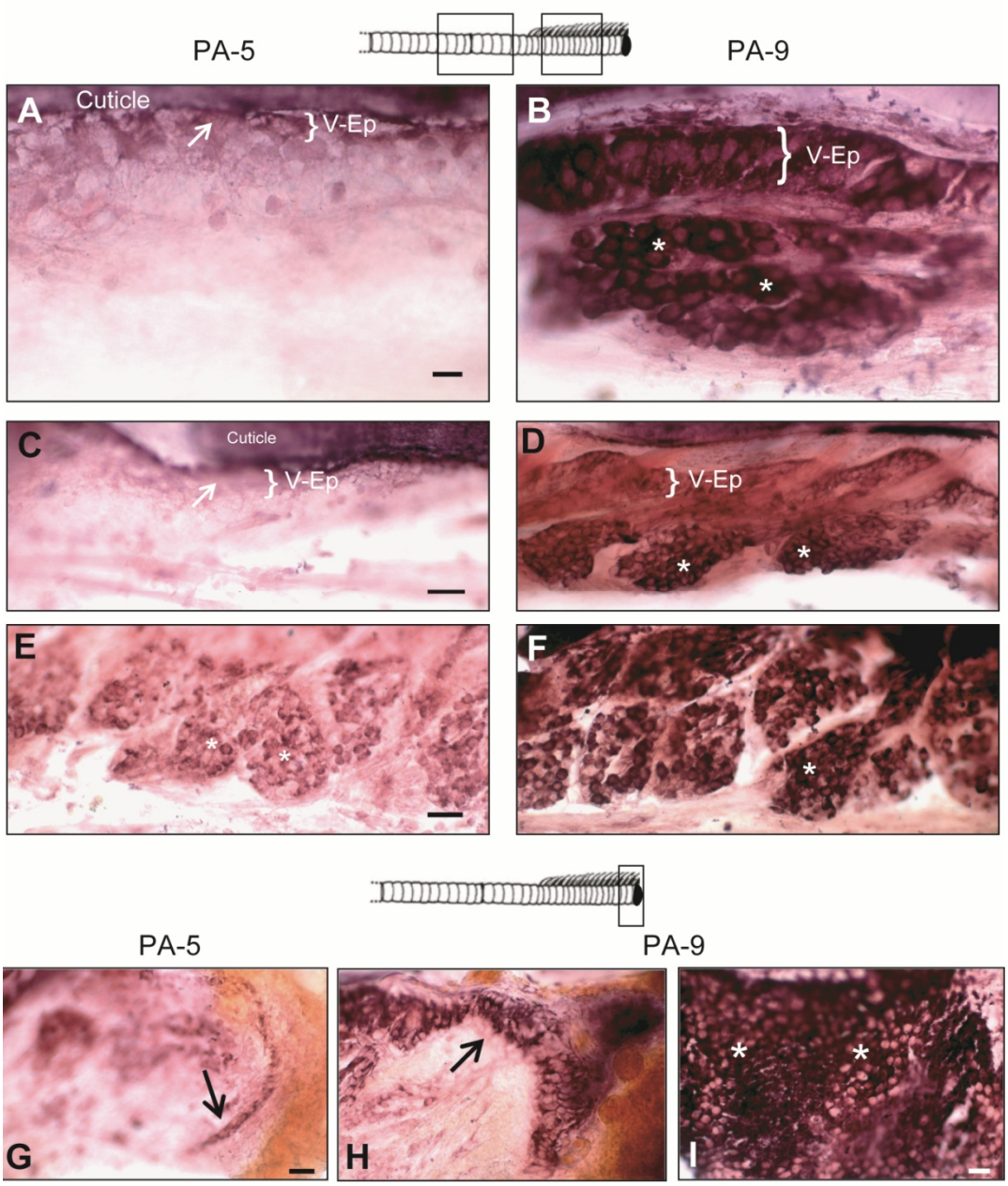

Figure 2-7 Ablation-induced *splash* labeling in antennular lateral flagella of intermolt animals.

Schematic drawing showing unilaterally-ablated lateral flagellum and areas examined at post-ablation days 5 and 9 (PA-5 and PA-9 respectively). **A**, **B**:Proximal PZ. **C**, **D**: Middle PZ. **E-F**: Distal PZ. **G-I**: Mature zone. **A** The proximal PZ at PA-5 showed faint intensity *splash* labeling in some ventral epithelial cells. The ORN clusters were not *splash*+. **B** The proximal PZ at PA-9 showed very intense *splash* labeling in the ventral epithelial cells and in numerous ORN clusters (asterisk). **C** Middle PZ at PA-5 did not show *splash* labeling in ventral epithelium (V-Ep) (arrow). **D** PA-9 V-Ep in middle region appeared to detach from the cuticle. Most if not all epithelial cells and ORN clusters (asterisks) had very intense *splash* labeling compared to PA-5.**E** ORN clusters inPA-5 distal PZ were labeled with *splash* (asterisks). There were many unlabeled ORNs within clusters containing labeled ORNs. **F** Distal PZ PA-9 showed very intense *splash* labeling in most of the epithelial cells and ORNs (asterisk). Similar to PA-5, some

ORNs were unlabeled. **G** At PA-5, the epithelium most proximal to the blastema had intense *splash* labeling. **H** At PA-9 and most proximal to the blastema, there were many epithelial cells with very intense *splash* labeling. **I** Lateral and mesial epithelial cells proximal to the blastema contained the most intense labeling and the greatest number of cells labeled with *splash* at PA-9 compared to PA-5. *Scale Bars* 50 µm (**A-D**), 20 µm (**E**, **F**), 20 µm (**G-I**)

Table 2-1 Median intensity rating for *splash* labeling in premolt and intermolt LF

	Premolt (N = 3)		**Intermolt (N = 3-5)**	
	Epithelium	**ORNs**	**Epithelium**	**ORNs**
pPZ	+++	*	++	*
mPZ	++	*	++	*
dPZ	++	+	++	+++
MZ	++	++	+++	+++

Symbols are as follows: not examined (*), no labeling (-), faint labeling (+), intense labeling (++), very intense labeling (+++). In intermolt animals, epithelial cells in the proximal, middle, and distal proliferation zone (pPZ, mPZ, dPZ) were intensely labeled with *splash*, and epithelial cells and ORNs in the mature zone (MZ) had very intense *splash* labeling. In premolt animals, epithelial cells in the pPZ, mPZ, dPZ, and MZ had intense *splash* labeling, and ORNs in the dPZ had faint *splash* labeling.

Table 2-2 Median intensity rating for *splash* labeling in ablated antennular lateral flagella of intermolt animals.

	P5 (N = 3)		P9 (N = 3)	
	Epithelium	**ORNs/ precursor**	**Epithelium**	**ORNs/ precursor**
pPZ	+	-	+++	+++
dPZ	++	++	+++	+++
Site of injury	++	*	+++	*

Symbols are as follows: not examined (*), no labeling (-), faint labeling (+), intense labeling (++), very intense labeling (+++). Post-ablation days 5 and 9 (PA-5 and PA-9 respectively). Epithelial cells showed faint intensity of *splash* labeling in PA-5 proximal proliferation zone (pPZ) and no *splash* labeling in ORN precursors. PA-9 epithelial cells and ORN precursors in pPZ and ORNs in dPZ had very intense *splash* labeling. Epithelial cells in the site of injury of PA-9 animals had very intense *splash* labeling, compared with PA-5 animals which had intense labeling.

CHAPTER 3: MECHANISMS UNDERLYING SPONTANEOUS AND ODOR-EVOKED CALCIUM RESPONSES IN OLFACTORY RECEPTOR NEURONS OF SPINY LOBSTERS, *PANULIRUS ARGUS*

Publication: This chapter is a manuscript that will be submitted to the journal *Chemical Senses*

Authors: Tizeta Tadesse*, Manfred Schmidt, and Charles D. Derby

Affiliation: Neuroscience Institute and Department of Biology, Georgia State University, Atlanta, GA

***Corresponding Author:** Tizeta Tadesse, Neuroscience Institute, Georgia State University, P.O. Box 5030, Atlanta, GA30302-5030USA. Email: ttadesse@gsu.edu FAX 404-413-5446

Running title: Calcium responses in olfactory neurons of spiny lobsters

Acknowledgements

We thank Dr. Juan Aggio for help with data analysis and statistics and Jessica Haulk for assistance with data organization. Anti-GluR1 antiserum was kindly provided by Dr. Timothy McClintock. Supported by NIH DC00312, GSU Dissertation Grant, GSU Brains & Behavior seed grant, and GSU Brains & Behavior fellowship to TT.

3.1 Abstract

Olfaction in the spiny lobster, *Panulirus argus*, and other decapod crustaceans is mediated by primary olfactory receptor neurons (ORNs) located in the olfactory sensilla, called aesthetascs, located on the lateral flagella of the antennules. Using calcium imaging of *in situ* ORNs, we examined mechanisms underlying odor-induced Ca^{2+} transients and spontaneous Ca^{2+} oscillations in ORN somata. Odor-induced Ca^{2+} transients were reduced in amplitude under low extracellular Ca^{2+} and abolished when blocking Co^{2+} sensitive Ca^{2+} channels. Manipulation of intracellular Ca^{2+} with thapsigargin reduced the amplitude and increased the repolarization time. Blocking tetrodotoxin (TTX) sensitive channels did not affect the mean amplitude of odor-activated Ca^{2+} transients. Spontaneous Ca^{2+} oscillations were reduced under low extracellular Ca^{2+} and abolished by blocking Co^{2+} sensitive Ca^{2+} channels. In some ORNs, the frequency of spontaneous Ca^{2+} oscillations increased under low extracellular Ca^{2+} possibly mediated by intracellular Ca^{2+} stores. Both thapsigarin and TTX reduced the amplitude and frequency of spontaneous oscillations. These data suggest that extracellular Ca^{2+} is the major source for odor-activated Ca^{2+} transients and spontaneous oscillations, intracellular Ca^{2+} stores also have some contribution, and the Ca^{2+} response are largely not due to TTX-sensitive channels such as voltage-gated Na+ channels associated with action potentials but instead may be associated with channels involved in olfactory transduction. Odor activated influx of Ca^{2+} and the contribution of intracellular stores is a common feature of ORNs; however there is a discrepancy in the effect of spiking activity on Ca^{2+} transients. The mechanisms for odor-induced Ca^{2+} transient increases and spontaneous oscillations in spiny lobster ORNs in general are similar to ORNs from other organisms.

Key words: olfactory, sensory neuron, calcium imaging, calcium oscillation

3.1 Introduction

Animals, including humans, detect, identify, and respond to chemicals in their environment using their olfactory system. Caribbean spiny lobsters, *Panulirus argus*, use olfactory receptor neurons (ORNs) in aesthetasc sensilla located on the antennular lateral flagellum (LF) to mediate discrimination of and orientation to food-related chemicals (Steullet et al., 2001, 2002; Horner et al., 2004). These ORNs also mediate behavioral responses to conspecific social and sexual chemical cues and signals (Horner et al., 2008; Shabani et al., 2008, 2009) and for odor associative learning and odor discrimination, making them an established model system for studying chemoreception (Ache, 2002, 2005).

The LF is composed of pseudosegments called annuli, each containing about 20 aesthetasc sensilla. ORNs are densely packed in the olfactory organ of spiny lobsters. There are ca. 300 ORNs per aesthetasc, ca. 20 aesthetascs per annulus, and ca. 100 aesthetasc-bearing annuli per lateral flagellum (Fig. 1A), making a total of ca. 1,200,000 ORNs per lobster. Odors permeate through the thin cuticle of the aesthetasc sensilla (Grünert and Ache, 1988; Derby et al., 1997) and bind to receptor sites on the dendritic membrane of ORNs to initiate odor transduction. Patch clamp electrophysiological recordings showed that there are at least two populations of ORNs based on spontaneous activity: some ORNs have spontaneous tonic activity (Michel et al., 1991), and others have spontaneous bursting activity (Bobkov and Ache, 2007). Spiny lobster ORNs can respond with an inositol 1, 4, 5-triphosphate (IP_3) mediated excitation or cyclic adenosine 5'-monophosphate (cAMP) mediated inhibition, suggesting the presence of dual transduction pathways in an individual ORN (Boekhoff et al., 1994).

Ca^{2+} ions play a crucial role in odor activation, modulation, and adaptation (Schild and Restrepo, 1998; Menini, 1999; Matthews and Reisert, 2003). For example, in odor transduction in ORNs of vertebrates, odors bind to G-protein (G_{olf}) coupled receptors that activate adenylyl cyclase leading to cyclic AMP or IP_3 formation. Second messengers activate cyclic-nucleotide-gated (CNG) channels causing influx of Ca^{2+}, and activation of somatic voltage-gated channels. The intracellular increase in Ca^{2+} lasts for several seconds (Zufall et al., 2000), surpassing the voltage change which lasts in seconds. In insects, olfactory receptors (Ors) have been shown to act as ionotropic receptors (IR) (Benton et al., 2009). In lobsters, odors activate G-protein coupled receptors (Xu et al., 1999; Xu and McClintock 1999)

and possibly ionotropic receptors. An ionotropic glutamate receptor subunit GluR1 homolog (OET07) that is specifically expressed in all ORNs (*Homarus americanus*: Hollins et al., 2003; Stepanyan et al., 2004, 2006; *P. argus*: Tadesse et al., 2011) may act as a co-receptor functionally related to Or83b expressed in ORNs in *Drosophila* (Corey et al., 2010). Evolutionary and gene expression studies of IR25a, a homolog of GluR1, showed a broad expression in numerous olfactory and gustatory neurons (Croset et al., 2010) supporting a model of an ionotropic co-receptor.

Odor-induced increases in intracellular Ca^{2+} occur in ORNs from humans (Restrepo et al., 1991), rodents (Restrepo et al., 1993), chicks (Jung et al., 2005), amphibians (Zufall et al., 1997; Leinders-Zufall et al., 1998), channel catfish (Restrepo and Teeter 1990), insects (Stengl 1994; Nakagawa-Inoue et al., 1998; Pezier et al., 2007), and spiny lobsters (Ukhanov et al., 2011). The main source for odor-induced increases in intracellular Ca^{2+} is from extracellular stores for ORNs of chicks (Jung et al., 2005), humans (Restrepo et al., 1993a), and rodents (Restrepo et al., 1993b; Takeuchi and Kurahashi 2003). In cats (Gomez et al., 2005) and amphibians (Zufall et al., 2000), extracellular and intracellular Ca^{2+} stores both contribute to odor-induced increases in intracellular Ca^{2+}. In addition, spontaneous Ca^{2+} oscillations occur in ORNs of spiny lobsters (Ukanov et al., 2011) and other neuronal cells (Gao et al., 1998; Parri and Crunelli 2003; Kawai et al., 2009).

In this study, mechanisms underlying odor-induced Ca^{2+} transients and spontaneous oscillations in Ca^{2+} were examined in ORNs of *P. argus* using Ca^{2+} imaging. We established Ca^{2+} imaging of spiny lobster ORNs in an *in vitro* 'slice' preparation developed in parallel with that of Ukhanov et al. (2011). This slice preparation has the advantage of maintaining the structural integrity of the LF compared to isolated cells, thus revealing the *in situ* properties of these cells. To elucidate the contribution of extracellular and intracellular Ca^{2+} on odor activated Ca^{2+} transients and Ca^{2+} oscillations, we reduced extracellular Ca^{2+}, blocked cobalt-sensitive Ca^{2+} channels, and blocked the sarco/endoplasmic Ca^{2+} -ATPase (SERCA) using thapsigargin. To determine whether the Ca^{2+} transients are a reflection of spiking activity or transduction events, we blocked TTX-sensitive Na^{+} channels. We show that the odor-induced transient increase in intracellular Ca^{2+} is predominantly mediated by influx of extracellular Ca^{2+}

but also to a lesser degree by release of intracellular Ca^{2+}. Spontaneous Ca^{2+} oscillations are mediated by both extracellular and intracellular Ca^{2+}. Blocking TTX-sensitive Na^{+} channels had no major effect on odor-induced Ca^{2+} transients, suggesting that the Ca^{2+} transients may reflect odor transduction events.

3.2 Methods

Animals

Young adult male and female Caribbean spiny lobsters (*Panulirus argus*) of 50-75 mm carapace length were collected near the Florida Keys Marine Laboratory and shipped to Georgia State University where they were held in 400-liter aquaria with re-circulated, filtered, and aerated artificial seawater (Instant Ocean™, Aquarium Systems Inc., Mentor, OH, USA) at 20-25ºC. Animals were maintained in a 12 hr: 12 hr light: dark cycle and fed shrimp or squid three times per week.

Chemicals

All chemicals are of > 99% purity and obtained from Sigma Aldrich (St. Louis, MO) unless otherwise noted.

Tissue preparation

Antennular lateral flagella (LF) were collected from intermolt spiny lobsters and immersed in *P. argus* saline (459 mM NaCl, 13.4 mM KCl, 13.6 mM $CaCl_2 \cdot 2H_2O$, 3 mM $MgCl_2 \cdot 6H_2O$, 14.1 mM Na_2SO_4, 9.8 mM HEPES, pH 7.4, 977 mOsmol). Guard sensilla were removed and two-annulus pieces were cut from the mature zone. These pieces of LF, which we call 'LF slices' (Fig. 3-1C), were immersed for 5 min in a solution consisting of 2 mL *P. argus* saline, 8 mg of L-cysteine, and 500 µL of 2.5 mg/ml papain, for enzymatic digestion. LF slices were rinsed in *P. argus* saline for 15-20 min on a shaker followed by desheathing of ORN clusters using forceps. Pilot data were collected using the following acetoxymethyl (AM) ester Ca^{2+} indicator dyes: Fluo-4 AM, Fluo-3 AM, Fluo-5F AM, and Oregon green BAPTA AM (OGB) (Molecular Probes, Invitrogen, Carlsbad, CA). All the Ca^{2+} indicator dyes showed

odor-induced Ca^{2+} transients however, OGB was selected for use in subsequent studies because it loaded the maximum number of ORNs and showed a robust response. 50 µg of OGB was dissolved in 45-50 µL Pluronic ® F127 with DMSO (Invitrogen, Carlsbad, CA). OGB was diluted to a final concentration of 50-60 µM, according to Stosiek et al. (2003) and Grewe et al. (2010), in *P. argus* saline in an Eppendorf tube. LF slices were transferred to the Eppendorf tube using forceps and placed on a horizontal shaker set at medium speed in the dark for 1 hr at room temperature. Loaded LF slices were rinsed in saline for 20 min then transferred into another dish containing saline until imaging.

Calcium imaging

LF slices were secured on a dish containing a layer of Sylgard® (Fig. 3-1C) and mounted on the stage of an upright epifluorescence microscope (Zeiss Axioplan 2, Jena, Germany) equipped with a 40 X water immersion objective with long working distance (Fig. 3-1E). LF slices were continuously perfused with *P. argus* saline at a rate of 3.0-3.6 ml/min for the duration of the experiment. Excitation light (320-680 nm) was provided by a monochromator (Polychrome V, Till Photonics, Munich, Germany), and fluorescent images (688 x 520 pixels and 2 x 2 binning) were captured with a fast CCD camera (Imago QE, Till Photonics). An experimental protocol was customized in Vision software that synchronized image acquisition with an external processor (Imaging System Controller), allowing us to control the stimulus onset and offset (Vision, Till Photonics). For Ca^{2+} signal quantification, a Region of Interest (ROI) was outlined for each OBG-loaded ORN soma, and the average pixel value of mean fluorescence intensity was calculated using Vision software, then transferred to Microsoft Excel (Redmond, WA) for further analysis.

Chemical preparation and delivery

Odorants were prepared in *P. argus* saline as described by Michel et al. (1991). Briefly, 2 g of TetraMarine (TetM) were mixed in 60 ml of *P. argus* saline for ~ 3 hr, centrifuged at 1400 x g for 20 min,

filtered, aliquoted, and stored at -20°C until used for each experiment. *P. argus* saline was used as a negative control. We constructed a multi-barrel stimulation pipette that consisted of a center suction channel (250 µm inner diameter) surrounded by 6 pressurized stimulus channels (100 µm inner diameter) (Fig. 3-1D). We used a picospritzer and two sets of solenoid valves to control the delivery of odorants. The suction channel was continuously open and closed briefly when a stimulus event was triggered. The triggering of an event by the imaging system opened the solenoid valve of a selected stimulus channel for 1s and simultaneously closed the suction channel to allow stimulus delivery. After 1s the stimulus solenoid valves closed and the suction valve opened. We designed an experimental flow-through chamber mounted on a microscope stage equipped with a water-immersion objective lens (Fig. 3-1E). The stimulating pipette was set on a micromanipulator and the LF slice preparation was secured onto the bottom of the flow-through chamber covered by a layer of Sylgard®. Visualization of the stimulus distribution by application of saline with food coloring or fluorescein to the AE showed that the stimulus reached the AE but not the ORN somata (Fig. 3-1F). To confirm visually that an odorant was delivered exclusively to the aesthetasc sensilla, we used a 1s-long pulse of saline with 0.001% of either fast green or fluorescein (Fig. 3-1F). Quantification of the mean fluorescence intensity of fluorescein at the AE and at the ORNs confirmed that the stimulus reached the AE and not the ORNs and it provides a measure of the time course of the odor stimulus at the AE (Fig. 3-1G).

Experiments

The goal of these experiments was to determine the effect of four treatments on the responses of ORNs to odorants. These four treatments were: 1) low calcium; 2) cobalt chloride; 3) thapsigargin; or 4) TTX. Each treatment was performed on at least 4 LF slices collected from at least 2 spiny lobsters. Each experiment consisted of three phases: pre-treatment, treatment, and post-treatment recovery. In each phase of each experiment, two odorants were tested: 1% TetM, and *P. argus* saline as a negative control. Each test lasted for ca. 80 s: a 15-s pre-stimulus time, a 0.6-1.0 s stimulus time (duration of solenoid

activation), and ca. 65-s post-stimulus time. For each 80-s test, 500 - 800 images were acquired at 100 ms / frame. The time between tests was 2 min. We also examined spontaneous Ca^{2+} oscillations by imaging LF slices and not stimulating AE (no-stimulation).

The four treatments were the following:

Treatment 1: Low calcium saline was prepared as follows: 459 mM NaCl, 13.4 mM KCl, 0.1 mM $CaCl_2 \cdot 2H_2O$, 3 mM $MgCl_2 \cdot 6H_2O$, 14.1 mM Na_2SO_4, 9.8 mM HEPES, pH 7.4. LF slices were bathed in low Ca^{2+} saline for 5 - 6 min and continuously bathed during testing. LF slices were bathed in normal saline for 6 min then continuously bathed during re-testing in saline.

Treatment 2: A 0.5 M stock of $CoCl_2 \cdot 6H_20$ (Co^{2+}) was prepared in *P. argus* saline. On the day of the experiment, 20 mM cobalt chloride was prepared and LF slices were bathed for approximately 3 min. LF slices were continuously bathed during testing, and then bathed in normal saline for 8–18 min before re-testing.

Treatment 3: A stock of 10 mM thapsigargin (Tocris Bioscience, Ellisville, MO) was prepared in normal saline and aliquots were stored at -20° C. Immediately before the experiment, an aliquot was thawed and diluted to 1 µM. LF slices were continuously bathed during testing in thapsigargin for 15-18 min. Post-treatment recovery phase was not conducted as thapsigargin is a known irreversible blocker.

Treatment 4: A 10 mM stock of tetrodotoxin citrate (TTX) (Tocris Bioscience) was prepared in normal saline and stored in -20° C until immediately before the experiment at which time it was diluted to a final concentration of 1 or 8 µM. LF slices were continuously bathed during testing in TTX for 5 min before testing. Recovery from treatment was allowed by bathing in normal saline for 8 min before retesting.

Data analysis

Spike2 software (Cambridge Electronic Design, Cambridge, England) was used for analyzing the mean fluorescence intensity. Two scripts were written to analyze odor-induced Ca^{2+} transients and

spontaneous Ca^{2+} oscillations. An ORN was considered to respond if an odor-induced fluorescence signal was greater than the response criterion (i.e. 2 standard deviations or more above the mean pre-stimulus level). Based on this, peak amplitude and 80% repolarization time (i.e., the time it takes the Ca^{2+} signal to return to 80% of the mean pre-stimulus level) were determined (Fig. 3-2E). Mean fluorescence intensity from the 'No stimulation' was used to determine the amplitude and frequency of spontaneous Ca^{2+} oscillations. A spontaneous event is defined as having two troughs and one peak that exceeds a preset threshold. This threshold filters out miniscule events and takes into account larger and visible peaks. The amplitude of each peak was calculated as Peak / Average of pre- and post-troughs. For each ORN, the amplitude, repolarization time, frequency, and amplitude of spontaneous oscillations were normalized to the respective values during the pre-treatment phase (set to 100%). SigmaPlot 8.0 (Systat Software Inc., San Jose, CA) was used to generate bar graphs showing median and interquartile range and representative time courses of Ca^{2+}. Illustrations of time courses of Ca^{2+} are presented as relative fluorescence changes from baseline ($\Delta F/F$). All statistical analyses were conducted using PASW Statistics 18 (SPSS Inc., Chicago, IL). Friedman's Two-Way Analysis of Variance by Ranks (ANOVA) and *post-hoc* analysis with Wilcoxon Signed Ranks Test and a Bonferroni correction were used. Final figures were generated using SigmaPlot.

3.4 Results

Calcium imaging of spiny lobster ORNs

Two paired-antennules make up the major chemosensory organ in decapod crustaceans (Derby, 2000). Each antennule has a lateral flagellum (LF) that houses specialized chemoreceptive aesthetasc sensilla. Each aesthetasc is innervated by the outer dendrites of ca. 300 bipolar olfactory receptor neurons (ORNs) (Fig. 3-1A). Immunocytochemical labeling of *P. argus* ORNs with an antibody against a ionotropic glutamate receptor subunit cloned from the American lobster, *Homarus americanus* (Hollins et al., 2003) (i.e., anti-GluR1), and counterstaining with Hoechst 33258, a nuclear marker, selectively labels

the somata (Fig. 3-1B) and inner dendritic segments of mature ORNs. For Ca^{2+} imaging of spiny lobster ORNs, we made LF slice preparations, each consisting of two aesthetasc-bearing annuli and maintaining the structural integrity of ORNs (Fig. 3-1C).

Fluorescence images of ORNs loaded with Oregon green BAPTA AM (OGB) showed numerous loaded ORNs (Fig. 3-1H) and showed a robust increase (grey to white) in somatic Ca^{2+} when stimulated with high KCl (460mM KCl and 13.4mM NaCl compared to the normal physiological saline 13.4mM KCl and 460mM NaCl). TetraMarine (TetM), a fish food mixture, was used as an odorant due to its ability to cause excitation in many ORNs (Michel et al. 1991) and cause a transient increase in somatic Ca^{2+} (Ukhanov et al., 2011). We stimulated AE with 1% TetM and also found a transient increase in somatic Ca^{2+}. Pseudocolor fluorescence images of OGB-loaded ORNs before stimulation with 1% TetM (Fig. 3-1J) and after stimulation (Fig. 3-1K) are shown for 4 ORNs. Time course for mean fluorescence of the 4 ORNs (Fig. 3-1L-O) showed a mean increase in somatic Ca^{2+} following stimulation with 1% TetM. Overall, this demonstrates the functionality of the Ca^{2+} imaging set-up for spiny lobster ORNs.

Odor-induced Ca^{2+} transients and spontaneous Ca^{2+} oscillations of ORNs

To examine the Ca^{2+} response to odor presentation in spiny lobster ORNs, OGB-loaded ORNs were imaged for 60 to 80-s and 800 images were acquired at 100 ms / frame. Each test consisted of a 15-s pre-stimulus time, a 1.0-s stimulus with 1% TetM, and ca. 65-s post-stimulus time, with a 2-min interval between tests. Stimulation of AE with 1% TetM caused a transient increase in mean fluorescence intensity which we call 'Ca^{2+} transient'. Time courses of Ca^{2+} transients for 2 ORNs are shown in response to 1% TetM (Fig. 3-2A, C) and a negative control saline (B, D) without the Ca^{2+} transient. Repeated stimulation of the same ORN with 1% TetM (Trials 1, 2 and 3) with a 2-min inter-trial interval showed reproducible Ca^{2+} transients (Fig. 3-2E-G). The quantification of odor-induced Ca^{2+} transients is illustrated in Fig. 3-2E (1-Baseline, 2-Peak, 3-Amplitude, and 4-Repolarization to 80%). If an odor-

induced fluorescence signal was greater than the response criterion (i.e. 2 standard deviations or more above the mean pre-stimulus level), then an ORN was considered to respond to an odor.

Mature ORNs showed one of two types of Ca^{2+} transients when stimulated with 1% TetM. Some ORNs had no spontaneous Ca^{2+}oscillations and responded to 1% TetM with a Ca^{2+} transient (Fig. 2H) and not to a negative control saline. Some spontaneously oscillating ORNs responded with an odor-induced Ca^{2+} transient (ORN 2 and 3 in Fig. 3-2I, J) and not to a negative control saline. In total, 67% of loaded ORNs responded to TetM (n = 214 ORNs, N = 3 lobsters, LF slices = 6). Spontaneous Ca^{2+}oscillations (Fig. 3-2K-M) were observed in 31.9% of ORNs (n = 86 ORNs, N = 3 lobsters, LF slices = 9) under normal physiological conditions with a mean frequency of 0.25 Hz (range 0.12 - 0.37) and mean peak amplitude of 5.26 $\Delta F/F$ (n = 21 ORNs, N = 2 lobsters, LF slices = 5). These data demonstrate that mature ORNs are heterogeneous in their normal Ca^{2+} state and in their responsiveness to odors.

Source of Ca^{2+} in odor-induced transients and spontaneous oscillations

To elucidate the underlying source of Ca^{2+} in odor-induced Ca^{2+} transients and spontaneous Ca^{2+} oscillations in ORN somata, we conducted four experiments. The first experiment addressed the contribution of extracellular [Ca^{2+}] by reducing [Ca^{2+}] in saline. The second experiment focused on the role of Ca^{2+} channels by application of blocking agent, cobalt. The third experiment blocked the sarco/endoplasmic Ca^{2+} - ATPase pump (SERCA) using thapsigargin thereby reducing Ca^{2+} in the endoplasmic reticulum that is available for release into the cytosol. Thus, this experiment determined the contribution of intracellular Ca^{2+} stores. The fourth experiment used TTX to determine if Ca^{2+} transients depend on action potentials and therefore reflect spiking activity of ORNs in response to odor stimulation.

Effect of reducing extracellular [Ca^{2+}] on odor-induced transients and spontaneous oscillations

To assess the contribution of extracellular [Ca^{2+}] on odor-induced somatic Ca^{2+} transients, we reduced [Ca^{2+}] in saline to 0.1 mM from the normal physiological concentration of 13.6 mM. An

example of ORNs at the peak of the odor-induced response in normal saline and in low extracellular [Ca^{2+}] is shown in Fig. 3-3A. Many ORN somata show reduced relative fluorescence intensity in low extracellular [Ca^{2+}] compared with pre-treatment. Representative Ca^{2+} transients illustrate either a reduction (Fig. 3-3B) or elimination of odor-induced response (Fig. 3-3C) in low extracellular [Ca^{2+}] followed by partial recovery in post-treatment. We found a significant effect of low extracellular [Ca^{2+}] on the peak amplitude (Friedman's ANOVA: (χ^2 (2) = 73.145, $P< 0.05$) and on the repolarization time (χ^2 (2) = 60.733, $P< 0.05$) of odor-induced response (Fig. 3C) (n = 44 ORNs, N = 3 lobsters, LF slices = 7). Low extracellular Ca^{2+} significantly reduced the peak amplitude compared with pre-treatment (*post-hoc* analysis using Wilcoxon Signed Ranks Test with a Bonferroni correction significance level $P \leq 0.017$, Z = -6.037, $P<0.001$). The response partially recovered, since the post-treatment peak amplitude was greater than during treatment (Z = -5.540, $P<0.001$), and less than pre-treatment (Z = -4.995, $P<0.001$). There was also a significant decrease in repolarization time under low extracellular [Ca^{2+}] compared with pre-treatment (Z = -6.037, $P<0.001$). There was complete recovery, since the post-treatment repolarization time was greater than during treatment (Z = -5.527, $P<0.001$) and similar to pre-treatment (Z = -1.449, $P = 0.147$). These data demonstrate that extracellular Ca^{2+} is critical for odor-induced somatic response, since there are significant effects on the magnitude and the termination of the Ca^{2+} transients in low extracellular [Ca^{2+}].

To determine whether extracellular [Ca^{2+}] contributes to spontaneous Ca^{2+} oscillations, we examined ORNs that were not stimulated with odorants (Fig. 3-3D-H). Representative traces illustrate a decrease in spontaneous Ca^{2+} oscillations in low extracellular [Ca^{2+}] (Fig. 3-3D, E). We found that low extracellular [Ca^{2+}] significantly affected the peak amplitude (Friedman's ANOVA: χ^2 (2) = 23.333, $P<0.05$) and frequency (Friedman's ANOVA: χ^2 (2) = 24.400, $P<0.05$) of spontaneous Ca^{2+} oscillations (n = 15 ORNs, N = 2 lobsters, LF slices = 5). *Post hoc* analysis shows that both the peak amplitude (Z = -3.527, $P< 0.001$) and frequency (Z = -3.527, $P<0.001$) were significantly reduced under low extracellular [Ca^{2+}] and were significantly increased in post-treatment recovery (Z = -3.408, $P = 0.001$) (Z = -3.295, *P*

= 0.001), respectively (Fig. 3F). These data suggest that extracellular [Ca^{2+}] contributes to spontaneous Ca^{2+} oscillations in ORN somata.

Low extracellular [Ca^{2+}] increased the frequency of spontaneous Ca^{2+} oscillations in a sub-population of ORNs compared to saline (Fig. 3-3G). Quantification of the spontaneous frequency shows a significant effect of low extracellular [Ca^{2+}] (Friedman's ANOVA: (χ^2 (2) = 6.870, P< 0.05) (Fig. 3-3H). *Post hoc* analysis shows the difference in frequency is between pre-treatment and low extracellular [Ca^{2+}] (T =-1.417, P= 0.014) and not in post-treatment recovery (T= -.333, P= 0.564) or pre-treatment to post-treatment recovery (T= 1.083, P= 0.061). These data demonstrate that reduction in extracellular [Ca^{2+}] differentially affects ORNs by inducing somatic Ca^{2+}oscillations in some ORNs but reducing or eliminating them in others.

Co^{2+} blocked both odor-induced [Ca^{2+}] transients and spontaneous oscillations.

To confirm that Ca^{2+} influx through voltage-gated Ca^{2+} channels mediates the odor-induced somatic Ca^{2+} transients, we used 20 mM cobalt chloride as a blocker. Representative time courses show Ca^{2+} transients are abolished with Co^{2+} treatment and partially recovered when returned to normal saline (Fig. 3-4A, B). Quantification of the Ca^{2+} transients also showed that Co^{2+} abolished odor-induced Ca^{2+} response by significantly reducing the peak amplitude (Friedman's ANOVA: (χ^2 (2) = 96.547, P<0.05) and repolarization time (χ^2 (2) = 77.310, P< 0.05) (n = 51 ORNs, N = 2 lobsters, LF slices = 5) (Fig. 3-4C). *Post-hoc* analysis with Wilcoxon Signed Ranks Test and a Bonferroni correction (significance level α = 0.017) showed a significant reduction in peak amplitude and repolarization time, respectively (Z = -7.141, P<0.01) (Z = -7.141, P<0.01), between pre-treatment and Co^{2+} treatment. There was an increase in peak amplitude and repolarization time (Z = 6.031, P<0.01) (Z = -6.031, P<0.01) between Co^{2+} and post-treatment recovery. There was also a significant difference between pre-treatment and recovery for both peak amplitude and repolarization time (Z = 5.727, P<0.01) (Z = 2.524, P = 0.012), suggesting that the

response partially recovered. This suggests that odor-induced somatic Ca^{2+} transients are due to Ca^{2+} influx through Co^{2+}-sensitive Ca^{2+} channels.

Co^{2+} treatment also abolished spontaneous Ca^{2+} oscillations (Fig. 3-4D-F). There was a significant effect on the peak amplitude (Friedman's ANOVA: (χ^2 (2) = 35.707, $P < 0.05$) and spontaneous frequency (χ^2 (2) = 31.760, $P < 0.05$) (n = 20 ORNs, N = 2 lobsters, LF slices = 5). Co^{2+} treatment significantly reduced both the peak amplitude (Z = -4.472, $P<0.001$) and spontaneous frequency (Z = -4.472, $P<0.001$). Responses partially recovered, since responses in post-treatment were higher than during treatment (amplitude: Z = -3.408, $P< 0.001$; frequency: Z = -3.408, $P< 0.001$) but lower than in pre-treatment (amplitude: Z = -3.889, $P<0.001$; frequency: Z = -3.216, $P = 0.01$). These data suggest that Ca^{2+} influx through Co^{2+} sensitive Ca^{2+} channels is essential for spontaneous somatic oscillations.

Thapsigargin affected odor-induced Ca^{2+} transients and spontaneous oscillations

Intracellular Ca^{2+} stores contribute to odor-induced increases in Ca^{2+} in ORNs of other species (Zufall et al., 2000; Gomez et al., 2005). To elucidate the role of intracellular Ca^{2+} on odor-induced Ca^{2+} transients and spontaneous Ca^{2+}oscillations in spiny lobster ORN, we used thapsigargin, a known irreversible blocker of sarco/endoplasmic reticulum Ca^{2+} ATPase pump (SERCA). Blocking SERCA depletes Ca^{2+} from the endoplasmic reticulum thereby reducing its availability for release into the cytosol. Thapsigargin had different effects on different ORNs. Representative time courses of Ca^{2+} in ORNs during thapsigargin treatment show examples of a decrease in the amplitude (Fig. 5A) and an increase in the amplitude and repolarization time (Fig. 3-5B). Quantifications also show that 1 µM thapsigargin significantly reduced the peak amplitude (Wilcoxon Signed Ranks Test, Z = -5.214, $P<0.001$) of the odor-induced Ca^{2+} response (Fig. 3-5C). It also increased the repolarization time of the odor-induced Ca^{2+} response (Z = -3.901, $P<0.001$) (n = 109 ORNs, N = 2 lobsters, LF slices = 5). This suggests that intracellular Ca^{2+} contributes to the rise and termination of odor-induced Ca^{2+} transients. Thapsigargin

significantly reduced the spontaneous frequency (Z = -2.756, P = 0.006) and peak amplitude (Z = -2.992, P = 0.003) (Fig. 3-5D- F) (n = 12 ORNs, N = 2 lobsters, LF slices = 4) of spontaneous Ca^{2+} oscillations. These data suggest that intracellular Ca^{2+} contributes to the spontaneous Ca^{2+}oscillations.

Blocking TTX-sensitive Na^+ channels does not block Ca^{2+} transients

Previous studies using electrophysiological recordings showed that spiny lobster ORNs have action potentials mediated by voltage-gated Na^+ and K^+ currents (McClintock and Ache 1989; Schmiedel-Jakob et al., 1989). Applying TTX to the somatic regions of these cells blocked production of action potentials, though application of TTX to the dendritic region of these cells did not (McClintock and Ache 1989; Schmiedel-Jakob et al., 1989). Simultaneous recording with patch-clamping and Ca^{2+} imaging from ORNs of spiny lobsters showed a correlation between odor-induced spiking activity and Ca^{2+} transients. There was also a correlation between spontaneous bursts of action potentials with spontaneous Ca^{2+} oscillations (Ukhanov et al., 2011). In our experiments, to determine the contribution of spiking activity on the Ca^{2+} response, we used TTX to block TTX-sensitive Na^+ channels. Figure 6A and B shows the effect of TTX on the time courses of odor-activated Ca^{2+} transients for two typical ORNs. In both cases, the odor-activated Ca^{2+} transient is not noticeably reduced by TTX treatment. However, a decrease in amplitude is observed during post-treatment recovery. Analysis of the effect of TTX on a population of 95 ORNs provides quantitative statistical support for the conclusion that TTX does not block odor-activated Ca^{2+} responses (Fig. 3-6C). Comparison of pre-treatment, TTX treatment, and post-treatment recovery shows a significant effect on the peak amplitude (Friedman's ANOVA: χ^2 (2) = 27.937, P< 0.05) and repolarization time (χ^2 (2) = 24.897, P< 0.05) (n = 95 ORNs, N = 2 lobsters, LF slices = 6) on odor induced Ca^{2+} transients (Fig. 3-6C). However, comparison of TTX treatment to pre-treatment control shows no significant difference in the peak amplitude (Z = -0.082, P = 0.935) or repolarization time (Z = 2.395, P = 0.017). There was a significant reduction in the peak amplitude between TTX and post-treatment recovery (Z = -3.708, P<0.001) and pre-treatment to post-treatment (Z

= 4.510, $P<0.001$). There was a significant increase in repolarization time between pre-treatment to post-treatment recovery (Z = -5.735, $P<0.001$), but no difference between TTX to post-treatment recovery (Z = -2.183, $P = 0.029$). To eliminate the possibility that TTX requires longer incubation time, we incubated for 8 min at 1 μM TTX and for 5 min at 8 μM TTX. In both cases, the Ca^{2+} transients were not abolished, suggesting that duration of treatment or concentration were not factors causing the lack of TTX's effect on the mean amplitude and repolarization time of the Ca^{2+} transients. These data demonstrate that TTX did not affect the mean amplitude and repolarization time for odor-induced somatic Ca^{2+} transients.

We compared the frequency distributions of odor-induced response in normal saline and in TTX for the peak amplitude (Fig. 3-6D) and repolarization time (Fig. 3-6E). A Two-sample Kolmogorov-Smirnov Test showed a significant difference in both peak amplitude (Z = 1.577, $P = 0.014$) and repolarization time (Z = 1.414, $P = 0.037$), with the responses in TTX having broader frequency distributions in the response amplitude and repolarization time compared than the pre- or post-treatment. These data demonstrate that TTX causes some ORNs to increase and other ORNs to decrease the amplitude and repolarization time of odor-induced Ca^{2+} responses. Taken together, our data suggests heterogeneity in odor-induced response of ORNs in spiny lobsters.

We examined the effect of TTX on spontaneous Ca^{2+} oscillations. Figure 6F shows the results for a typical ORN, with a reduction in the amplitude and frequency during TTX treatment. Analysis of the effect of TTX on 14 spontaneously oscillating ORNs, unlike odor-induced response, showed statistical support for a TTX-mediated reduction of spontaneous Ca^{2+} oscillations (Fig. 3-6G). Comparison of pre-treatment, TTX treatment, and post-treatment recovery showed a significant difference in peak amplitude (Friedman's ANOVA: (χ^2 (2) = 19.018, $P< 0.05$) and spontaneous frequency (χ^2 (2) = 11.382, $P< 0.05$) (n = 14 ORNs, N = 2 lobsters, LF slices = 4) (Fig. 3-6E). *Post-hoc* analysis with Wilcoxon Signed Ranks Test and a Bonferroni correction (significance level $p < 0.017$) for both amplitude and frequency of spontaneous oscillations showed a significant reduction between pre-treatment and treatment (Z = -3.299, $P = 0.001$, Z = -2.419, $P = 0.016$, respectively). There was also a difference between pre-treatment and post-treatment in the peak amplitude (Z = -2.919, $P = 0.004$). All other comparisons showed no

significant difference (see Fig. 3-6 legend). These data show that TTX reduced spontaneous Ca^{2+} oscillations but did not abolish them. This suggests that TTX-sensitive Na^{+} channels are necessary for some of the spontaneous Ca^{2+} oscillations.

3.5 Discussion

This study examined the roles of extracellular and intracellular Ca^{2+} in odor-induced Ca^{2+} transient responses and in spontaneous Ca^{2+} oscillations of spiny lobster ORNs using calcium imaging. We found that odor-induced Ca^{2+} transient responses and spontaneous Ca^{2+} oscillations in ORN somata are primarily mediated by an influx of extracellular Ca^{2+} through Co^{2+} -sensitive Ca^{2+} channels, but that intracellular Ca^{2+} stores also have some contribution. These odor-induced Ca^{2+} transients occur in the presence of TTX and are thus probably independent of TTX-sensitive Na^{+} channels, suggesting that either these Ca^{2+} responses may be a reflection of receptor potentials or other signal transduction related events. A subset of ORNs has Ca^{2+} oscillations that appear only in low extracellular Ca^{2+}, and these may be mediated by intracellular Ca^{2+} stores.

Ca^{2+} influx through Co^{2+} sensitive Ca^{2+} channels mediates Ca^{2+} transients

We show odor-induced increases in intracellular Ca^{2+}in ORNs of *P. argus* (Fig. 3-2). Our data also demonstrate that a low extracellular [Ca^{2+}] significantly reduced odor-induced Ca^{2+} transients in spiny lobster ORNs (Fig. 3-3). This has also been observed in ORNs of catfish (see Schild and Restrepo 1998 for review), rats (Tareilus et al., 1995), and humans (Restrepo et al., 1993). Blocking Co^{2+} -sensitive Ca^{2+} channels abolished odor-induced Ca^{2+} transients in spiny lobster ORNs (Fig. 3-4). In channel catfish, blocking L-type Ca^{2+}channels abolished the Ca^{2+} rise following odor activation (Restrepo and Teeter 1990). Collectively, these results demonstrate the central role of an influx of Ca^{2+} in the odor activation of ORNs in animals in general.

Odor-activated increases in intracellular Ca^{2+} may not arise solely from Ca^{2+} in the extracellular environment but also from intracellular stores as previously demonstrated in salamanders (Zufall et al., 2000). Ca^{2+} is released from the endoplasmic reticulum through ryanodine receptors and inositol triphosphate receptors ($InsP_3$) (Murmu et al., 2010) and restored by the sarco/endoplasmic Ca^{2+} - ATPase (SERCA). A SERCA homolog has been identified in the antennule of *P. argus* (Mandal et al., 2009). To elucidate the contribution of intracellular Ca^{2+} stores to odor-induced Ca^{2+} transients in spiny lobster ORNs, we blocked the SERCA pump using thapsigargin, thus preventing the replenishment of the endoplasmic reticulum with Ca^{2+} (Zufall et al., 2000). Thapsigargin reduced the amplitude and increased the duration of odor-induced Ca^{2+} transients (Fig. 3-5). Based on our data, we hypothesize that the release of intracellular Ca^{2+} may be through ryanodine receptors or $InsP_3$ receptors from the endoplasmic reticulum similar to that in insect ORNs (Murmu et al., 2010).

Spontaneous Ca^{2+} oscillations

Spiny lobsters have at least two types of ORNs based on the nature of their spontaneous activity. Some ORNs have spontaneous bursts of activity and others have tonic spiking activity (Michel et al., 1991; Bobkov and Ache 2007; Ukhanov et al., 2011). Spontaneous bursts were correlated with Ca^{2+} oscillations (Ukhanov et al., 2011). In our study, we intended to understand the mechanisms behind spontaneous Ca^{2+} oscillations. Our data demonstrate that spontaneous Ca^{2+} oscillations in most ORNs were significantly reduced in peak amplitude and frequency in low extracellular Ca^{2+} (Fig. 3-3) and abolished in Co^{2+} treatment (Fig. 3-4), suggesting that extracellular Ca^{2+} is the primary source for spontaneous Ca^{2+} oscillations. Intracellular stores also contribute to spontaneous Ca^{2+} oscillations, as manipulation of the SERCA pump significantly reduced the peak amplitude and frequency of spontaneous Ca^{2+} oscillations (Fig. 3-5). Interestingly, application of TTX reduced the peak amplitude and frequency of spontaneous oscillations (Fig. 3-6) but did not completely abolish them. Because TTX is known to block voltage-gated Na^+ channels and the production of action potentials in spiny lobster ORNs

(McClintock and Ache 1989; Schmiedel-Jakob et al., 1989), it appears that these channels, and thus spiking activity, is not necessary for spontaneous oscillations of Ca^{2+} levels in these cells. This runs counter to the expectation based on a correlation between Ca^{2+} oscillations and spiking responses in spiny lobster ORNs (Ukhanov et al., 2011). Taken together, these data suggests that influx of extracellular Ca^{2+} through Ca^{2+} channels is the primary source for spontaneous Ca^{2+} oscillations.

Lastly, low extracellular Ca^{2+} induced Ca^{2+} oscillations in a subset of ORNs (Fig. 3-3G). This may result from release of Ca^{2+} from intracellular stores through InP_3 receptors as observed in astrocytes (Zanotti and Charles, 1997) or through ryanodine receptors. Further experiments in conjunction with manipulations of intracellular stores of Ca^{2+} are necessary to understand this phenomenon. Possible mechanisms for spontaneous Ca^{2+} oscillations include Ca^{2+} release from intracellular stores, such as endoplasmic reticulum, or influx of extracellular Ca^{2+} through Ca^{2+} channels.

Ca^{2+} transients are independent of TTX-sensitive Na^{+} channels

Spiny lobster ORNs respond to odors with action potentials that are mediated by typical TTX-sensitive Na^{+} channels (Schmiedel-Jakob et al., 1989; McClintock and Ache 1989). Odor-induced spiking activity was recently correlated with Ca^{2+} transients using patch-clamping recordings and Ca^{2+} imaging (Ukhanov et al., 2011). In our study, however, application of TTX did not abolish odor-activated Ca^{2+} transients. This lack of effect was not due to TTX treatment not reaching the somata due to the fact that other effects were observed. The reduction in amplitude and frequency of spontaneous oscillations in addition to the broadening of the frequency distribution in odor-induced response measurements: peak amplitude and repolarization time during TTX treatment suggests that TTX has an effect on ORNs.

There are at least two possible explanations for the presence of Ca^{2+} transients during TTX treatment. Firstly, odor activated Ca^{2+} transients may be a reflection of odor transduction rather than spike generation. Using odor transduction model for ORNs based on results from *H. americanus* and *P. argus*, we know that odors activate G-proteins (Gαq and Gβ) that associate with phospholipase C-β (Xu

and McClintock 1999; Xu et al., 1999) to mediate synthesis of the 2nd messenger inositol 1,4,5-triphosphate (IP_3) (Fadool and Ache, 1992; Boekhoff et al., 1994). IP_3 activates cyclic nucleotide gated non-selective cation (CNG) channels, which causes an influx of Na^+ and Ca^{2+}. Ca^{2+} activated Cl^- channels depolarize the cell further, activating somatic voltage-gated Na^+ and Ca^{2+} channels, which further depolarize the cell and result in spiking activity in the axon. One hypothesis is that the Ca^{2+} transients occur prior to the activation of TTX-sensitive Na^+ channels; therefore, blocking these channels will not have a major effect.

Secondly, spike generation may predominantly be driven by Ca^{2+} currents and not Na^+ currents. Although in ORNs of many species including *P. argus*, Na^+ currents are responsible for spike generation, it is possible that Ca^{2+} currents may also contribute to spike generation similar to ORNs of salamanders and rats. In salamander ORNs, Co^{2+} and not TTX blocked a transient inward current (Trotier, 1986), and later Kawai et al. (2009) demonstrated that the spike generation was due to Ca^{2+} currents. T-type Ca^{2+} channels are responsible for the Ca^{2+} transients in ORNs of rats (Gautam et al., 2007a) and pigs (Gautam et al., 2007b). In rat ORNs, T-type Ca^{2+} channels mediate propagation of receptor potentials from cilia to dendritic knob to soma. Replacing extracellular Na^+ had no effect on Ca^{2+} transients (Gautam et al., 2007a), suggesting that Na^+ is not necessary to generate spikes in ORNs. It is also possible that some *P. argus* ORNs express TTX-insensitive Na^+ channels that will not be affected; however, it does not account for the number of ORNs that still had Ca^{2+} transients in TTX (Fig. 3-6). There may also be additional effects of TTX on other channels that we are unaware of.

3.6 References

Ache, B.W. 2002. Crustaceans as animal models for olfactory research. In: K. Wiese, editor. Crustacean experimental systems in neurobiology. Springer: Berlin Press. p.189-199.

Ache BW, Young JM. 2005. Olfaction: diverse species, conserved principles. Neuron. 48:417-430.

Benton R, VanniceKS, Gomez-Diaz C, Vosshall LB. 2009. Variant ionotropic glutamate receptors as chemosensory receptors in *Drosophila*. Cell. 136:149-162.

Boekhoff I, Michel WC, Breer H, Ache BW. 1994. Single odors differentially stimulate dual second messenger pathways in lobster olfactory receptor cells.J Neurosci. 14:3304-3309.

Bobkov YV, Ache BW. 2007. Intrinsically bursting olfactory receptor neurons. J Neurophysiol. 97:1052-1057.

Corey EA, Bobkov Y, Ache BW. 2010. Molecular characterization and localization of olfactory-specific ionotropic glutamate receptors in lobster olfactory receptor neurons. Chem Senses 3: P157.

Corey EA, Bobkov Y, Ukhanov K, Ache BW. 2012. Characterization and expression of lobster olfactory variants of ionotropic glutamate receptors. Chem Senses P209.

Croset V, Rytz R, Cummins SF, Budd A, Brawand D, Kaessmann H, Gibson TJ, Benton R. 2010. Ancient protostome origin of chemosensory ionotropic glutamate receptors and the evolution of insect taste and olfaction. PLoS Genet. 6: e1001064.

Derby CD, Cate HS, Gentilcore LR. 1997. Perireception in olfaction: molecular weight sieving by aesthetasc sensillar cuticle determines odorant access to receptor sites in the Caribbean spiny lobster *Panulirus argus*. J. Exp. Biol. 200: 2073-2081.

Fadool DA, Ache BW. 1992. Plasma membrane inositol 1,4,5-trisphosphate-activated channels mediate signal transduction in lobster olfactory receptor neurons.Neuron. 9:907-918.

Gao ZY, Chen M, Collins HW, Matschinsky FM, Lee VM, Wolf BA. 1998. Mechanisms of spontaneous cytosolic Ca^{2+} transients in differentiated human neuronal cells. Eur J Neurosci. 10:2416-2425.

Gautam SH, Otsuguro KI, Ito S, Saito T, Habara Y. 2007a. T-type Ca^{2+} channels mediate propagation of odor-induced Ca^{2+} transients in rat olfactory receptor neurons. Neuroscience. 144:702-713.

Gautam SH, Otsuguro K, Ito S, Saito T, Habara Y. 2007b. T-type Ca^{2+} channels contribute to IBMX/forskolin- and K^{+}-induced Ca^{2+} transients in porcine olfactory receptor neurons. Neurosci Res. 57:129-139.

Grewe BF, Langer D, Kasper H, Kampa BM, Helmchen F. 2010. High-speed in vivo calcium imaging reveals neuronal network activity with near-millisecond precision. Nat Methods. 7:399-405.

Grünert U, Ache BW. 1988. Ultrastructure of the aesthetasc (olfactory) sensilla of the spiny lobster *Panulirus argus.* Cell Tiss Res 251:95-103.

Hollins B, Hardin D, Gimelbrant AA, McClintock TS. 2003. Olfactory-enriched transcripts are cell-specific markers in the lobster olfactory organ. J Comp Neurol 455:125-138.

Horner AJ, Weissburg MJ, Derby CD. 2004. Dual antennular chemosensory pathways can mediate orientation by Caribbean spiny lobsters in naturalistic flow conditions. J Exp Biol 207:3785-3796.

Horner AJ, Weissburg MJ, Derby CD. 2008. The olfactory pathway mediates sheltering behavior of Caribbean spiny lobsters, *Panulirus argus*, to conspecific urine signals. J Comp Physiol A 194:243-253.

Jung Y, Wirkus E, Amendola D, Gomez G. 2005. Characteristics of odorant elicited calcium fluxes in acutely-isolated chick olfactory neurons. J Comp Physiol A. 191:511-520.

Kawai T, Abe H, Wakabayashi K, Oka Y. 2009.Calcium oscillations in the olfactory nonsensory cells of the goldfish, *Carassius auratus*. Biochim Biophys Acta.1790:1681-1688.

Leinders-Zufall T, Greer CA, Shepherd GM, Zufall F. 1998. Imaging odor-induced calcium transients in single olfactory cilia: specificity of activation and role in transduction. J Neurosci. 18:5630-5639.

Leinders-Zufall T Greer CA, Shepherd GM, Zufall F.1998. Visualizing odor detection in olfactory cilia by calcium imaging. Ann N Y Acad Sci. 855:205-207.

Mandal A, Arunachalam SC, Meleshkevitch EA, Mandal PK, Boudko DY, Ahearn GA. 2009. Cloning of sarco-endoplasmic reticulum Ca^{2+-}ATPase (SERCA) from Caribbean spiny lobster *Panulirus argus*. J Comp Physiol B. 179:205-214.

Matthews HR, Reisert J. 2003. Calcium, the two-faced messenger of olfactory transduction and adaptation. Curr Opin Neurobiol. 13:469-475.

McClintock TS, Ache BW 1989. Ionic currents and ion channels of lobster olfactory receptor neurons. J Neurophysiol. 94: 1085-1099.

Menini A.1999. Calcium signaling and regulation in olfactory neurons. Curr Opin Neurobiol. 9:419-426.

Michel WC, McClintock TS, Ache BW. 1991. Inhibition of olfactory receptor cells by and odor-activated potassium conductance. J Neurophysiol. 65:446-453.

Murmu MS, Stinnakre J, Martin JR. 2010. Presynaptic Ca^{2+} stores contribute to odor-induced responses in *Drosophila* olfactory receptor neurons. J Exp Biol. 213:4163-4173.

NakagawaInoueA, KawaharaS, KirinoY, SekiguchiT. 1998. Odorant-evoked increase in cytosolic free calcium in cultured antennal neurons of blowflies.Zool Sci 15*:*661–666*.*

Parri HR, Crunelli V. 2003. The role of Ca^{2+} in the generation of spontaneous astrocytic Ca^{2+} oscillations. Neuroscience. 120:979-992.

Restrepo D, Teeter JH. 1990. Olfactory neurons exhibit heterogeneity in depolarization-induced calcium changes. Am J Physiol. 258:1051-1061.

Restrepo D, Okada Y, Teeter JH, Lowry LD, Cowart B, Brand JG. 1993a. Human olfactory neurons respond to odor stimuli with an increase in cytoplasmic Ca^{2+}. Biophys J. 64:1961-1966.

Restrepo D, Okada Y, Teeter JH. 1993b. Odorant-regulated Ca^{2+} gradients in rat olfactory neurons. J Gen Physiol. 102:907-924.

Schild D, Restrepo D. 1998. Transduction mechanisms in vertebrate olfactory receptor cells. Physiol Rev. 78:429-466.

Schmiedel-Jakob I, Anderson PAV, Ache BW. 1989. Whole cell recording from lobster olfactory receptor cells: responses to current and odor stimulation. J Neurophysiol. 61: 994-1000.

Schmidt M, Tadesse T, Derby CD. 2010. Calcium imaging of response properties of olfactory receptor neurons of spiny lobsters, *Panulirus argus*. Chem Senses 5:P159.

Shabani S, Kamio M, Derby CD. 2008. Spiny lobsters detect conspecific blood-borne alarm cues exclusively through olfactory sensilla. J Exp Biol 211:2600-2608.

Shabani S, Kamio M, Derby CD. 2009. Spiny lobsters use urine-borne olfactory signaling and physical aggressive behaviors to influence social status of conspecifics. J Exp Biol 212:2464-2474.

Steullet P, Dudar O, Flavus T, Zhou M, Derby CD. 2001. Selective ablation of antennular sensilla on the Caribbean spiny lobster *Panulirus argus* suggests that dual antennular chemosensory pathways mediate odorant activation of searching and localization of food. J Exp Biol 204:4259-4269.

Steullet P, Krützfeldt DR, Hamidani G, Flavus T, Ngo V, Derby CD. 2002. Dual antennular chemosensory pathways mediate odor-associative learning and odor discrimination in the Caribbean spiny lobster *Panulirus argus*. J Exp Biol 205:851-867.

Stepanyan R, Hollins B, Brock SE, McClintock TS. 2004. Primary culture of lobster (*Homarus americanus*) olfactory sensory neurons. Chem Senses 29:179-187.

Stepanyan R, Day K, Urban J, Hardin DL, Shetty RS, Derby CD, Ache BW, McClintock TS. 2006. Gene expression and specificity in the mature zone of the lobster olfactory organ. Physiol Genom 25:224-233.

Stosiek C, Garaschuk O, Holthoff K, Konnerth A. 2003. *In vivo* two-photon calcium imaging of neuronal networks. Proc Natl Acad Sci U S A. 100:7319-7324.

Tadesse T, Schmidt M, Derby CD. 2011. Calcium imaging of olfactory receptor neurons in the spiny lobster, *Panulirus argus*. 573.01/CC5. Neuroscience Meeting Planner. Washington, DC: Society for Neuroscience. Online.

Takeuchi H, Kurahashi T. 2003. Identification of second messenger mediating signal transduction in the olfactory receptor cell.J Gen Physiol.122:557-567.

Trotier D.1986. A patch-clamp analysis of membrane currents in salamander olfactory receptor cells. Pflügers Arch. 407: 589-595.

Ukhanov K, Bobkov Y, Ache BW. 2011. Imaging ensemble activity in arthropod olfactory receptor neurons in situ. Cell Calcium. 49:100-107.

Xu F, McClintock TS. 1999. A lobster phospholipase C-β that associates with G-proteins in response to odorants. J Neurosci. 19:4881-4888.

Xu F, Bose SC, McClintock TS.1999. Lobster G-protein coupled receptor kinase that associates with membranes and G_{β} in response to odorants and neurotransmitters.J Comp Neurol. 415:449-459.

Zufall F, Leinders-Zufall T, Greer CA.2000. Amplification of odor-induced Ca^{2+} transients by store-operated Ca^{2+} release and its role in olfactory signal transduction. J Neurophysiol. 83:501-512.

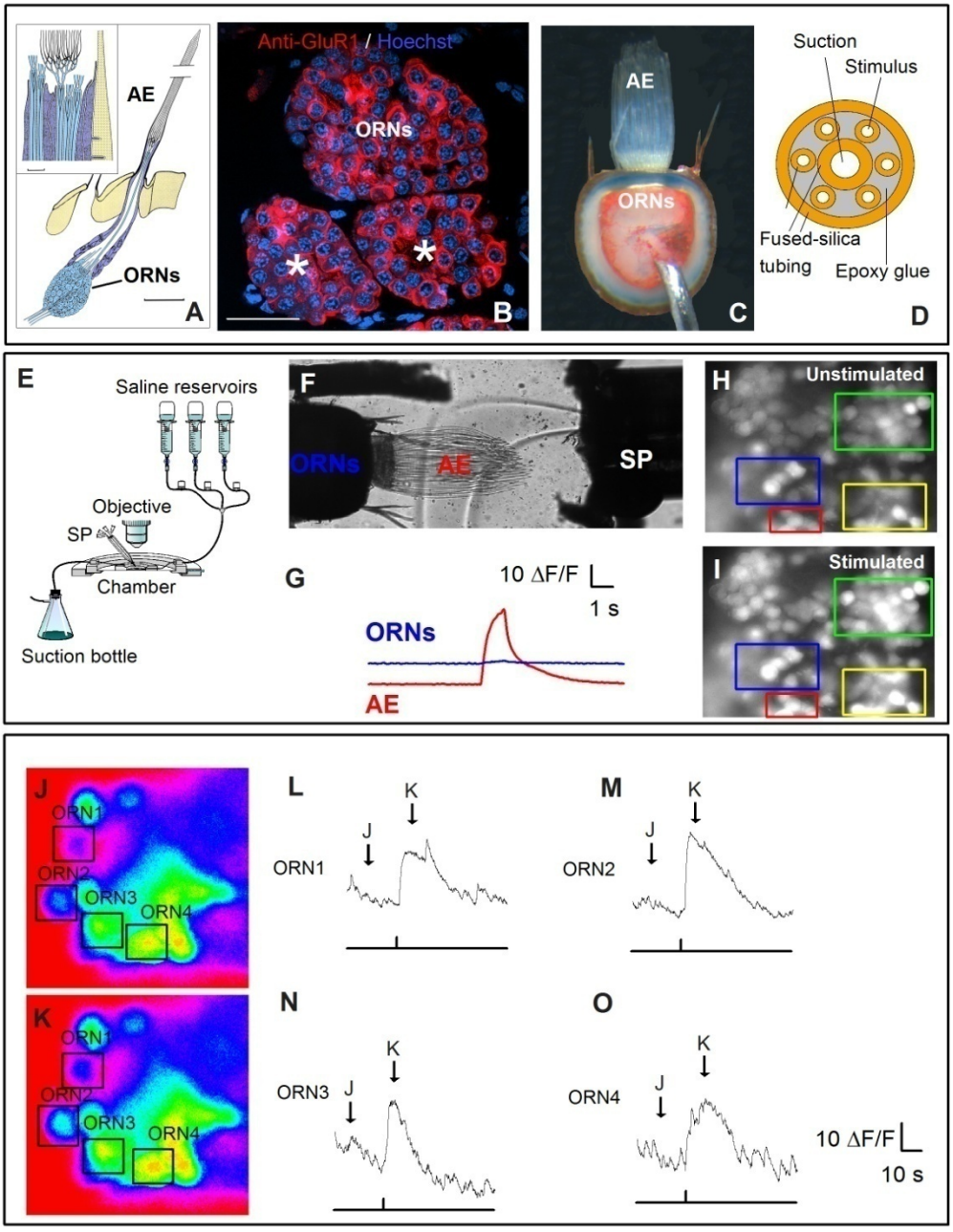

Figure 3-1 Calcium imaging of spiny lobster olfactory receptor neurons (ORNs).

(A) Schematic drawing of single aesthetasc (AE) sensillum (modified from Grünert and Ache, 1988). Each AE is innervated by the outer dendrites of ca. 300 ORNs. **(B)** Immunocytochemical labeling of ORNs (asterisks) with anti-GluR1, an antibody for an ionotropic glutamate receptor subunit, counterstained with Hoechst 33258, a nuclear marker. **(C)** Transmitted light microscopic image of lateral

flagellum (LF) slice preparation consisting of 2 aesthetasc-bearing annuli secured on a layer of Sylgard® used for Ca^{2+} imaging. **(D)** Schematic drawing of the multi-channel stimulus pipette (SP) in cross-section. The SP has 6 pressurized stimulus channels made of thin fused-silica tubes and a center suction channel made of a thicker fused-silica tube bonded together with epoxy glue. **(E)** Schematic drawing of the flow-through chamber (drawing by Lynn Milstead, Whitney Laboratory). **(F)** Visualization of stimulus distribution by application of saline containing Fast Green to the LF slice with the SP. Note that stimulus reaches the AE but not the ORN somata. **(G)** Time course of a 1s-long pulse of saline containing 0.001% fluorescein to the AE and obtained by quantification of the mean fluorescence intensity from AE (red) and ORN (blue) is shown. **(H)** Fluorescence images of un-stimulated ORNs loaded with Ca^{2+} indicator dye Oregon green BAPTA and **(I)** stimulated with high-KCl showed a robust increase in somatic Ca^{2+} (grey: low Ca^{2+}, white: high Ca^{2+}) Pseudocolor fluorescence images of Oregon green BAPTA loaded ORNs **(J)** before and **(K)** after AE stimulation with 1% TetraMarine (TetM). **(L-O)** Time courses of Ca^{2+} for ORNs 1 - 4 corresponding to images **J** and **K** showed an increase in Ca^{2+} following stimulation (time of stimulus is shown as a vertical bar on horizontal time line).

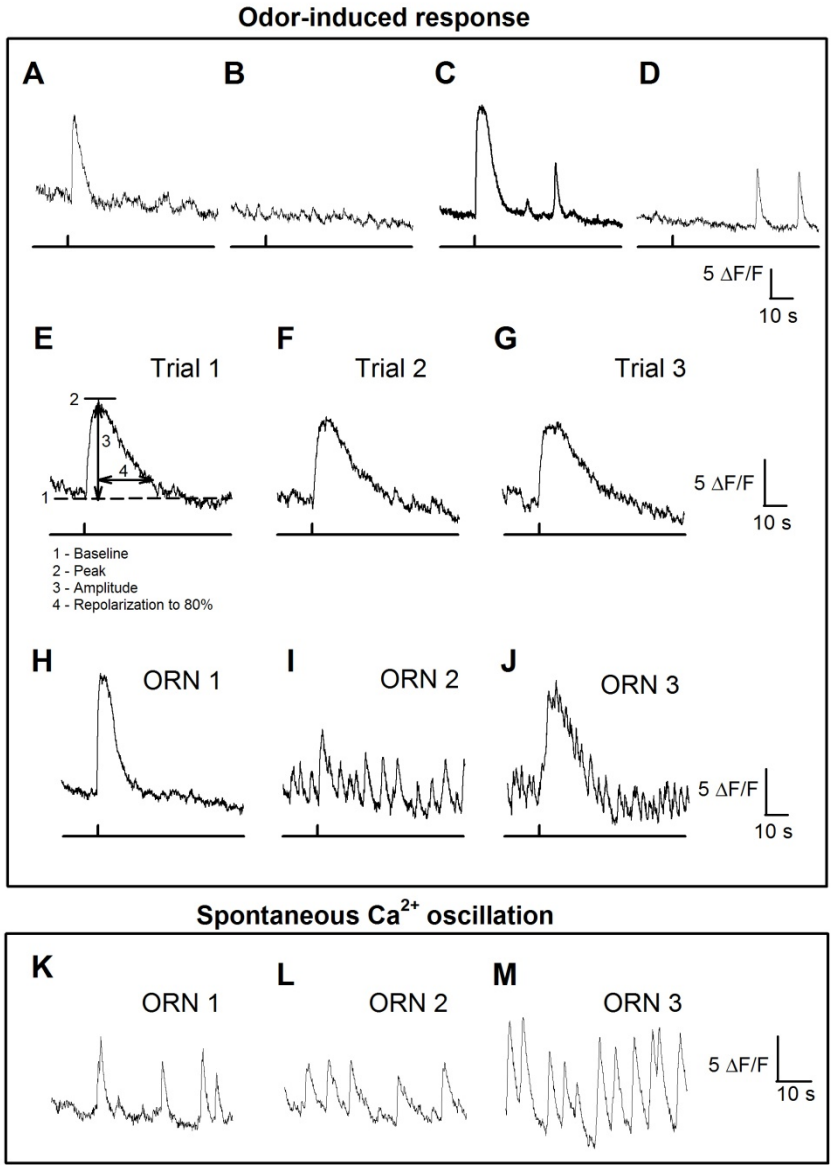

Figure 3-2 Characterization of somatic Ca^{2+} responses of ORNs.

Two examples of time courses of Ca^{2+} following stimulation with 1% TetM (**A**, **C**) and with negative control saline (**B**, **D**). **(E-G)** ORN stimulated with 1% TetM three times (Trials 1, 2 and 3) with a minimum 2-min inter-trial interval showed reproducible Ca^{2+} transients. The labeling of 1-Baseline, 2-Peak, 3-Amplitude and 4- Repolarization to 80% on trial 1 illustrates the parameters used to characterize the Ca^{2+} transients. **(H-J)** Representative somatic Ca^{2+} transients from three mature ORNs when stimulated with a 1-s pulse of 1% TetM. **(H)** ORN 1 had no spontaneous Ca^{2+} oscillations and responded to the 1-s odorant pulse with an increase in somatic Ca^{2+} that lasted many times longer than the stimulus. **(I)** ORN 2 spontaneously produced short, repetitive Ca^{2+} oscillations and responded with an odorant-entrained peak. **(J)** ORN 3 responded with a combination of an entrained peak and a long-lasting increase in Ca^{2+} which has oscillations. **(K-M)** Representative time courses of spontaneous Ca^{2+} oscillations in three ORNs with different amplitude and frequency of oscillations.

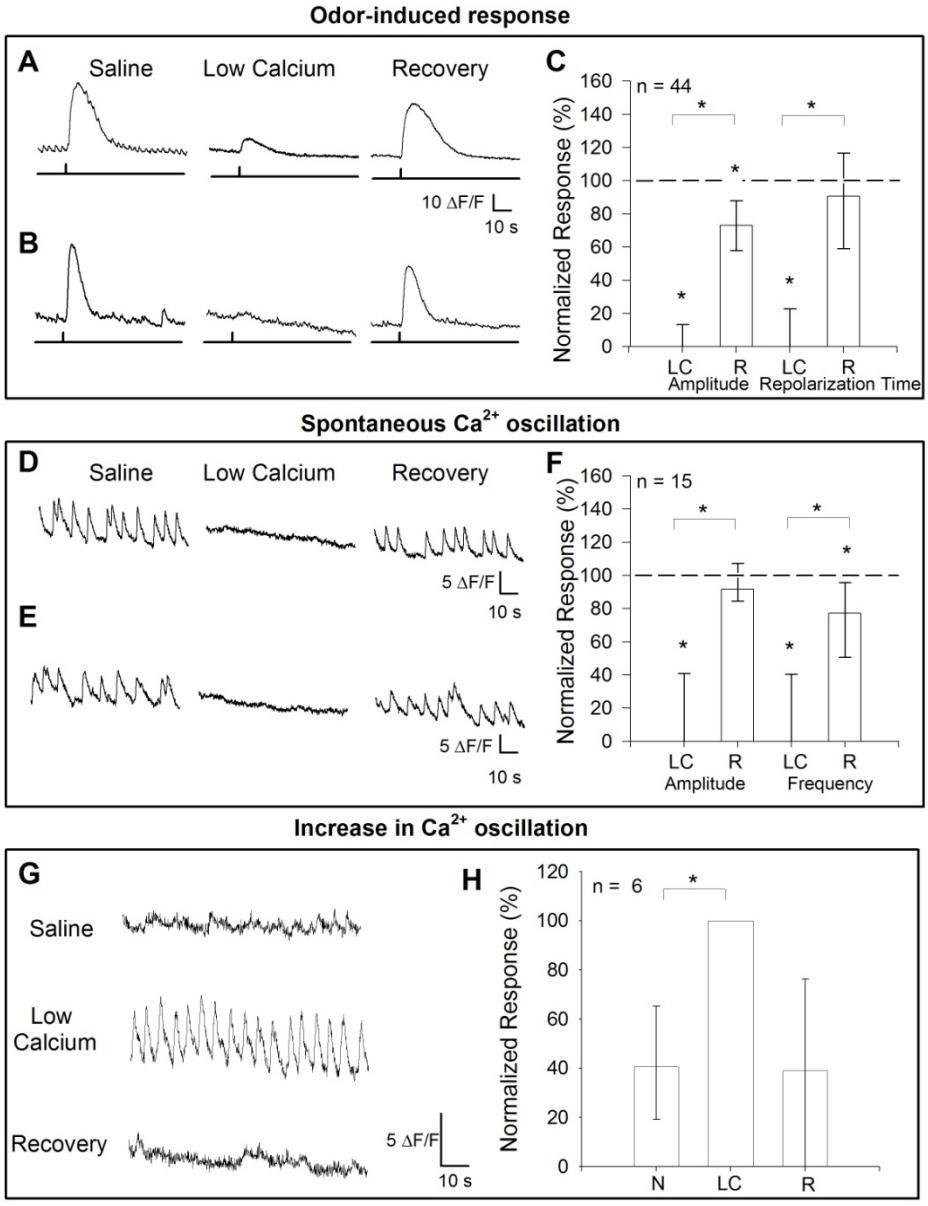

Figure 3-3 Effect of low extracellular Ca^{2+} on odor-induced Ca^{2+} transient responses and on spontaneous oscillations.

(A-B) Representative time courses of Ca^{2+} transients in normal saline, in low extracellular Ca^{2+} (0.1 mM $CaCl_2{\cdot}2H_2O$ from the normal physiological concentration of 13.6 mM), and post-treatment recovery. **(C)** Bar graph showing the percentage of normalized response and the median and interquartile range of peak amplitude and repolarization time [n = 44 ORNs, N = 3 lobsters, LF slices = 7]. **(D-E)** Representative time courses and **(F)** bar graph of spontaneous Ca^{2+} oscillations in normal saline, low extracellular Ca^{2+}, and recovery [n = 15 ORNs, N= 2 lobsters, LF slices = 5]. **(G)** Representative time course of an ORN with increase in spontaneous Ca^{2+} oscillations in low extracellular Ca^{2+}**(H)** and a bar graph showing median and interquartile ranges of frequency of oscillations normalized to low extracellular Ca^{2+} [n = 6 ORNs, N = 2 lobsters, LF slices = 3]. * Significance level $P< 0.05$. [LC-low extracellular Ca^{2+}, R-recovery, N-normal saline]

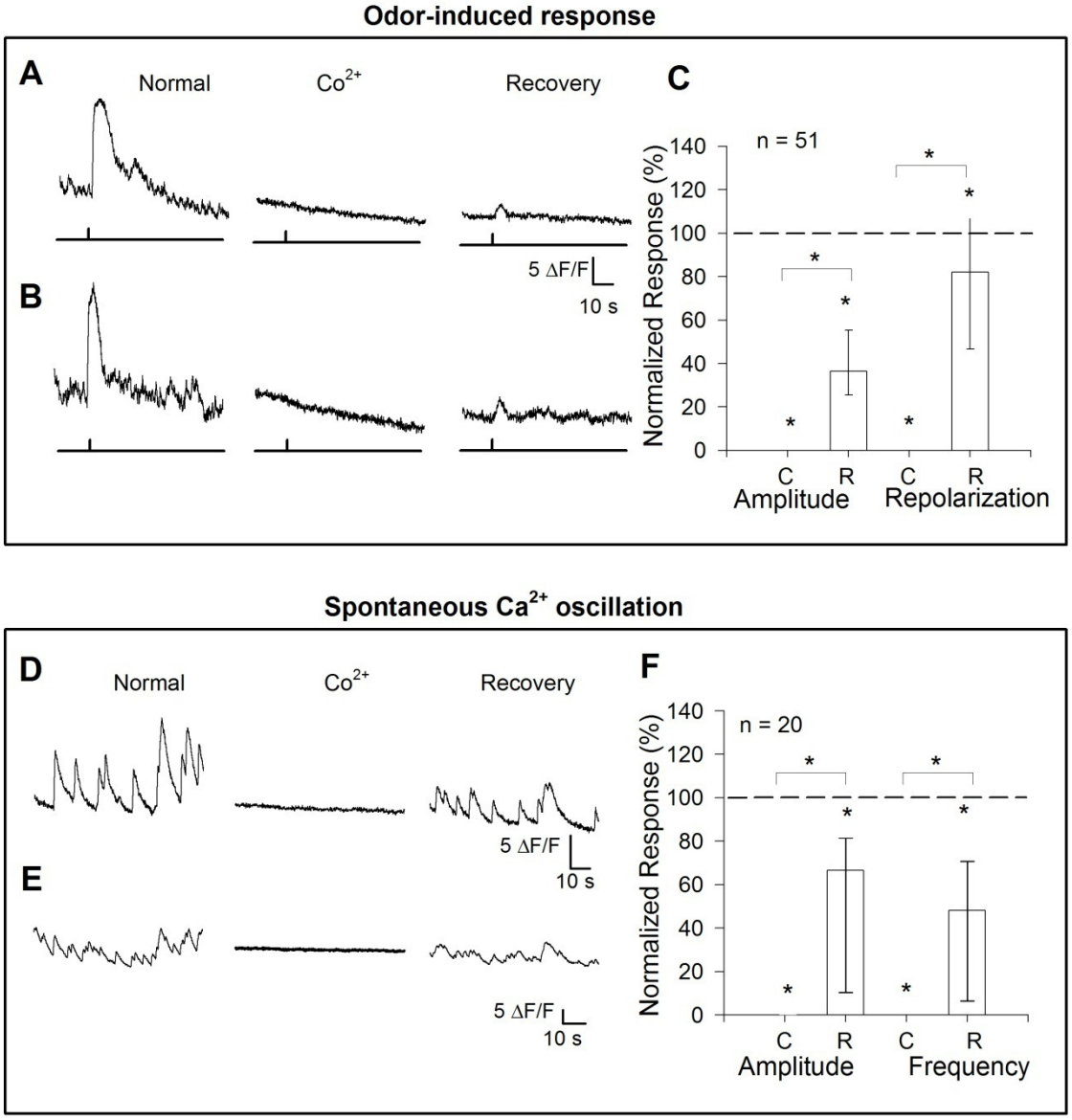

Figure 3-4 Effect of cobalt on odor-induced responses and spontaneous Ca^{2+} oscillations.

(A-B) Representative time course of Ca^{2+} transients [n = 51 ORNs, N = 2 lobsters, LF slices = 5] and **(D-E)** spontaneous Ca^{2+} oscillations [n = 20 ORNs, N = 2 lobsters, LF slices = 5] in normal saline, 20 mM cobalt, and recovery. **C** Bar graph shows the median and interquartile range of peak amplitudes and repolarization times for Ca^{2+} transients, expressed as percentage of normalized response. **(F)** Bar graph shows the amplitude and frequency for spontaneous oscillations. * Significance level $P < 0.017$. [C-cobalt, R-recovery]

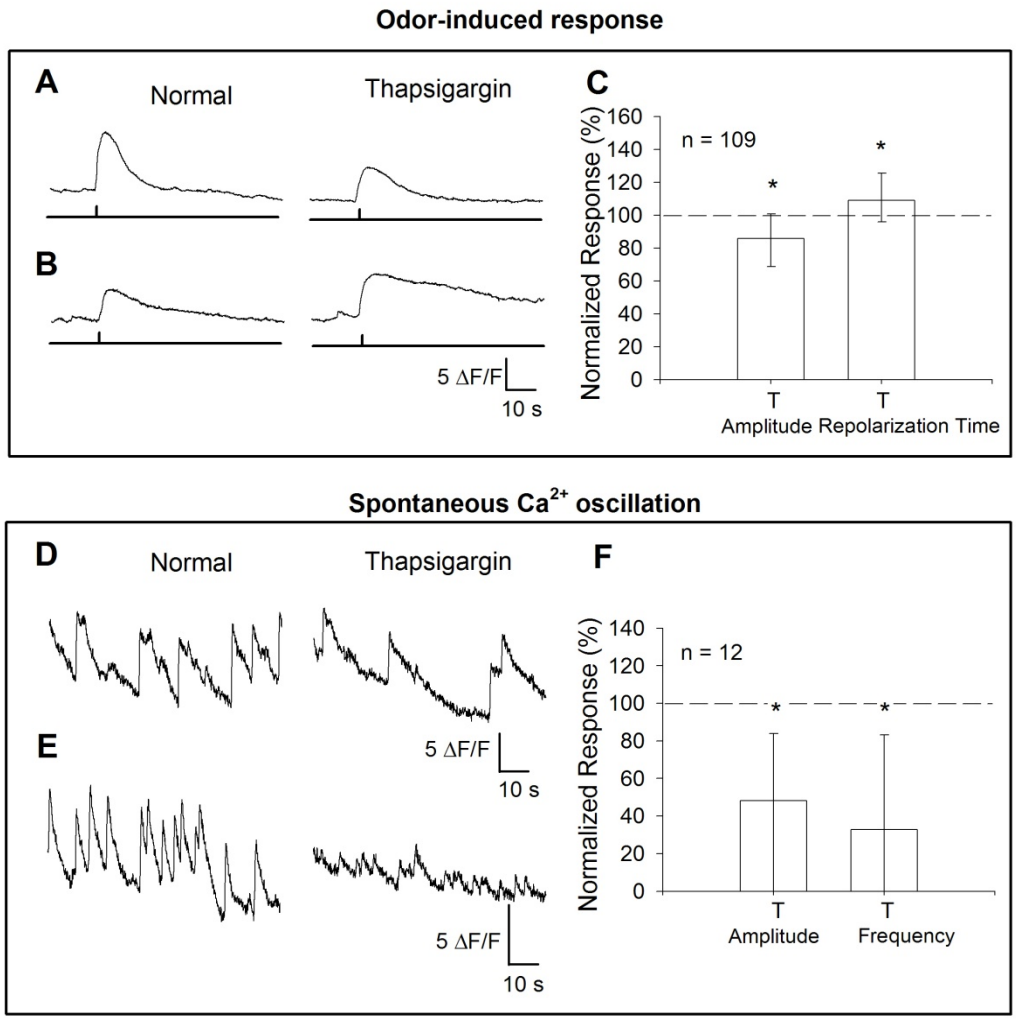

Figure 3-5 Effect of thapsigargin on odor-induced Ca^{2+} transient responses and on spontaneous oscillations.

(A, B) Representative time course of Ca^{2+} transients [n = 109 ORNs, N = 2 lobsters, LF slices = 5] and **(D, E)** spontaneous Ca^{2+} oscillations [n = 12 ORNs, N = 2 lobsters, LF slices = 4] in normal saline and in 1 μM thapsigargin. **(C, F)** Bar graphs show the median and interquartile range of peak amplitude and repolarization time for Ca^{2+} transients and peak amplitude and frequency for spontaneous oscillations. * Significance level $P < 0.05$. [T-Thapsigargin]

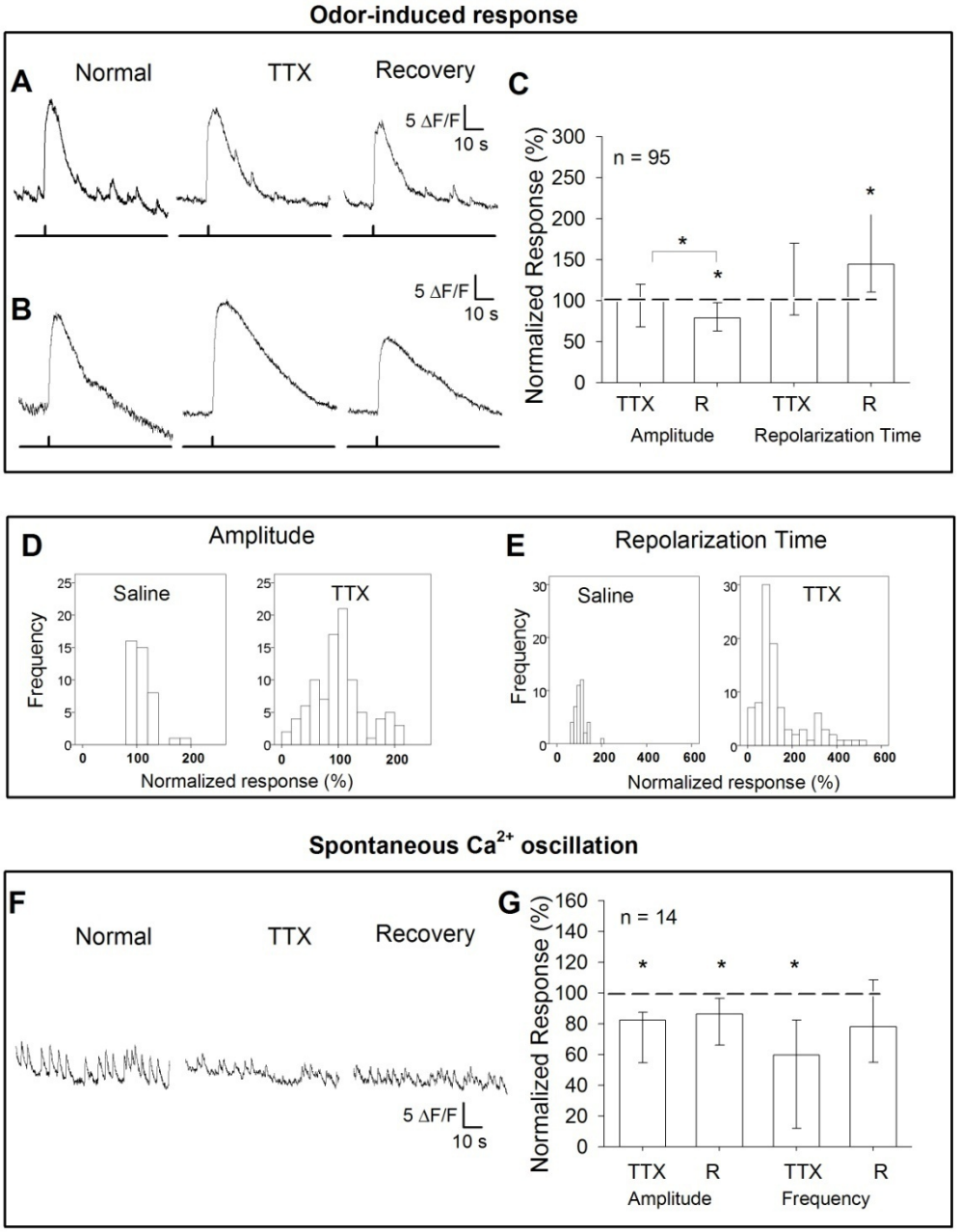

Figure 3-6 Effect of 1 µM TTX on odor-induced Ca^{2+} transient responses and on spontaneous Ca^{2+} oscillations.

(A-B) Representative time courses of Ca^{2+} transients [n = 95 ORNs, N = 2 lobsters, LF slices = 6] in normal saline, in TTX, and recovery. Bar graph shows the percentage of normalized response and the median and interquartile range of **(C)** peak amplitude and repolarization time for Ca^{2+} transients. Comparison of frequency distributions of odor-induced Ca^{2+} transient in saline and TTX shows a significant difference in **(D)** normalized response (%) of peak amplitude (ΔF/F) **(E)** normalized response (%) of repolarization time (two-sample Kolmogorov-Smirnov tests: for peak amplitude, Z = 1.577, *P* = 0.014; for repolarization time, Z = 1.414, p = 0.037).Representative time courses of **(F)** spontaneous Ca^{2+} oscillations[n = 14, N = 2, LF slices = 4] in normal saline, in TTX, and recovery. **(G)** Bar graph shows the

percentage of normalized response and the median and interquartile range of the amplitude and frequency for spontaneous oscillations. *Significance level $p < 0.017$. There was no difference between TTX and recovery in both peak amplitude ($Z = -1.083$, $P = 0.279$) and frequency ($Z = -1.572$, $P = 0.116$). There was also no significant difference between pre-treatment and recovery for spontaneous frequency ($Z = -1.412$, $P = 0.158$). [TTX-tetrodotoxin, R-recovery]

CHAPTER 4: PHYSIOLOGICAL CHANGES IN CALCIUM RESPONSES WITH MATURATION IN ADULT-BORN OLFACTORY RECEPTOR NEURONS OF SPINY LOBSTERS, *PANULIRUS ARGUS*

Authors: Tizeta Tadesse*, Manfred Schmidt, and Charles D. Derby

Affiliation: Neuroscience Institute and Department of Biology, Georgia State University, Atlanta, GA

***Corresponding Author:** Tizeta Tadesse, Neuroscience Institute, Georgia State University, P.O. Box 5030, Atlanta, GA 30302-5030 USA. Email: ttadesse@gsu.edu FAX 404-413-5446

Acknowledgements

Anti-GluR1 antiserum was kindly provided by Dr. Timothy McClintock. Supported by NIH DC00312, GSU Dissertation Grant, GSU Brains & Behavior seed grant, and GSU Brains & Behavior fellowship to TT.

4.1 Abstract

Sensory systems are critical for an organism to experience its environment. Olfactory receptor neurons (ORNs) of some species have continuous addition and turnover throughout adulthood. ORNs are susceptible to r environmental damage, and thus adult neurogenesis may be a compensatory mechanism to maintain olfactory reception. During embryonic development of mammals, sequential expression of odor transduction genes in ORNs coincides with changes in the ORNs' physiological response properties; whether a similar pattern of changes occurs in the functional maturation of adult-born ORNs is not known. Adult neurogenesis of ORNs occurs in some decapod crustaceans, including spiny lobsters, *Panulirus argus*. To test the hypothesis that adult-born ORNs of spiny lobsters change in odor specificity, sensitivity, or temporal responses as they age, we used calcium imaging of *in situ* ORNs to examine spontaneous Ca^{2+} oscillations and odor-induced Ca^{2+} transients in ORNs from the proliferation, mature, and senescence zones (PZ, MZ, SZ, respectively), using 4 odorants each at 4 concentrations. We found an increase in the percentage of odorant-responsive ORNs between PZ to MZ and a decrease in odorant-responsive ORNs between MZ and SZ. There was a decrease in the percentage of ORNs that had spontaneous Ca^{2+} oscillations, an increase in the spontaneous amplitude from PZ to SZ, but no change in spontaneous frequency. Using lifetime sparseness as a measure of response specificity, MZ had a higher specificity compared to SZ but not to PZ. Although not significant, there was a strong trend of lower specificity in SZ than PZ. A hierarchical cluster analysis representing differences in response profiles revealed that ORNs formed 5 clusters and 11 sub-clusters. Further analysis showed the sub-clustering of ORNs was based on their responsiveness to the two most effective odorants. Taurine-best cells that also responded strongly to AMP were the predominant cell type in PZ, taurine-best cells in MZ, and glutamate-best in SZ. Comparison of the amplitude of the Ca^{2+} responses for 4 odorants at 4 concentrations across zones revealed that there were more taurine-responsive cells than glutamate-, AMP-, and ammonium-responsive cells. Mature ORNs were more odor responsive than immature or old cells. There were changes in odor sensitivity with age. These data demonstrate that three physiological response

properties – odor specificity, odor sensitivity, and odor-activated temporal responses – change as adult-born ORNs age.

Key words: olfactory, sensory neuron, maturation, aging, neurogenesis, calcium imaging

4.2 Introduction

Sensory systems are used by organisms to experience their environment. Every sensory system has peripheral detectors that detect environmental cues and transfer this information to specific areas of the brain that are involved in sensory perception. The emergence of deficits in sensory perception (Chen 2009; Frisina 2009; Linford et al., 2011) may be due to changes in tuning properties and response threshold, which are features of all mature sensory neurons. The olfactory and gustatory systems in some adult animals have the ability to regenerate sensory cells (Lindsey and Tropepe 2006; Miura and Barlow 2010). Some adult animals also have continuous addition and turnover of peripheral sensory neurons and central neurons throughout adulthood (Lindsey and Tropepe 2006; Ming and Song 2011). Adult neurogenesis of olfactory receptor neurons (ORNs) occurs in humans (Mackay-Sim 2010), mammals (Calof et al., 1996), and crustaceans (Steullet et al., 2000a; Harrison et al., 2001). Thus, understanding adult neurogenesis and more specifically functional maturation of adult-born ORNs may reveal mechanisms for age-related sensory deficits.

Functional maturation of mammalian ORNs during embryogenesis results from molecular, physiological, biochemical, and structural changes (Mair 1986). For example in rats, the sequence of odor transduction gene expression coincides with functional maturation of ORNs. The half maximal gene expression shows at embryonic day E16 GTP binding protein (G_{olf}) expression, at E19 olfactory cation channel, at E19 ~E-20 odorant receptor (OR), and at ~E22 olfactory marker protein (OMP) is the sequence of expression (Margalit and Lancet 1993). The physiological responses of ORNs also change, i.e. they become more selective as they develop (Gesteland et al., 1982). Adult-born ORNs may also have similar temporal expression of odor transduction genes similar to embryonic ORN development. There may be increases in both odor selectivity and sensitivity during functional maturation.

Functional maturation of adult-born ORNs is only recently beginning to be investigated. In adult mice, functional maturation of ORNs is mediated by the expression of olfactory marker protein (OMP) (Lee et al., 2011). In adult frogs, ablation-induced regenerating immature ORNs show similar odor-selectivity in their responses as their mature counterparts (Lidow et al., 1987). Humans have a loss in odor-selectivity of ORNs with age (Rawson et al., 2011). As far as we know, there is no study addressing the physiological changes during functional maturation of adult-born ORNs.

Adult crustaceans have indeterminate growth, thereby increasing in size, and thus continuously adding sensors, throughout their life (Derby, 2007). Adult spiny lobsters, *Panulirus argus*, have continuous proliferation and turnover of ORNs and associated structures (Steullet et al., 2000a; Harrison et al., 2001, 2003). The external olfactory organ is easily accessible, all stages of development of ORNs are present and spatially separated on a horizontal axis (Steullet et al., 2000a), and damage-induced regeneration is a common feature in *P. argus* (Harrison et al., 2003, 2004). Therefore, this is a good model system for studying adult neurogenesis specifically, functional maturation and aging of ORNs.

In decapod crustaceans, ORNs are housed in aesthetasc sensilla on the lateral flagellum (LF) of the paired first antennae, or antennules (Fig. 4-1A). Aesthetascs of *P. argus* are exclusively located on the ventral-distal region of the LF, where specific types of non-aesthetasc sensilla are also located, collectively forming a 'tuft'. The LF is organized as repeating cuticular units called annuli, containing ca. 100 aesthetasc-bearing annuli per LF, ca. 20 aesthetascs per annulus, and ca. 300 ORNs per aesthetasc sensilla (Fig. 4-1B) for a total of ca. 1,200,000 ORNs per animal. ORNs are assembled beneath the cuticular seta as a dense cluster of cell bodies (Grünert and Ache, 1988). Immunocytochemical labeling using anti-GluR1 antiserum (ionotropic glutamate receptor, originally identified in *H. americanus*: Hollins et al., 2003; Stepanyan et al., 2004, 2006) and Hoechst 33258, a nuclear marker, shows labeling of numerous mature ORN clusters (Fig. 4-1C). Aesthetasc sensilla have thin cuticle that allow odors to permeate (Grünert and Ache, 1988; Derby et al., 1997). Aesthetascs and their ORNs are added in the proximal proliferation zone (PZ) of the LF (Steullet et al., 2000a) (Fig. 4-1A). These ORNs mature (i.e. become responsive to chemical stimuli in the mature zone (MZ). Aesthetasc sensilla and their associated

ORNs become old in the senescence zone (SZ) and are gradually shed with each molt (Harrisonet al., 2001, 2003).

Functional maturation of adult-born ORNs in *P. argus* has been examined using taurine-like immunoreactivity and agmatine-based odor-induced activity labeling (Steullet et al., 2000a, 2000b). Taurine-like immunoreactivity is high in immature ORNs and low in mature ORNs. Agmatine activity labeling is low in immature ORNs and high in mature and senescent ORNs. Electrophysiological recordings and agmatine activity labeling showed that mature *P. argus* ORNs have different selectivity and sensitivity to odors (Michel et al., 1991; Simon and Derby 1995; Steullet et al., 2000b).

The aim of this study was to describe the changes in the physiological response properties of adult-born ORNs with their age in the spiny lobster. We recently established Ca^{2+} imaging of lobster ORNs in an *in vitro* 'LF slice' preparation from the MZ (Schmidt et al., 2010; Tadesse et al., 2011) in parallel with Ukhanov et al. (2011). In the current study, we also study LF slices from the PZ and SZ. We examined spontaneous Ca^{2+} oscillations and odor-induced Ca^{2+} transients across these zones. Our data demonstrate that adult-born ORNs change in odor specificity, sensitivity, and temporal responses with aging.

4.3 Material and Methods

Animals

Young adult male and female Caribbean spiny lobsters (*Panulirus argus*) of 50-75 mm carapace length were collected near the Florida Keys Marine Laboratory and shipped to Georgia State University. Spiny lobsters were placed in 400-liter aquaria with re-circulated, filtered, and aerated artificial seawater (Instant Ocean™, Aquarium Systems Inc., Mentor, OH, USA) at 20-25ºC, maintained in a 12 hr: 12 hr light: dark cycle and fed shrimp or squid three times per week.

Tissue preparation

Tissue preparation and Ca^{2+} imaging of lobster ORNs in an *in vitro* 'LF slice' preparation was conducted as described in Chapter 3 and Tadesse et al. (2011) with some modifications. Unilateral LF from adult intermolt spiny lobsters was excised using scissors and placed in *P. argus* saline (459 mM NaCl, 13.4 mM KCl, 13.6 mM $CaCl_2 \cdot 2H_2O$, 3 mM $MgCl_2 \cdot 6H_2O$, 14.1 mM Na_2SO_4, 9.8 mM HEPES, pH 7.4, 977 mOsmol). Guard sensilla were removed and the LF was further cut into two-annulus pieces (LF slices) (Fig. 4-1D) (Tadesse et al., 2011). The annuli numbering is as described by Schmidt et al. (2006) and Tadesse et al. (2011). PZ is represented by annuli -10 to 12, with the middle PZ being annuli -4 to 4. The mature zone is represented by annuli 13 to 52, and the senescence zone is represented by annuli 53 and greater. LF slices were taken from the PZ (+1 to +6), MZ and SZ. LF slices were enzymatically digested by immersing slices for 5 min in 2 mL *P. argus* saline, 8 mg of L-cysteine, and 500 µL of 2.5 mg/ml papain. LF slices were rinsed in *P. argus* saline for 20 min on a shaker, then ORN clusters were desheathed using forceps. Fifty µg of acetoxymethyl (AM) ester Ca^{2+} indicator dye Oregon green BAPTA (OGB) was dissolved in 45-50 µL Pluronic ® F127 in DMSO (Invitrogen, Carlsbad, CA). OGB was diluted to a final concentration of 50-60 µM, according to Stosiek et al. (2003) and Grewe et al. (2010), in saline in an Eppendorf tube. LF slices were transferred to the Eppendorf tube using forceps and placed on a horizontal shaker set at medium speed in the dark for 1 hr at room temperature. Loaded LF slices were rinsed in saline for 20 min then transferred into another dish containing saline until imaging.

Odor preparation and delivery

Stocks of 10 mM taurine, AMP, L-glutamate, and ammonium chloride (NH_4) were prepared in *P. argus* saline and aliquots were stored at -20°C. On the day of experiments, aliquots were removed and diluted in *P. argus* saline to a final concentration of 10^{-4} M for odor selectivity experiments or 10^{-3}, 10^{-4}, 10^{-5}, and 10^{-6} M for odor sensitivity experiments, and the remainder was discarded. Two g of Tetramarine (TetM) (Petsolutions, Beavercreek, OH)was mixed in 60 ml of *P. argus* saline for ~ 3 hr,

centrifuged at 1400 x g for 20 min, filtered, and aliquots were stored at -20°C. On the day of experiments, aliquots were diluted in *P. argus* saline to 1% TetM. Odorants were applied using a picospritzer pressurized multi-barrel spritzing pipette (five stimulus channels and one suction channel) to the aesthetasc sensilla and Ca2+ responses were imaged in the somata (Tadesse et al., 2011; Chapter 3).

Calcium imaging

LF slices were secured on a dish containing a layer of Sylgard® and mounted on a stage of an upright epifluorescence microscope (Zeiss Axioplan 2, Jena, Germany) equipped with a 40 X water immersion objective. LF slices were continuously perfused with *P. argus* saline at a rate of 3.0-3.6 ml/min for the duration of the experiment. Excitation light (320-680 nm) was provided by a monochromator (Polychrome V, Till Photonics, Munich, Germany), and fluorescent images (688 x 520 pixels and 2 x 2 binning) were captured with a fast CCD camera (Imago QE, Till Photonics). An experimental protocol was customized in Vision software that synchronized image acquisition with an external processor (Imaging System Controller), allowing us to control the stimulus onset and offset (Vision, Till Photonics). For quantification of Ca^{2+} signals, a Region of Interest (ROI) was outlined for each OGB-loaded ORN soma, and the average pixel value of mean fluorescence intensity was calculated using Vision software, then transferred to Microsoft Excel (Redmond, WA) for further analysis.

Experiments

Each test lasted for ca. 80 s: a 15-s pre-stimulus time, a 0.6-1.0 s stimulus time (duration of solenoid activation), and ca. 65-s post-stimulus time. For each 80-s test, 500 - 800 images were acquired at 100 ms / frame. The time between tests was 2 min. The two odorants were 1% TetM and *P. argus* saline as a negative control. We also examined spontaneous Ca^{2+} oscillations by imaging LF slices and not stimulating AE (no-stimulation).

Data analysis

Spike2 software (Cambridge Electronic Design, Cambridge, England) was used for analyzing the mean fluorescence intensity. An ORN was considered to respond if an odor-induced fluorescence signal was greater than the response criterion (i.e. 2 standard deviations or more above the mean pre-stimulus level), and the peak amplitude was determined. The mean fluorescence intensity from the 'No-stimulation' was used to determine the amplitude and frequency of spontaneous Ca^{2+} oscillations. A spontaneous event is defined as Ca^{2+} signal having two troughs and one peak that exceeds a preset threshold. As mentioned in the results, some ORNs were normalized to the response of the best-odorant (set to 100%). Illustrations of time courses of Ca^{2+} responses are presented as relative fluorescence changes from baseline ($\Delta F/F$).

Lifetime sparseness (S_L) was used as a measure of response selectivity (Davison and Katz 2007; Tan et al., 2010). S_L formula was written in Microsoft Excel $[\{1 - [(\sum r_i /N)^2 / \sum (r_i^2)/N]\} / [1- (1/N)]]$ (Tan et al., 2010) where r_i = response strength (amplitude) and N = total number of stimuli. Mean S_L was computed using responses to taurine, glutamate, AMP, and NH_4. A high sparseness ($S_L = 1$) is a neuron that responds to only one odorant, and a low sparseness ($S_L = 0$) is a neuron that responds to all odorants equally.

A hierarchical cluster analysis was used to determine the odor-activated response profiles of ORNs. The amplitude of the Ca^{2+} responses to the 4 odorants was normalized to the maximum response for each ORN. A hierarchical cluster analysis was conducted with a Pearson's correlation coefficient as a measure of the distances between clusters and a dendrogram and scree plot were generated.

All statistics were conducted using either PASW Statistics 18 (SPSS Inc., Chicago, IL) or DIG Stats, a free online source. Dendrograms of the results of cluster analyses were generated from PASW, and all graphs and final figures were generated using SigmaPlot 8.0 (Systat Software Inc., San Jose, CA).

4.4 Results

Adult-born spiny lobster ORNs may become more odor selective and sensitive during functional maturation, similar to embryonic ORNs of vertebrates. We hypothesized that adult-born ORNs change in odor specificity, sensitivity, or temporal responses as they age. We tested our hypothesis using Ca^{2+} imaging of ORN somata in LF slice preparations (Fig. 4-1D) loaded with Ca^{2+} indicator dye OGB (Fig. 4-1E). Spontaneous Ca^{2+} oscillations (Fig. 4-1H) and odor-induced Ca^{2+} transients (Fig. 4-1F, G) (following odor stimulation of aesthetascs for 1 s) were examined for three variables: (1) zone (proliferation, mature, and senescence), (2) odorant type (taurine, L- glutamate, AMP, NH_4, 1% TetM), and (3) odorant concentration (10^{-6}, 10^{-5}, 10^{-4}, 10^{-3} M for taurine, L- glutamate, AMP, NH_4).

Percentage of ORNs that are odor-responsive or with spontaneous Ca^{2+} oscillations differs across zones

To assess whether the frequency of odorant-responsive ORNs changes as ORNs age, we sampled 826 OGB-loaded ORNs (357 in PZ, 290 in MZ, and 179 in SZ) and calculated the percentage of ORNs in each zone that responded to any of the 4 odorants (taurine, L- glutamate, AMP, NH_4) at 10^{-4} M (Fig. 4-2E). In the PZ, 10.64% of the ORNs were odor-responsive and spontaneously oscillating, 2.24% responded but did not oscillate, and 87.11% did not respond. In the MZ, 27.93% responded and oscillated, 15.52% responded but did not oscillate, and 56.55% did not respond. In the SZ, 11.17% responded and oscillated, 5.59% responded but did not oscillate, and 83.24% did not respond. Chi-square test for homogeneity showed that the frequency distribution of the three type of responses differed across the three zones [χ^2 (4, N = 826) = 92.562, $p < 0.001$]. There was a significant difference in the frequency distributions between PZ and MZ [χ^2 (2, N = 647) = 80.789, $p < 0.001$] and between MZ and SZ [χ^2 (2, N = 469) = 35.554, $p < 0.001$], and no difference between PZ and SZ [χ^2 (2, N = 536) = 4.213, $p = 0.122$]. These results reflect an increase in the percentage of odorant-responsive ORNs as they age from newly-born cells to maturation (PZ vs. MZ) and a decrease in odorant-responsive ORNs as they become even older (MZ vs. SZ).

To determine whether the frequency of ORNs showing spontaneous Ca^{2+} oscillations changes as ORNs age, we calculated for these same 826 OGB-loaded ORNs the percentage of cells that oscillated and responded to any of the 4 odorants, oscillated and did not respond, and those that did not oscillate from the total (Fig. 4-2F). In PZ, 10.64% oscillated and responded, 48.74% oscillated but did not respond, and 40.6% did not oscillate. In MZ, 27.93% oscillated and responded, 23.79% oscillated but did not respond, and 48.28% did not oscillate. In SZ (n=179), 11.17% oscillated and responded, 17.88% oscillated but did not respond, and 70.95% did not oscillate. Chi-square test for homogeneity showed significant difference in the distributions of spontaneous Ca^{2+} oscillations across zones [χ^2 (4, N = 826) = 101.204, $p < 0.001$]. There were significant differences between all of the zones: PZ vs. MZ χ^2 (2, N = 647) = 54.644, $p < 0.001$; MZ vs. SZ χ^2 (2, N = 469) = 26.227, $p < 0.001$; PZ vs. SZ χ^2 (2, N = 536) = 51.195, $p < 0.001$. These data suggest a decrease in the percentage of ORNs that undergo spontaneous Ca^{2+} oscillations as the ORNs age.

Frequency and amplitude of spontaneous Ca^{2+} oscillations differ across zones

To examine whether the parameters of spontaneous Ca^{2+} oscillations change as ORNs age, we examined their frequency and amplitude in PZ, MZ, and SZ. Representative time courses of spontaneous Ca^{2+} oscillations from two ORNs taken from PZ, MZ, and SZ (Fig. 4-3 A-F) reveal differences in both parameters. Quantification and statistical analysis confirmed the qualitative differences across zones in the frequency and the amplitude of spontaneous Ca^{2+} oscillations [ANOVA Kruskal Wallis ($H(2) = 23.663$, $p< 0.001$; $H(2) = 10.015$, $p = 0.007$), respectively]. *Post-hoc* analysis for Ranks with a Bonferroni's correction (significance level $p < 0.017$) showed that ORNs in PZ oscillate at a lower frequency compared to MZ ($p < 0.001$) and compared to SZ ($p = 0.012$). There was no difference in the frequency of oscillations between MZ and SZ ($p = 0.162$).

Post-hoc analysis for Ranks with a Bonferroni's correction (significance level $p < 0.017$) showed that ORNs in SZ have significantly smaller amplitude of oscillation compared with MZ ($p = 0.002$). There was no significant difference between PZ and SZ ($p = 0.136$), but there was a strong trend of smaller amplitude in PZ compared to MZ ($p = 0.030$) [PZ median = 3.656 RF, range = 18.78, n = 76) MZ median = 5.138 RF, range = 11.86, n = 28; SZ median = 3.452, range = 5.14, n = 45]. Taken together, these data suggest that the amplitude of spontaneous Ca^{2+} oscillations increases as adult-born ORNs age.

Odor selectivity of ORNs differs across zones

Representative responses to taurine, glutamate, AMP, and NH_4, each at 10^{-4} M, are shown for ORNs from PZ (Fig. 4-4A-D), MZ (Fig. 4-4E-H), and SZ (Fig. 4-4I-L). Qualitative assessment shows differences in the odorant type responses across zones. To analyze the changes in the odor selectivity across zones, we compared lifetime sparseness (S_L) for ORNs in different zones (Fig. 4-4M), based on amplitude of responses to the four single odorants (taurine, glutamate, AMP, and NH_4, each at 10^{-4} M). S_L values differed across zones (ANOVA: $F(2) = 5.167$, $p = 0.007$, for 102 ORNs from 12 LF slices from 4 spiny lobsters). A *post-hoc* analysis with Bonferroni significance level ($p < 0.017$) showed that S_L values were significantly higher in MZ than in SZ ($P = 0.014$). There was no significant difference between PZ and MZ ($P = 1.00$). There was no significant difference in S_L values between PZ and SZ, but there was a strong trend of lower S_L values in SZ ($P = 0.021$). These data suggest that ORNs become more broadly tuned as they age.

Response profiles of ORNs differ across zones

To determine whether the odorant-activated response profiles of ORNs changes as adult-born ORNs age, we first used cluster analysis (Fig. 4-5) to characterize the response profiles of the ORNs to

the four single odorants, and then we compared whether the frequency distributions of ORNs with different response profiles changed as ORNs age (Fig. 4-6). To characterize the response profiles, we conducted a hierarchical cluster analysis using the amplitude of the Ca^{2+} responses to the 4 odorants for 102 ORNs, based on responses that are normalized to the maximum response for each ORN. Pearson's correlation coefficient was used as a measure of the distances between clusters. A dendrogram representing differences in response profiles (Fig. 4-5A), together with a scree plot, revealed that based on their response profiles to these four odorants, the ORNs form 5 clusters and 11 sub-clusters. We assessed the basis for these clusters by characterizing each ORN according to the most effective odorant (i.e. 'best' odorant) and mapping this onto the clusters. ORNs in cluster A (n =49) were taurine-best (mean S_L=0.616), cluster B (n=27) were glutamate-best (mean S_L= 0.528), cluster C (n=11) were ammonium-best (mean S_L= 0.706), cluster D (n=3) were glutamate-, AMP-, and ammonium-best (mean S_L= 0.182), and cluster E (n = 12) were AMP-best (mean S_L= 0.722). These data show that four of the five clusters were based on the best response of ORNs to only one of the 4 tested odorants.

We further examined 11 sub-clusters based on a second inflection point on the scree plot. Cluster A had three sub-clusters: all were taurine-best (Fig. 4-5B), but A1 (n=23) had very low responses to the other odorants (mean S_L= 0.722), A2 (n=26) responded strongly to AMP (mean S_L=0.530), and A3 (n=1) responded strongly to AMP and ammonium but not to glutamate (mean S_L= 0.341). Cluster B had two sub-clusters: all were glutamate-best (Fig.4-5C), but B1 (n=11) responded strongly to taurine (mean S_L=0.451), and B2 (n=16) responded only weakly to the other odorants (mean S_L= 0.581). Cluster C had two sub-clusters: both were ammonium-best (Fig. 4-5D), but C1 (n=4) also responded strongly to AMP (mean S_L=0.578), and C2 (n=7) responded weakly to the other odorants (mean S_L=0.779). Cluster D had two sub-clusters: D1 (n=2) responded strongly to glutamate (Fig. 4-5E) and also to AMP and ammonium (mean S_L= 0.198, and D2 (n=1) responded strongly to ammonium, glutamate, and AMP (mean S_L=0.149). Cluster E had two sub-clusters: both were AMP-best (Fig. 4-5F), but E1 (n=9) responded weakly to the other three odorants (mean S_L= 0.786), while E2 (n=3) responded strongly to glutamate (mean S_L=

0.528). These data suggest that the sub-clustering of ORNs is based on their responsiveness to the two most effective odorants.

We examined whether the frequency distributions of the sub-clusters were different across zones (Fig. 4-6A, F, K). We used only 8 of the 11 sub-clusters, omitting A1, D1, and D2 due to low sample size. Chi-square analysis showed that the frequency distributions for these sub-clusters differed across the three zones (χ^2 (14, n= 98) = 50.06, $p < 0.001$). Pair-wise comparisons showed a differences between all zones (MZ vs. SZ: χ^2 (7) = 18.67, $p < 0.005$; PZ vs. SZ: χ^2 (7) = 28.60, $p < 0.005$; PZ vs. MZ: χ^2 (7) = 32.26, $p < 0.005$). Representative responses of the predominant cell type in PZ (Fig. 4-6 B-E), MZ (Fig. 4-6G-J), and SZ (Fig. 4-6L-O) are shown for single ORNs in response to the four odorants. In PZ, taurine-best cells (A2, n=26) that also responded strongly to AMP were the predominant cell type. Taurine-best cells (A1, n=23) were the predominant cell type in MZ. In SZ, the majority of cells were glutamate-best (B2, n=16). Thus, the response profile changed as adult-born ORNs aged and the changes are due to the most effective odorant.

Odor sensitivity of ORNs differs across zones

To determine whether there are changes in odor sensitivity across zones, we compared the amplitude of the Ca^{2+} responses to each of the four odorants at four concentrations: 10^{-6}, 10^{-5}, 10^{-4}, and 10^{-3} M. A two-way ANOVA with repeated measures [zone (3 levels), odorant type (4 levels), odorant concentration (4 levels)] showed an overall significant effect [F (90, 27312.921) = 4.460, $p< 0.001$ (n=262) and met the assumption for sphericity (Mauchly's Test of Sphericity, $\chi2$ (5) = 6.987, p= 0.222)].

There was a significant effect of zone (Fig. 4-7A) [F(2) = 9.375, $p < 0.001$]. Pairwise comparisons with Bonferroni significance level $p < 0.017$ showed that the response amplitude of ORNs in MZ (mean = 48.257, n= 118) was significantly higher than in PZ (mean = 39.083, n = 90, $p < 0.001$). Thus, response amplitude increases as adult-born ORNs mature.

There was a significant effect of odorant type (Fig. 4-7B) [$F(3) = 18.174$, $p < 0.001$]. Pairwise comparisons with Bonferroni significance level $p < 0.017$ showed that the response amplitude to taurine (mean= 55.613, n= 70) was significantly higher than for glutamate (mean=40.771, n=69, $p< 0.001$), AMP (mean= 39.034, n = 71, $p< 0.001$), or NH_4 (mean= 38.772, n = 53, $p< 0.001$).

There was no significant effect of odorant concentration alone (Fig. 4-7C) [$F(3) = 1.710$, $p=0.165$]; however, there were significant interactions. There were differences between odorant concentration and odorant type [$F(9) = 8.631$, $p< 0.001$]. There were differences between odorant concentration and zone [$F(6) =5.066$, $p< 0.001$]. Lastly, there were differences in odorant concentration, odorant type, and zone [$F(18) = 4.628$, $p< 0.001$]. To further assess the effect of odorant concentration, we examined the response trends in each zone for each odorant using 10^{-6} and 10^{-3} M concentrations. In PZ, there was an increase (for taurine) and a decrease (for glutamate, AMP, and ammonium) in the normalized response amplitude with an increase in odorant concentration from 10^{-6} to 10^{-3} M (Fig. 4-7D). In MZ, there was an increase (taurine, AMP and ammonium) and a decrease (glutamate) in the normalized response amplitude with increased concentration (Fig. 4-7E). Lastly in SZ, there was an increase (glutamate, AMP and ammonium) and a decrease (taurine) in the normalized response amplitude (Fig. 4-7F). These data demonstrate heterogeneity in response to odorant concentration based on zone and odorant type, and thus the normalized means may show lack of statistical significant difference. Taken together, these data suggest that as adult-born ORNs age, their sensitivity changes.

4.5 Discussion

The goal of this study was to elucidate which functional changes adult-born ORNs undergo when they mature and age. We tested the hypothesis that adult-born ORNs in spiny lobsters change in odor specificity, sensitivity, or temporal responses as they age. Using Ca^{2+} imaging of ORN somata in LF slice preparations, we analyzed the spontaneous Ca^{2+} oscillations and odor-induced Ca^{2+} transients and examined as variables developmental zone (three zones representing the age of ORNs), odorant type (five compounds tested), and odorant concentration (four concentrations tested). We found an increase in the

percentage of odorant-responsive ORNs as they age from newly-born cells to mature, and a decrease in odorant-responsive ORNs as they get old. As adult-born ORNs age, we show a decrease in the percentage of ORNs that produce spontaneous Ca^{2+} oscillations and an increase in the amplitude of oscillation. ORNs become more broadly tuned as they get old and the response profile, defined by the responses to all odorant types tested, change as adult-born ORNs age. The most effective odorant is the major player for the changes in the response profile. We also show ORNs change in their odor sensitivity with age. This study demonstrates that in spiny lobster the physiological response properties of adult-born ORNs change with their chronological age.

Functional maturation may result from changes due to cellular machinery

Functional maturation of adult-born ORNs may be regulated by the temporal and spatial expression pattern of proteins involved in odor transduction. We recently showed that extracellular Ca^{2+} is the major source of Ca^{2+} for both odor-activated Ca^{2+} transients and spontaneous oscillations, and intracellular Ca^{2+} stores also have some contribution in mature ORNs (Tadesse et al., 2011). In addition, the odor-activated Ca^{2+} responses Ca^{2+} responses may be a reflection of receptor potentials or other signal transduction related events (Tadesse et al., 2011). Our results show an increase in the percentage of odorant-responsive ORNs from proliferation zone (PZ) to mature zone (MZ) and a decrease from MZ to senescence zone (SZ). We also showed a decrease in the percentage of ORNs that undergo spontaneous Ca^{2+} oscillations, an increase in amplitude, and no change in frequency of Ca^{2+} oscillations with age. However, there was no difference in the above parameters between PZ and SZ. These data suggest that adult-born ORNs become more odor-responsive from newly-born cells to mature cells. There is a loss in spontaneous Ca^{2+} oscillations with age.

Our experiments are based on using Ca^{2+} imaging to examine changes in the physiological properties during functional maturation of adult-born ORNs. The changes may be solely due to changes in Ca^{2+} channel expression. Ca^{2+} is an important second messenger in cells since it has numerous and

diverse roles. Ca^{2+} is involved in neuronal development, including proliferation and differentiation (Leclerc et al., 2011), and in mature cells in aging and dying (Gleichmann and Mattson 2011; Toescu and Vreugdhenhil 2010). Ca^{2+} channels in the plasma membrane and in the endoplasmic endoplasmic reticulum are known to maintain Ca^{2+} homeostasis (Clapham 2007). Aging associated changes in Ca^{2+} homeostasis in the brain of mammals and humans have been documented (Toescu and Vreugdenhil 2010). It is highly likely that during maturation of adult-born ORNs in spiny lobsters, voltage-gated Ca^{2+} channels on the plasma membrane of ORN somata and ryanodine receptors / inositol triphosphate receptors ($InsP_3$) on the endoplasmic reticulum also change in expression. These changes in odor-activated Ca^{2+} responses in spiny lobster ORNs may also be due to temporal expression of proteins involved in odor-transduction pathways, similar to what is known during embryonic olfactory development in mammals (Margalit and Lancet 1993; Menco et al., 1994). Mature ORNs in mammals are identified by high levels of expression of cytoplasmic OMP. OMP begins to be expressed during embryonic development and reaches adult-like expression by postnatal day 30 in rats (Margalit and Lancet 1993). A recent study also showed that OMP is necessary for adult-born functional maturation of ORNs expressing mouse odorant receptor 23 (Lee et al., 2011).

There are two hypotheses for odor transduction in spiny lobsters. One hypothesis is that similar to vertebrates, odors activate G-protein-coupled receptors, which through second messenger cascades lead to elicitation of action potentials. Some odor transduction proteins such as G-protein subunits (Gαq and Gβ) and phospholipase C-β, as well as candidate genes for other molecules involved in olfactory physiology, have been identified from the mature zone of clawed lobsters, *Homarus americanus* (Xu and McClintock 1999; Xu et al., 1999; Stepanyan et al., 2006). Rapid changes in IP_3 and cAMP were measured following odor activation (Boeckoff et al., 1994). It would be interesting to see if any of these molecules are associated with functional maturation of ORNs. The second hypothesis is that odors activate ionotropic receptors similar to ORNs in *Drosophila* (Benton et al., 2009). Ionotropic glutamate receptor subunit, GluR1, cloned from *H. americanus* (Hollins et al., 2003) and *P. argus* (Tadesse et al., 2011) showed expression in the somata of all mature ORNs (Hollins et al., 2003; Stepanyan et al., 2004, 2006; Tadesse

et al., 2011). GluR1 in lobsters may be an ionotropic receptor similar to ORNs of *Drosophila* (Benton et al., 2009). IR25, a homolog of GluR1, is expressed in chemoreceptors of arthropods (Croset et al., 2010). Regardless of whether or not GluR1 has a similar function to insect co-receptor Or83b expressed in all ORNs, it may be associated with functional maturation of adult-born ORNs similar to OMPs in rodents.

Although further examination is necessary, association of GluR1 with functional maturation of adult-born ORNs is partially supported by preliminary data using immunocytochemistry labeling for GluR1 subunit and anti-BrdU (an S-phase marker following systemic injection with 5-bromo-2-deoxyuridine). We found fewer ORNs labeled with anti-GluR1 in PZ where more BrdU-positive cells are seen, compared with MZ. Molt stage, which also affects proliferation of ORNs, affected GluR1 labeling (Appendix A). Taken together, these data lead us to hypothesize that GluR1 is involved with functional maturation of adult-born ORNs.

ORNs differs in selectivity and sensitivity with age

Patch clamp electrophysiological recordings from LF slices of mature *P. argus* ORNs showed selectivity to odors (Michel et al., 1991, 1993; Simon and Derby 1995). Our study using Ca^{2+} imaging examined the responses of many ORNs simultaneously, which is a tremendous advantage compared to prior studies. We showed that mature ORNs were odor selective and had a single best response (Figs. 4-5, 6). This suggests that the Ca^{2+} imaging is an effective method to assess odor selectivity.

Our data showed that S_L values were significantly higher in ORNs from the MZ than from the SZ (Fig. 4-4), suggesting lower odor selectivity as ORNs senesce. Ca^{2+} imaging of ORNs biopsied and isolated from middle aged ($\leq$ 45 years old) and older ($\geq$ 65 years old) humans also showed a decrease in odor selectivity based on the response to two odor mixtures: ORNs of young adults responded to only one mixture, while older adults responded to two both mixtures (Rawson et al., 2011). Although our study examined different ages of ORNs in an adult animal and Rawson et al. (2011) examined different ages of humans, they demonstrate ORNs become more broadly tuned as they senesce.

One possible reason that we did not observe a difference in selectivity between PZ and MZ may be due to the quality of the LF slice preparations taken from more distal PZ. On the horizontal developmental axis, the most proximal aesthetasc-bearing PZ (+1 to +3, data not shown) did not produce odor-activated Ca^{2+} transients and thus were not included in our analysis. This was also true for the most distal SZ, which had brittle LF slices making them difficult to manage. Thus, the more proximal SZ was selected for the study. It is highly likely that more immature or older ORNs exist that were not included in our study, and those might show greater differences in selectivity.

Patch clamp electrophysiological recordings of *P. argus* also showed ORNs were sensitive to odors (Michel et al., 1993; Simon and Derby 1995). Most non-olfactory chemoreceptor neurons also found on the antennules had a threshold range of 10^{-9} to10^{-6} M (Schmidt and Melon, 2010). In the current study using Ca^{2+} imaging, the lowest concentration tested was 10^{-6} M which may possibly be a high or saturating concentration. Our data showed that the response amplitude of ORNs was greater in mature than immature ORNs. The response to taurine was greater than the response to glutamate, AMP, or NH_4. Our data suggest that as adult-born ORNs age, their sensitivity also changes. Our data also demonstrates that the Ca^{2+} imaging is superior to patch clamping because we show that it is selective to changes in odorant concentration and the LF slice preparation fairly long lasting.

Changes in odor selectivity and odor sensitivity may be due to changes in the receptor type expression, changes in receptor cell density or change in odor-binding affinity (DeMaria and Ngai 2010). The genes for the odorant receptors have not been identified in crustaceans thus far. However we know based on receptor binding and biochemical assays of sensilla innervated by mature *P. argus* ORNs have different receptor types and different binding affinities. For example, taurine (Olson et al., 1992; Olson and Derby 1995; Sung et al., 1996; Gentilcore and Derby 1998), AMP (Blaustein et al., 1993; Gentilcore and Derby 1998), and glutamate (Burgess and Derby 1997; Gentilcore and Derby 1998) receptors have been characterized. Future studies comparing receptor expression from sensilla innervated by immature and old ORNs will elucidate the role of receptor expression with functional maturation.

Response profiles of ORNs differ across zones

Our cluster analysis suggests that the response profile, defined according to the two most effective odorants, changed as adult-born ORNs age. Immature ORNs had more taurine-best cells that also responded strongly to AMP, mature ORNs had more taurine-best cells, and senescence ORNs had more glutamate-best cells. One hypothesis is that taurine-sensitive receptors may decrease in expression while glutamate-sensitive receptors increase in expression during functional maturation of ORNs. The possible changes in receptor type expression may also account for changes in odor-selectivity (DeMaria and Ngai 2010).

In conclusion, we show that adult-born ORNs change in odor specificity, sensitivity, and temporal responses. We hypothesize that these changes may result from changes in the cellular machinery required for odor-transduction.

4.6 References

Benton R, Vannice KS, Gomez-Diaz C, Vosshall LB. 2009. Variant ionotropic glutamate receptors as chemosensory receptors in *Drosophila*. Cell. 136:149-162.

Blaustein DN, Simmons RB, Burgess MF, Derby CD, Nishikawa M, OlsonKS. 1993. Ultrastructural localization of 5'-AMP odorant receptor sites on the dendrites of olfactory receptor neurons of the spiny lobster. J Neurosci. 13:2821-2828.

Boekhoff I, Michel WC, Breer H, Ache BW. 1994. Single odors differentially stimulate dual second messenger pathways in lobster olfactory receptor cells.J Neurosci. 14:3304-3309.

Burgess MF, Derby CD.1997. Two novel types of L-glutamate receptors with affinities for NMDA and L-cysteine in the olfactory organ of the Caribbean spiny lobster *Panulirus argus*. Brain Res.771:292-304.

Calof AL, Hagiwara N, Holcomb JD, Mumm JS, Shou J. 1996. Neurogenesis and cell death in olfactory epithelium. J Neurobiol. 30:67-81.

ClaphamDE. 2007. Calcium signaling. Cell. 131:1047-1058.

Chen WG. 2009. Symposium overview: A systems approach to studying chemical senses and aging: moving from populations to mechanisms. Ann N Y Acad Sci. 1170:702-7.

Corey EA, Bobkov Y, Ache BW. 2010. Molecular characterization and localization of olfactory-specific ionotropic glutamate receptors in lobster olfactory receptor neurons. Chem Senses 3: P157.

Corey EA, Bobkov Y, Ukhanov K, Ache BW. 2012. Characterization and expression of lobster olfactory variants of ionotropic glutamate receptors. Chem Senses P209.

Croset V, Rytz R, Cummins SF, Budd A, Brawand D, Kaessmann H, Gibson TJ, Benton R. 2010. Ancient protostome origin of chemosensory ionotropic glutamate receptors and the evolution of insect taste and olfaction. PLoS Genet. 6: e1001064.

DeMaria S and Ngai J. 2010. The cell biology of smell. J Cell Biol. 191:443-452.

Derby CD, Cate HS, Gentilcore LR. 1997. Perireception in olfaction: molecular weight sieving by aesthetasc sensillar cuticle determines odorant access to receptor sites in the Caribbean spiny lobster *Panulirus argus*. J. Exp. Biol. 200: 2073-2081.

Derby CD. 2007. Why have neurogenesis in adult olfactory systems? The Presidential Symposium at the 2006 AChemS Conference. Chem Senses 32: 361-363.

Frisina RD. 2009. Age-related hearing loss: ear and brain mechanisms. Ann N Y Acad Sci. 1170:708-717.

Gentilcore LR, Derby CD. 1998. Complex binding interactions between multicomponent mixtures and odorant receptors in the olfactory organ of the Caribbean spiny lobster *Panulirus argus*. Chem Senses. 23:269-281.

Gesteland RC, Yancey RA, Farbman AI. 1982. Development of olfactory receptor neuron selectivity in the rat fetus. Neuroscience. 7:3127-3136.

Gleichmann M, Mattson MP. 2011. Neuronal calcium homeostasis and dysregulation. Antioxid Redox Signal. 14:1261-1273.

Grewe BF, Langer D, Kasper H, Kampa BM, Helmchen F. 2010. High-speed in vivo calcium imaging reveals neuronal network activity with near-millisecond precision. Nat Methods. 7:399-405.

Grünert U, Ache BW. 1988. Ultrastructure of the aesthetasc (olfactory) sensilla of the spiny lobster *Panulirus argus.* Cell Tiss Res 251:95-103.

Harrison PJH, Cate HS, Swanson ES, Derby CD. 2001. Postembryonic proliferation in the spiny lobster antennular epithelium: rate of genesis of olfactory receptor neurons is dependent on molt stage. J Neurobiol 47:51-66.

Harrison PJH, Cate HS, Steullet P, Derby CD. 2003. Amputation-induced activity of progenitor cells leads to rapid regeneration of olfactory tissue in lobsters. J Neurobiol 55:97-114.

Harrison PJH, Cate HS, Derby CD. 2004. Localized ablation of olfactory receptor neurons induces both localized regeneration and widespread replacement of neurons in spiny lobsters. J Comp Neurol 471:72-84.

Hollins B, Hardin D, Gimelbrant AA, McClintock TS. 2003. Olfactory-enriched transcripts are cell-specific markers in the lobster olfactory organ. J Comp Neurol 455:125-138.

Lazarini F, Lledo PM. 2011. Is adult neurogenesis essential for olfaction? Trends Neurosci. 34: 20-30.

Leclerc C, Néant I, Moreau M. 2011. Early neural development in vertebrates is also a matter of calcium. Biochimie. 93:2102-2111.

Lee AC, He J, Ma M. 2011. Olfactory marker protein is critical for functional maturation of olfactory sensory neurons and development of mother preference. J Neurosci. 31:2974-2982.

Lidow MS, Gesteland RC, ShipleyMT, Kleene SJ. 1987. Comparative study of immature and mature olfactory receptor cells in adult frogs. Brain Res. 428:243-258.

Lindsey BW, Tropepe V. 2006. A comparative framework for understanding the biological principles of adult neurogenesis. Prog Neurobiol. 80:281-307.

LinfordNJ, Kuo TH, Chan TP, Pletcher SD. 2011. Sensory perception and aging in model systems: from the outside in. Annu Rev Cell Dev Biol. 27:759-785.

Mackay-Sim A. 2010. Stem cells and their niche in the adult olfactory mucosa. Arch Ital Biol. 148:47-58.

Mair RG. 1986. Ontogeny of the olfactory placode. Experientia. 42:213-223.

Margalit T, Lancet D.1993. Expression of olfactory receptor and transduction genes during rat development. Brain Res Dev Brain Res. 73:7-16.

Michel WC, McClintock TS, Ache BW. 1991. Inhibition of olfactory receptor cells by and odor-activated potassium conductance. J Neurophysiol. 65:446-453.

Michel WC, Trapido-Rosenthal HG, Chao ET, Wachowiak M. 1993. Stereoselective detection of amino acids by lobster olfactory receptor neurons. J Comp Physiol A.171:705-712.

Ming GL, Song H. 2011. Adult neurogenesis in the mammalian brain: significant answers and significant questions. Neuron. 70:687-702.

OlsonKS, Trapido-Rosenthal HG, Derby CD. 1992. Biochemical characterization of independent olfactory receptor sites for 5'-AMP and taurine in the spiny lobster. Brain Res. 583:262-270.

OlsonKS, Derby CD. 1995. Inhibition of taurine and 5'AMP olfactory receptor sites of the spiny lobster Panulirus argus by odorant compounds and mixtures. J Comp Physiol A. 176:527-540.

Rawson NE, Gomez G, Cowart BJ, Kriete A, Pribitkin E, Restrepo D. 2011. Age-associated loss of selectivity in human olfactory sensory neurons. Neurobiol Aging. Nov 8. [Epub ahead of print]

Schmidt M, Melon DeF. 2010. Neuronal processing of chemical information in crustaceans. In Thomas Breithaupt and Martin Thiel. Chemical communications in crustaceans. Springer. p.123-148.

Schmidt M, Tadesse T, Derby CD. 2010. Calcium imaging of response properties of olfactory receptor neurons of spiny lobsters, *Panulirus argus*. Chem Senses 5:P159.

Simon TW, Derby CD.1995. Mixture suppression without inhibition for binary mixtures from whole cell patch clamp studies of in situ olfactory receptor neurons of the spiny lobster. Brain Res. 678:213-224.

Steullet P, Cate HS, Derby CD. 2000a. A spatiotemporal wave of turnover and functional maturation of olfactory receptor neurons in the spiny lobster *Panulirus argus*. J Neurosci 20:3282-3294.

Steullet P, Cate HS, Michel WC, Derby CD. 2000b. Functional units of a compound nose: Aesthetasc sensilla house similar populations of olfactory receptor neurons on the crustacean antennule. J Comp Neurol 418:270-280.

Stepanyan R, Hollins B, Brock SE, McClintock TS. 2004. Primary culture of lobster (*Homarus americanus*) olfactory sensory neurons. Chem Senses 29:179-187.

Stepanyan R, Day K, Urban J, Hardin DL, Shetty RS, Derby CD, Ache BW, McClintock TS. 2006. Gene expression and specificity in the mature zone of the lobster olfactory organ. Physiol Genom 25:224-233.

Stosiek C, Garaschuk O, Holthoff K, Konnerth A. 2003. *In vivo* two-photon calcium imaging of neuronal networks. Proc Natl Acad Sci U S A. 100:7319-7324.

Sung DY, Walthall WW, Derby CD. 1996. Identification and partial characterization of putative taurine receptor proteins from the olfactory organ of the spiny lobster. Comp Biochem Physiol B 115:19-26.

Tadesse T, Schmidt M, Derby CD. 2011. Calcium imaging of olfactory receptor neurons in the spiny lobster, *Panulirus argus*. 573.01/CC5. Neuroscience Meeting Planner. Washington, DC: Society for Neuroscience. Online.

Toescu EC, Vreugdenhil M. 2010. Calcium and normal brain ageing. Cell Calcium. 47:158-164.

Ukhanov K, Bobkov Y, Ache BW. 2011. Imaging ensemble activity in arthropod olfactory receptor neurons in situ. Cell Calcium. 49:100-107.

Xu F, McClintock TS. 1999. A lobster phospholipase C-β that associates with G-proteins in response to odorants. J Neurosci. 19:4881-4888.

Xu F, Bose SC, McClintock TS.1999. Lobster G-protein coupled receptor kinase that associates with membranes and G_{β} in response to odorants and neurotransmitters.J Comp Neurol. 415:449-459.

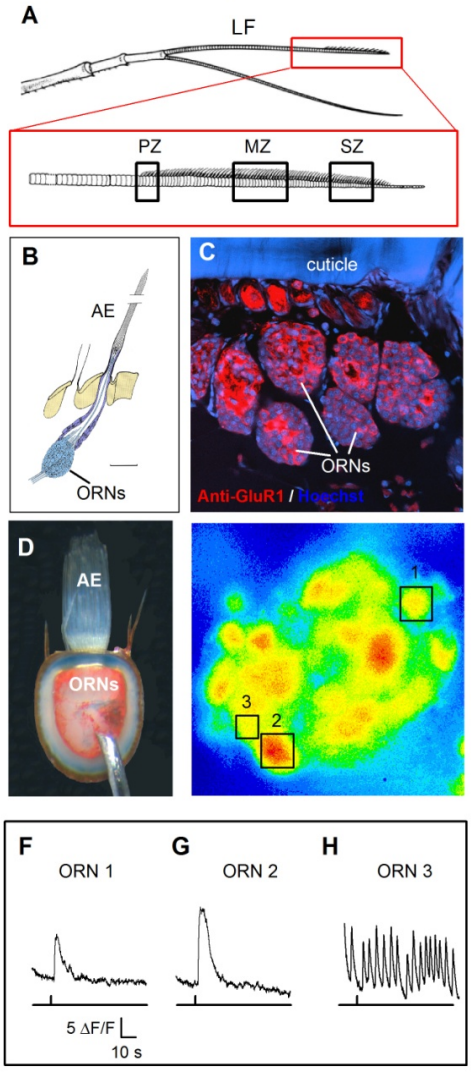

Figure 4-1 Antennular lateral flagellum of the adult spiny lobster, *Panulirus argus*.

(**A**) A schematic drawing of an antennule showing a lateral flagellum (LF) and a medial flagellum, each composed of repeated cuticular units called annuli. The ventral distal region of the LF (red box) contains the aesthetasc sensilla (AE). Inset shows the spatial pattern of ages of aesthetasc sensilla and their olfactory receptor neurons (ORNs), or developmental zones, which result from adult neurogenesis in the LF, with the youngest ORNs in the proliferation zone (PZ), mature ORNs in the mature zone (MZ), and

oldest ORNs in the senescence zone (SZ). (**B)** Schematic drawing of an AE, showing the innervation of the outer dendrites of ca. 300 olfactory receptor neurons (ORNs) (modified from Grünert and Ache, 1988). (**C)** A confocal image of labeling with anti-GluR1 antibody (red) and Hoechst 33258 (blue), a nuclear marker, shows labeling of ORNs in the mature zone. (**D)**Transmitted light micrograph, showing LF slice preparation from the MZ used for Ca^{2+} imaging. Preparation, consisting of 2 aesthetasc-bearing annuli, shows the AE (site of stimulation) and ORNs (site of imaging). **(E)**Mature ORNs loaded with Ca^{2+} indicator dye Oregon Green BAPTA-488. Pseudocolor fluorescent image shows the peak Ca^{2+} transient in response to 1-s stimulation with 1% TetM. (**F-H**) Corresponding time courses of Ca^{2+} signals in ORNs 1 and 2 show responses to 1% TetM. Time course of Ca^{2+} signal in ORN 3 shows spontaneous Ca^{2+}oscillations. This cell does not respond to 1% TetM.

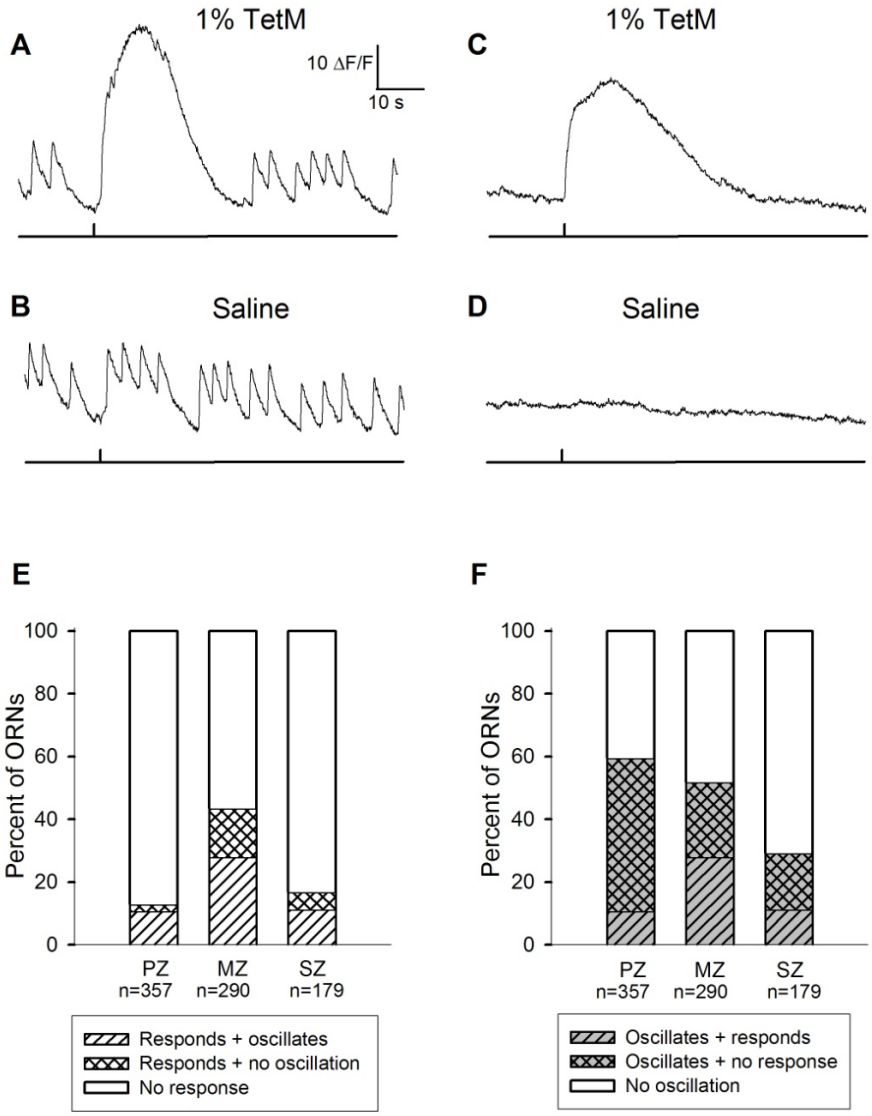

Figure 4-2 Comparison of odor-responsiveness and spontaneous Ca^{2+} oscillations of ORNs in the three developmental zones (PZ, MZ, SZ).

(**A, C**) Representative time course of Ca^{2+} signals of an ORN with spontaneous Ca^{2+} oscillations responds with a Ca^{2+} transient to stimulation with odor, 1% TetM (**A**), but not to saline **(C). (B, D)** Representative

time courses of Ca^{2+} signals of an ORN with no spontaneous Ca^{2+} oscillations responds with a Ca^{2+} transient to stimulation with 1% TetM (**B**) but not to saline **(D)**. (**E-F**) Physiological characterization (odor-responsiveness and spontaneous oscillations) and their distribution across zones for 826 OGB-loaded ORNs. **(E)** Stacked bar graphs show the percentage of cells out of the OGB loaded cells that are odor-responsive and which are with and without spontaneous oscillation. There was a significant difference in the odor-responsiveness across zones. **(F)** Stacked bar graphs show the percentage of cells that have spontaneous oscillation and which were odor responsive or not-odor-responsive. There was a significant difference in the frequency distribution in spontaneous Ca^{2+} oscillations across zones.

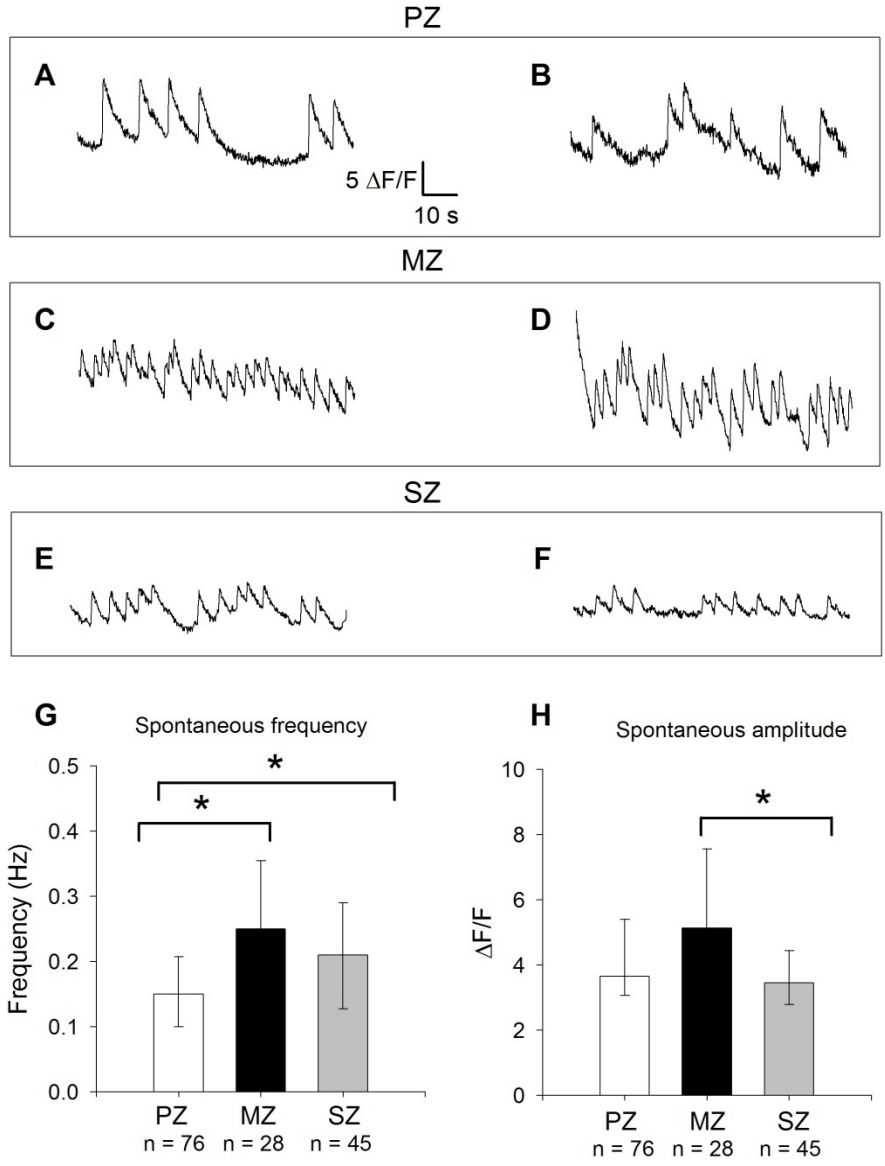

Figure 4-3 Spontaneous Ca^{2+} oscillations of ORNs across zones.

Representative time courses of spontaneous Ca^{2+} oscillations from the PZ (**A, B**), MZ (**C, D**), and SZ (**E, F**). (**G-H**) Bar graphs show the median and 25^{th} /75^{th} percentile of frequency **(G)** and amplitude (**H**) of spontaneous Ca^{2+} oscillations across zones. There was an overall difference in frequency of spontaneous Ca^{2+} oscillations across zones [ANOVA Kruskal Wallis H (2) = 23.663, $p< 0.001$, n = 149; There was

also an overall difference in amplitude of spontaneous Ca^{2+} oscillations across zones [ANOVA Kruskal Wallis (H (2) = 10.015, p = 0.007, n = 149). PZ was significantly lower in the frequency of spontaneous Ca^{2+} oscillations compared with MZ (p = 0.012). There was no significant difference between PZ and SZ (p = 0.136), but there was a strong trend of smaller amplitude in PZ compared to MZ (p = 0.030). SZ was significantly smaller in spontaneous amplitude compared with MZ (p = 0.002). All *post-hoc* analysis for Ranks was adjusted using Bonferroni's correction (significance level p < 0.017).

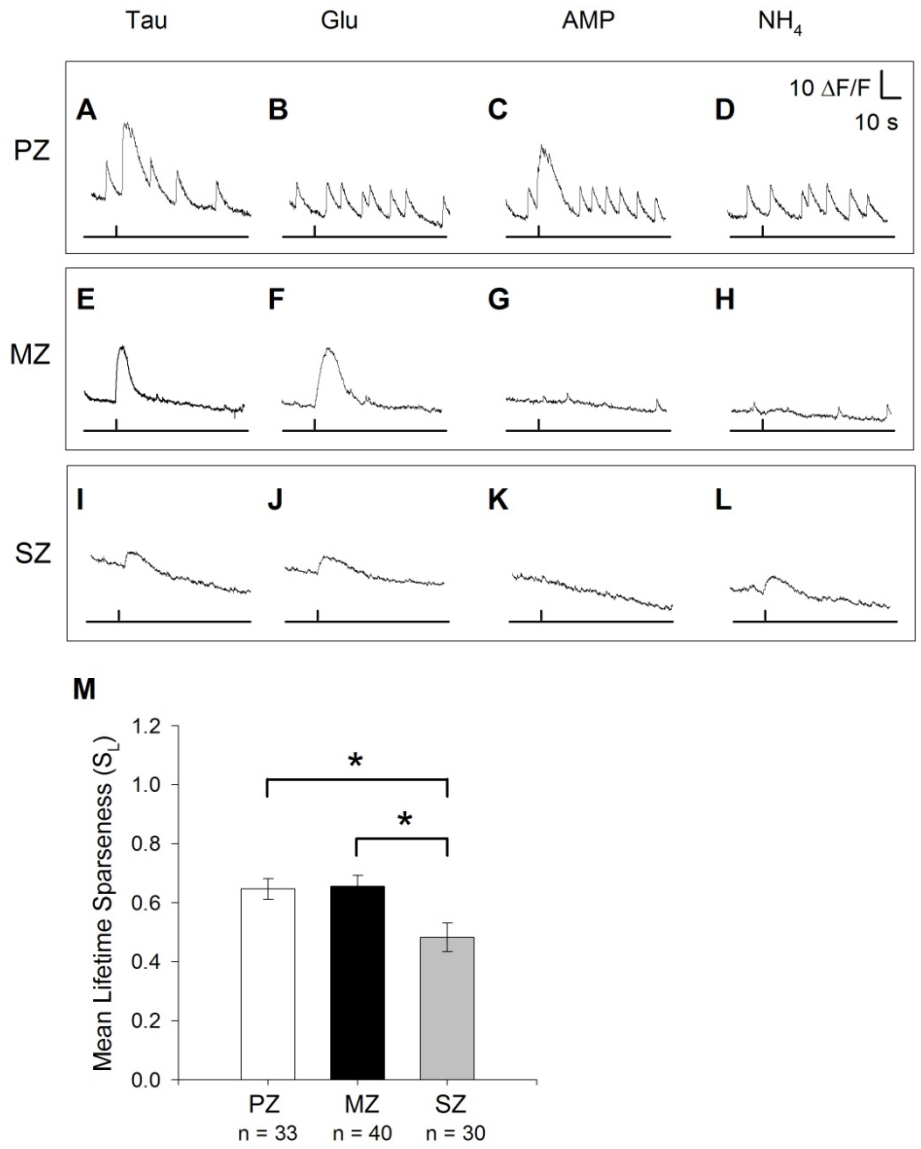

Figure 4-4 Comparison of odor selectivity across zones.

(**A-L**) Representative time courses of Ca^{2+} transients in individual ORNs in response to single odorants taurine (Tau), glutamate (Glu), AMP, and NH_4, each at 10^{-4} M. ORNs in PZ (**A-D**), ORNs in MZ (**E-H**), ORNs in SZ (**I-L**). **M** Bar graph showing the mean lifetime sparseness (S_L) for PZ, MZ, and SZ. ORNs responding to only 1 odorant have a high sparseness (S_L = 1) and ORNs responding equally to each odorant have low sparseness (S_L = 0). There was an overall difference in S_L values across zones (ANOVA: F(2) = 5.167, p = 0.007, for 102 ORNs from 12 LF slices from 4 lobsters). S_L was significantly

higher in MZ than SZ ($P = 0.014$) but not significantly different than PZ ($P = 1.00$). There was no significant difference in S_L between PZ and SZ but there was a strong trend of lower S_L in SZ ($P = 0.021$). *Post-hoc* analysis was adjusted for Bonferroni significance level ($p < 0.017$).

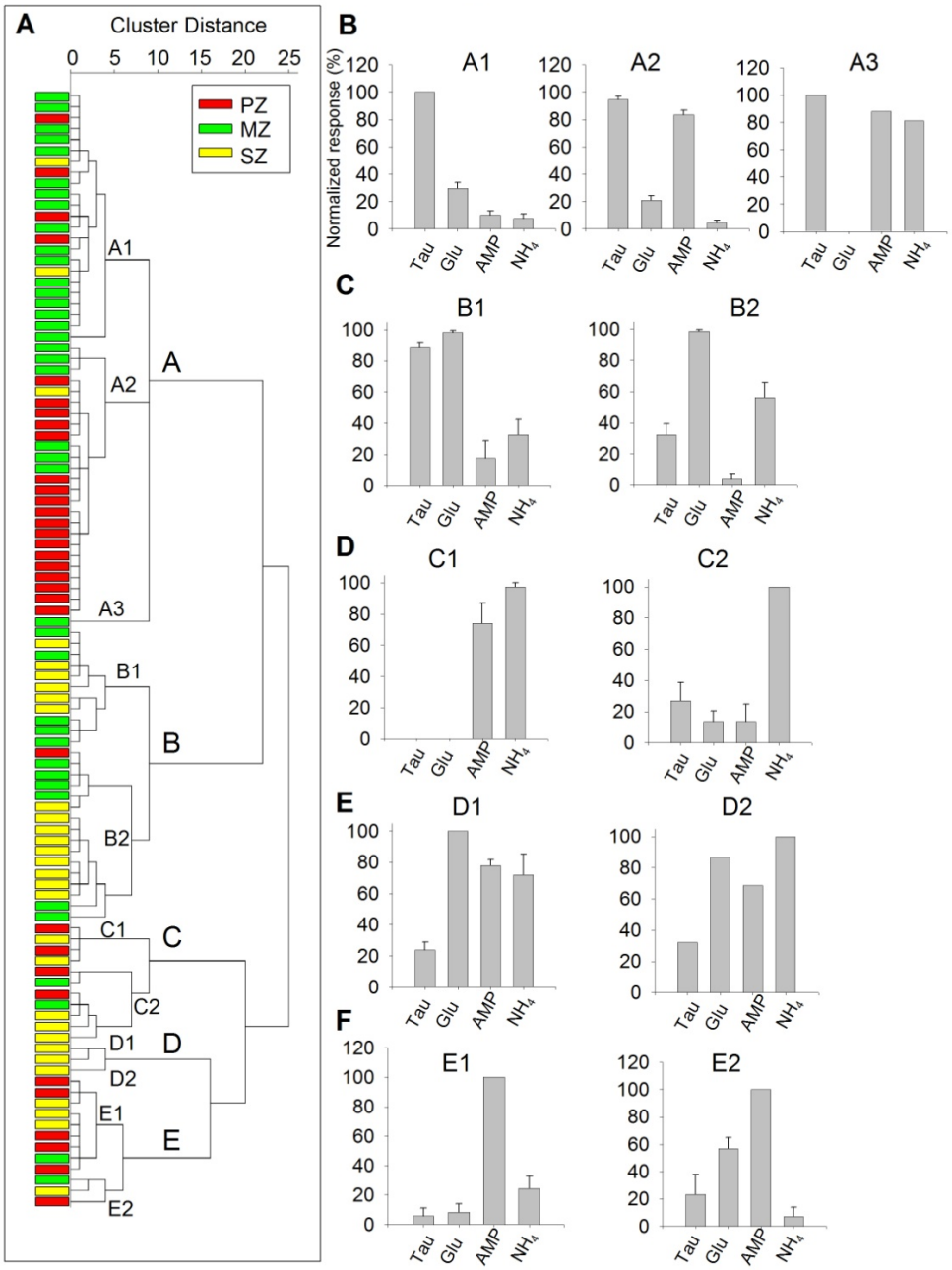

Figure 4-5 Characterization of ORN response profiles using cluster analysis.

(A) Dendrogram showing 5 clusters (A-E) and 11 sub-clusters (A1-E2) of ORNs based on the differences in response profiles to the four odorants taurine (Tau), glutamate (Glu), AMP, and NH_4. Also shown on the dendrogram is the mapping of the developmental zone from which each ORN was recorded: PZ (red), MZ (green), SZ (yellow). **(B-F)** Bar graphs show mean normalized responses ± SEM to the most effective odorant type mapped onto the sub-clusters.

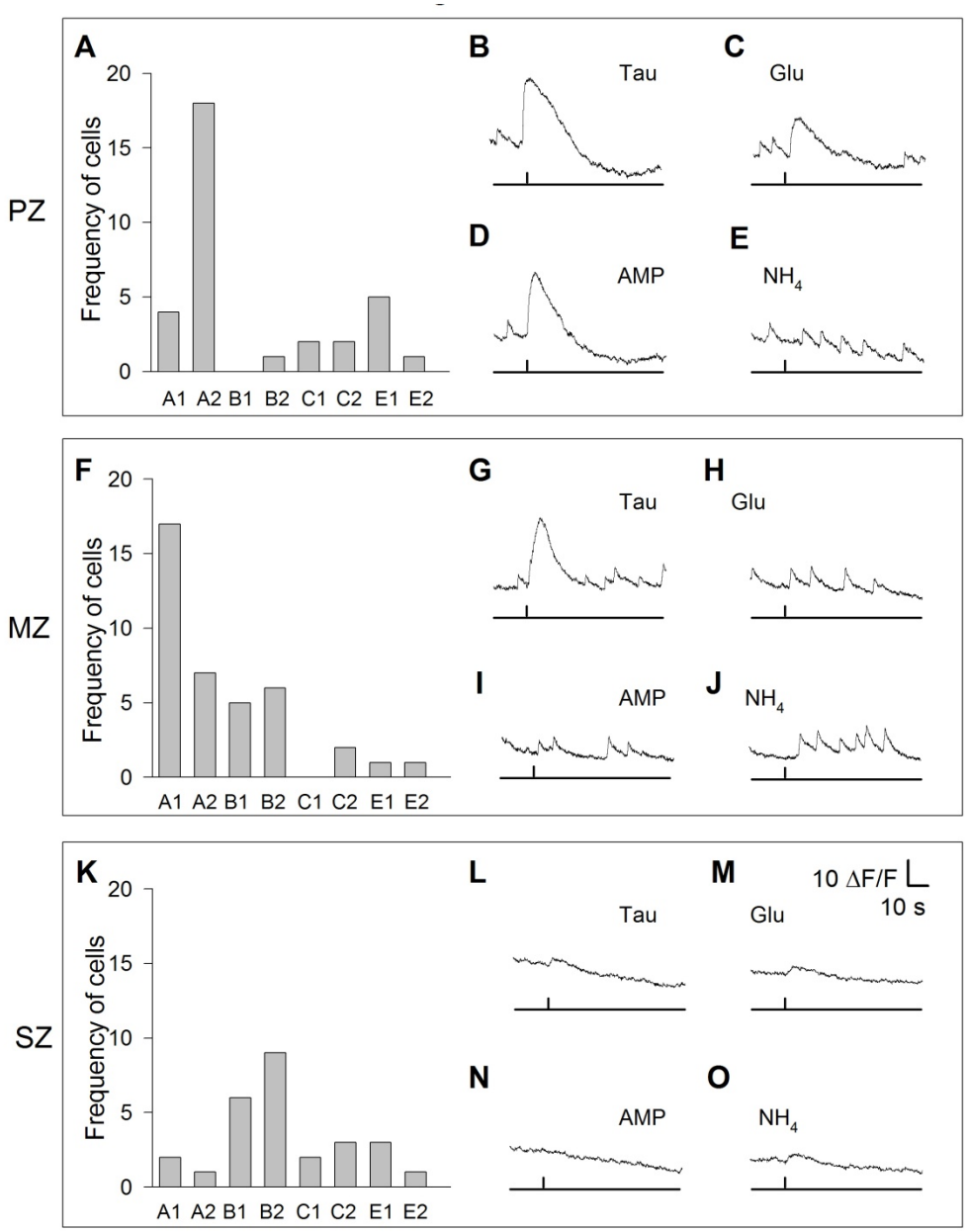

Figure 4-6 Comparison of frequency distributions of ORNs with different response profiles across zones.

(A, **F, K)** show frequency distributions of 8 sub-clusters for the PZ, MZ, and SZ, respectively. There was a significant difference in the distributions (χ^2 (14, n= 98) = 50.06, $p < 0.001$). The differences were between all zones [MZ vs. SZ: χ^2 (7) = 18.67, $p < 0.005$; PZ vs. SZ: χ^2 (7) = 28.60, $p < 0.005$; PZ vs. MZ: χ^2 (7) = 32.26, $p < 0.005$]. Sub-cluster A2, which are taurine-best cells (n=26) that also responded strongly to AMP and weakly to glutamate, was the predominant cell type in PZ. Sub-cluster A1, which are taurine-best cells (A1, n=23), were the predominant cell type in MZ. Sub-cluster B2, which are glutamate-best cells (B2, n=16), were the predominant cell type in SZ. Representative time courses of Ca^{2+} transients in response to single odorants taurine (Tau), glutamate (Glu), AMP, and NH_4 at 10^{-4} M, are shown for one ORN each from PZ (**B-E**), MZ (**G-J**), and SZ (**L-O**).

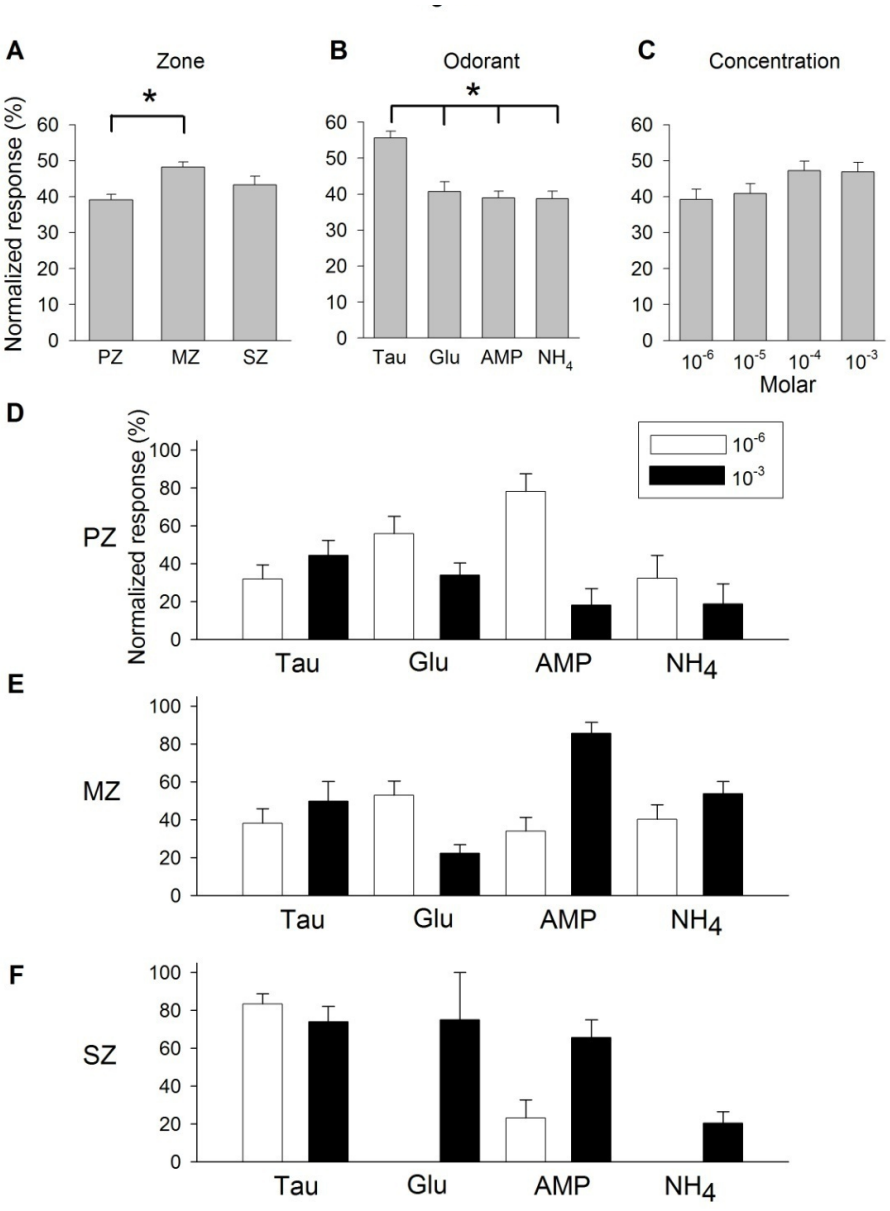

Figure 4-7 Effect of odorant type, concentration of odorant, and developmental zone on the amplitude of the Ca^{2+} response of ORNs.

A two-way ANOVA with repeated measures [zone (3 levels), odorant type (4 levels), odorant concentration (4 levels)] showed an overall significant effect [F (90, 27312.921) = 4.460, p< 0.001 (n=262) and met the assumption for sphericity (Mauchly's Test of Sphericity, $\chi 2$ (5) = 6.987, p= 0.222)]. Bar graphs for the mean normalized Ca^{2+} response amplitude and pairwise comparisons with Bonferroni significance level p < 0.017 are shown for **(A)** zone, **(B)** odorant type, and **(C**) odorant concentration. **(A)** Response amplitude of ORNs in MZ was significantly higher than in PZ (p< 0.001). **(B)** Response amplitude for taurine was significantly higher than for glutamate (p< 0.001), AMP (p< 0.001), or NH_4 (p< 0.001). **(C)** There was no significant effect of odorant concentration [F(3) = 1.710, p=0.165]. **(D, E, F)** Bar graphs showing trends in the mean normalized Ca^{2+} response for PZ, MZ and SZ at 10^{-6} (white bars) and 10^{-3} (black bars) M concentrations of taurine, glutamate, AMP and ammonium.

CHAPTER 5: GENERAL DISCUSSION

This dissertation addressed the molecular, cellular, and physiological changes during adult neurogenesis of ORNs in the antennular lateral flagellum (LF) of the spiny lobster *Panulirus argus.* The spiny lobster is a good model system for studying adult neurogenesis because there is continuous proliferation and turnover of ORNs and associated structures (Steullet et al., 2000; Harrison et al., 2001, 2003). The external olfactory organ is easily accessible, all stages of development of ORNs are present and spatially separated on a horizontal axis (Steullet et al., 2000), and damage-induced regeneration is common (Harrison et al., 2003, 2004).

achaete-scute complex (*ASC*) genes, which encode basic helix-loop-helix transcription factors, are known to regulate embryonic and adult neurogenesis in many animals. The results in Chapter 2 demonstrate that in *P. argus splash* (*sp*iny *l*obster *a*chaete *s*cute homolog) expression is not closely associated with the formation of sensory neurons under normal physiological conditions but may be involved in repair and regeneration. Ca^{2+} is a major contributor for odor activation, modulation, and adaptation of mature ORNs in diverse organisms. Chapter 3 demonstrates that extracellular Ca^{2+} is the major source for odor-activated Ca^{2+} transients and spontaneous oscillations, intracellular Ca^{2+} stores also contribute, and the Ca^{2+} response may not be a reflection of spiking activity. During embryonic development of mammals, sequential expression of odor transduction genes in ORNs coincides with changes in the ORNs' physiological response properties. Thus, the results in Chapter 4 demonstrate that three physiological response properties – odor specificity, odor sensitivity, and spontaneous Ca^{2+} oscillations – change as adult-born ORNs age.

splash may be involved with repair/ regeneration and other roles other than adult neurogenesis

In Chapter 2, the molecular and cellular factors associated with adult neurogenesis were addressed. During embryonic development in *Drosophila*, sensory organ formation originates from expression of *ASC* homologs in unspecified ectodermal cells that form a proneural cluster. The one cell that takes on a neural fate forms the sensory organ (Skeath and Carroll, 1994; Skeath and Doe, 1996). The hypothesis that *splash* is associated with but not restricted to sensory neuron formation in the olfactory organ was tested. If *splash* is a proneural gene and functions in ORN neurogenesis of adult spiny lobsters as do *ASC* homologs of insects, we expected to observe similar expression pattern as described in insects.

As far as we know, this is the first description of the cellular distribution of an *ASC* homolog in an adult arthropod. *splash*, is expressed in the adult antennular LF, a major chemosensory organ in decapod crustaceans. *splash* is expressed in both immature and mature ORNs and also in other cell types. Molt stage, which affects the extent of ORN proliferation, did not affect *splash* expression in proliferating ORNs but it did affect expression in mature ORNs. Damage to the LF, which induces regeneration, also enhanced *splash* expression, suggesting an association between *splash* with regeneration and repair. We conclude that *splash* is not closely associated with the formation of sensory neurons under normal physiological conditions but may be involved in repair and regeneration. We also propose that *splash* has additional roles other than neurogenesis in adult crustaceans.

Molecular mechanisms of adult neurogenesis and regeneration

One of the promising results from Chapter 2 is the association of *splash* with damage-induced repair and regeneration. Inhibiting *splash* expression in the PZ and at the site of damage and assessing the effect on repair and/or regeneration will elucidate the role of *splash*. An additional approach may be to induce local damage to the LF (Harrison et al., 2004) and examine *splash* expression to determine if the extent of LF damage affects the expression. Besides *ASC* homologs, there are numerous candidate genes

possibly involved in adult neurogenesis and regeneration that have yet to be examined. *atonal*, a gene encoding a basic helix loop helix transcription factor, is necessary and sufficient for specifying olfactory sensilla development in fruit flies (Gupta and Rodrigues 1997). Thus far, *atonal* homologue has not been successfully cloned from spiny lobster LF although attempts have been made. Future experiments using different degenerate PCR primers other than the ones previously used may aid in cloning *atonal* and examining the cellular expression patterns similar to the study for *splash*.

In the development of insect sensory neurons, ASC homologs activate *hairy enhancer of split*, which results in delamination of one sensillum progenitor cell and the maintenance of ectodermal fate in the remaining cells of the proneural cluster. The spiny lobster olfactory organ expresses a *hairy - enhancer of split* homolog (Chien et al., 2009), but its cellular localization has yet to be determined. During limb regeneration in fiddler crabs, an expressed sequence tag library of the blastema four days after limb removal identified an *enhancer of split* homolog (Durica et al., 2006). Thus, *splhairy* is another candidate gene that may be involved in adult neurogenesis and/or damage-induced repair and regeneration.

Lastly, there are others genes cloned from the LF of adult intermolt *P. argus* that may be involved in different aspects of adult neurogenesis. Preliminary data (Appendix B) show partial sequences for *notch* receptor (GQ252687.1), *delta* ligand (GQ252686.1), and *ephrin* (GQ252685.1). Notch receptor and delta ligand are involved in differentiation, proliferation, cell fate determination, and apoptosis in *Drosop*hila and other animals (Artavanis-Tsakonas et al., 1999). Eph/ephrins, are membrane-bound proteins expressed in the developing olfactory system of rodents (St John and Key 2001) and insects (Bosing and Brand 2002; Vidovic 2007) are involved with odotopic map formation (Cutforth et al., 2003; Chen and Flanagan 2006).

Future studies examining the above or other candidate genes using semi-quantitative PCR and or *in situ* hybridization will elucidate the molecular factors involved with adult neurogenesis. Comparing different molt stages, developmental zones, and tissues (brain and LF) and examining damage-induced changes may also be necessary. If a correlation with adult neurogenesis or regeneration is established,

then manipulating the gene expression will elucidate the molecular mechanisms. The ORNs from adult *H. americanus* had been successfully maintained in culture (Fadool et al., 1991; Stepanyan et al., 2004) so application of dsRNA interference (RNAi) or small interference (siRNA) is a way to inhibit gene expression. The effect of RNAi inhibition may be determined by using quantitative PCR. There is an advantage of using RNAi as it is easy to synthesize, it is specific to the gene sequence of interest, and it successfully works in an *in vitro* assay. The limitation of using RNAi is the irreversible effect and possibly additional unforeseen effects. If antibodies made against the proteins of the genes of interest become available, then those can also be used to block the protein. Overall, it is feasible to inhibit gene expression in the LF of spiny lobster in an *in vitro* assay.

Odor-induced Ca^{2+} transients and spontaneous Ca^{2+} oscillations in mature ORN

To propose mechanisms underlying changes in physiological responses during functional maturation of adult-born ORNs, and given that Ca^{2+} is a major contributor for odor activation, modulation, and adaptation (Schild and Restrepo 1998; Menini 1999; Matthews and Reisert 2003) in mature ORNs of diverse organisms, it was necessary to understand the role of Ca^{2+} in lobster ORNs. Odor-induced increases in intracellular Ca^{2+} occurs in ORNs across phyla. Odor transduction in mature ORNs of vertebrates is as follows: odors bind to G-protein (G_{olf}) coupled receptors and activate adenylyl cyclase, which leads to formation of cyclic AMP or IP_3. cAMP activates cyclic-nucleotide-gated (CNG) channels, causing an influx of Ca^{2+} and activation of somatic voltage-gated channels. Ca^{2+} is also an important second messenger in neuronal development, including proliferation and differentiation (Leclerc et al., 2011), and in mature cells in aging and dying (Gleichmann and Mattson 2011; Toescu and Vreugdhenhil 2010).

Thus, Chapter 3 examined the mechanisms underlying odor-induced Ca^{2+} transients and spontaneous Ca^{2+} oscillations in mature ORN somata. We established Ca^{2+} imaging of spiny lobster ORNs in an *in vitro* 'LF slice' preparation developed in parallel with Ukhanov et al. (2011). The

establishment of LF slice preparations for Ca^{2+} imaging provides a tremendous advantage for examining the responses of many ORNs simultaneously. This preparation and system is ideal for future studies examining peripheral olfactory coding.

The data show that odor-induced Ca^{2+} transients were reduced in amplitude under low extracellular Ca^{2+} and abolished when blocking Co^{2+} sensitive Ca^{2+} channels. Manipulation of intracellular Ca^{2+} with thapsigargin reduced the amplitude and increased the repolarization time. Blocking tetrodotoxin (TTX) sensitive channels did not affect the mean amplitude of odor-activated Ca^{2+} transients. Spontaneous Ca^{2+} oscillations were reduced and abolished under low extracellular Ca^{2+} and blockage of Co^{2+} sensitive channels, respectively. Both thapsigarin and TTX reduced the amplitude and frequency of spontaneous oscillations.

In summary, we found that extracellular Ca^{2+} is the major source for odor-activated Ca^{2+} transients and spontaneous oscillations, intracellular Ca^{2+} stores also have some contribution, and the Ca^{2+} response may reflect olfactory transduction. These data suggest that odor-induced Ca^{2+} transients may not be due to TTX-sensitive Na^{+} channel spiking activity. Odor-activated influx of Ca^{2+} and the contribution of intracellular stores is a feature of ORNs of other animals; however there is a discrepancy in Ca^{2+} transients and spiking activity in *P. argus*. Future experiments combining patch clamping with Ca^{2+} imaging may further elucidate the mechanism of odor-activated Ca^{2+} transients and spiking activity. The role of Ca^{2+} in odor adaptation or modulation can also be examined in future experiments. Examination of the Ca^{2+} transients following prolonged odor stimulation is a first step. Determining whether this is mediated by inhibition of CNG channels through calcium/calmodulin complex will address the role of Ca^{2+} in odor adaptation of *P. argus* ORNs.

Physiological changes and functional maturation of adult-born ORNs

During embryonic development of mammals, sequential expression of odor transduction genes in ORNs coincides with changes in the ORNs' physiological response properties; whether a similar pattern

of changes occurs in the functional maturation of adult-born ORNs is not known. Chapter 4 tested the hypothesis that adult-born ORNs of spiny lobsters change in odor specificity, sensitivity, or temporal responses as they age. Using calcium imaging of *in situ* ORNs, we found an increase in the percentage of odorant-responsive ORNs as they age from newly-born cells to mature ORNs, and a decrease in odorant-responsive ORNs as they get old. As adult-born ORNs age, we show a decrease in the percentage of ORNs that produce spontaneous Ca^{2+} oscillations and an increase in the amplitude of oscillation. These data suggest that adult-born ORNs become more odor-responsive from newly-born cells to mature cells. There is a decrease in spontaneous Ca^{2+} oscillations with age. ORNs become more broadly tuned as they senesce and the response profile, defined by the responses to all odorant types tested, change as adult-born ORNs age. The most effective odorant type is the major player for the changes in the response profile. We also show ORNs change in their odor sensitivity with age. This study demonstrates that the physiological response properties of adult-born ORNs change with functional maturation.

One hypothesis is that GluR1 is involved with functional maturation of adult-born ORNs. Preliminary data (Appendix A) using immunocytochemistry labeling for anti-GluR1 subunit and S-phase marker following systemic injection with 5-bromo-2-deoxyuridine (BrdU) showed the following: fewer ORNs labeled with anti-GluR1 in PZ where more BrdU-positive cells are seen, compared with MZ and molt stage affected GluR1 labeling, where premolt PZ and MZ had fewer ORNs labeled compared to intermolt. In the future, inhibiting GluR1 gene (GQ252689.1) expression using RNAi or inhibiting the protein using anti-GluR1 antibody, and repeating the experiments in Chapter 4 using LF slice preparation, may elucidate the role in functional maturation of adult-born ORNs.

Model for odor transduction in lobsters

There are two hypotheses for odor transduction in spiny lobsters. One hypothesis is that similar to vertebrates, odors activate G-protein-coupled receptors (OR), which through second messenger cascades lead to elicitation of action potentials (Fig. 5-1). The second hypothesis is that odors activate ionotropic

receptors (IR) similar to ORNs in *Drosophila* (Benton et al., 2009). Changes in odor selectivity and odor sensitivity may be due to changes in odor transduction machinery. Firstly, receptor cell density or changes in odor-binding affinity of ORs or IRs may affect the response properties. Receptor binding and biochemical assays of sensilla innervated by mature *P. argus* ORNs have different receptor types and different binding affinities. Secondly, based on the odor transduction model (Fig. 5-1) it is likely that there are differences in ion channel expression across the different zones of LF. Ion channel expression, more specifically, Ca^{2+} channels with developmental zone can be examined. Future studies can compare differences in receptor expression from sensilla innervated by immature, mature and old ORNs.

ORNs became more broadly tuned with age. It is possible that cell number may impact the breadth of tuning. If there are less ORNs in SZ compared to MZ, then cells in SZ may have to be broadly tuned to maintain optimal olfactory detection. Broadening of tuning may also be due to differences in receptor expression. It is possible that two cells have the same S_L value but maybe caused by different odorant receptor expression. This may result in a lack of odor discrimination, thus older cells at a given concentration may not distinguish two odorants. This result may also be affected by odor sensitivity. Older cells may require higher concentrations of odorants for optimal odor discrimination.

The results in Chapter 4 are based on Ca^{2+} responses to single odorants that are excitatory according to previous electrophysiological results. Examining the responses to other single odorants that give excitatory responses and odorants that give inhibitory responses may reveal whether the changes in physiological properties depend on the type of odorant/ receptor. Experiments using mixtures are more biologically relevant as animals typically are exposed to mixtures in their natural habitat and not to single odorants. Comparing the responses to mixtures that have different behavioral output, for example, food-related mixtures vs. pheromone blends will elucidate whether developmental age is a factor.

Spontaneous Ca^{2+} oscillations in ORNs

To our knowledge, the function of spontaneous Ca^{2+} oscillations in mature ORNs is not known. The TTX treatment suggests that some ORNs may contribute to spontaneous spiking activity. However, spontaneous Ca^{2+} oscillations in the majority of ORNs are unaffected by the TTX treatment, suggesting that those ORNs may have other functions. One hypothesis is that spontaneous Ca^{2+} oscillations in mature ORNs may affect gene transcription. Specifically, the frequency of oscillation could influence the expression of specific genes by activating a given transcription factor. It may affect the excitability of the ORN or may affect other signaling pathways that are involved in maintaining the cellular machinery.

Our experiments capture a short time (~80 sec) of the spontaneous Ca^{2+}oscillations. It is possible that the frequency of oscillation changes over a longer period of time. Nevertheless, changes in spontaneous Ca^{2+} oscillations across the different developmental zones may mean that the frequency of the same gene expression changes. It could also mean that different genes are expressed in the different zones depending on the frequency of oscillation. It is also possible that spontaneous Ca^{2+} oscillations have different functions depending on the developmental zone. For example, in PZ it may affect cellular proliferation and in SZ it may affect apoptosis. Lastly, the changes in spontaneous Ca^{2+} oscillations could be due to changes in plasma membrane and endoplasmic reticulum Ca^{2+} channel expression (Fig. 5-1).

Future directions for the field of adult neurogenesis

Adult neurogenesis occurs in restricted areas of the central and peripheral nervous system in diverse organisms but the mechanisms and functional significance of adult neurogenesis are not fully known. Although there is some progress in elucidating the mechanisms mediating adult neurogenesis across phyla, research on the functional significance of adult neurogenesis is lagging. Why do animals have adult neurogenesis? What do they use it for? To answer these types of questions, it will be necessary to link the genetic information to the behavioral output. One approach is to manipulate adult neurogenesis

in the periphery and examine the behavioral response. It is also important to understand how this peripheral manipulation affects the molecular and physiological response of neurons in the brain. Lastly, the link, or the lack thereof, between damage-induced repair and adult neurogenesis needs to be investigated. It is still not known whether the same mechanisms mediating adult neurogenesis are similar or different in adult regeneration. Understanding the mechanisms and function of adult neurogenesis will have a tremendous contribution for the advancement of therapeutics using adult neural stem cells.

5.1 References

Artavanis-Tsakonas S, Rand MD, Lake RJ. 1999. Notch signaling: cell fate control and signal integration in development. Science. 284: 770-776.

Benton R, Vannice KS, Gomez-Diaz C, Vosshall LB. 2009. Variant ionotropic glutamate receptors as chemosensory receptors in *Drosophila*. Cell. 136:149-162.

Bossing T and Brand AH. 2002. Dephrin, a transmembrane ephrin with a unique structure, prevents interneuronal axons from exiting the *Drosophila* embryonic CNS.Development. 129: 4205-4218.

Chen Y and Flanagan JG. 2006. Follow your nose: Axon pathfinding in olfactory map formation. Cell. 127: 881-884.

Chien H, Tadesse T, Liu H, Schmidt M, Walthall WW, Tai PC, Derby CD. 2009. Molecular cloning and characterization of homologs of *achaete–scute* and *hairy–enhancer of split* in the olfactory organ of the spiny lobster *Panulirus argus*. J Molec Neurosci. 39:294-307.

Cutforth T, Moring L, Mendelsohn M, Nemes A, Shah NM, Kim MM, Frisen J, Axel R. 2003. Axonal ephrin-As and odorant receptors: coordinate determination of the olfactory sensory map. Cell. 114: 311-322.

Durica DS, Kupfer D, Najar F, Lai H, Tang Y, Griffin K, Hopkins PM, Roe B. 2006. EST library sequencing of genes expressed during early limb regeneration in the fiddler crab and transcriptional responses to ecdysteroid exposure in limb bud explants. Integr Comp. Biol. 6:948-964.

Fadool DA, Michel WC, Ache BW. 1991. Sustained primary culture of lobster (Panulirus argus) olfactory receptor neurons. Tissue Cell. 23:719-731.

Gleichmann M, Mattson MP. 2011. Neuronal calcium homeostasis and dysregulation. Antioxid Redox Signal. 14:1261-1273.

Gupta BP, Rodrigues V. 1997. Atonal is a proneural gene for a subset of olfactory sense organs in *Drosophila*. Genes Cells. 2:225-233.

Harrison PJH, Cate HS, Swanson ES, Derby CD. 2001. Postembryonic proliferation in the spiny lobster antennular epithelium: rate of genesis of olfactory receptor neurons is dependent on molt stage. J Neurobiol. 47:51-66.

Harrison PJH, Cate HS, Steullet P, Derby CD. 2003. Amputation-induced activity of progenitor cells leads to rapid regeneration of olfactory tissue in lobsters. J Neurobiol. 55:97-114.

Harrison PJH, Cate HS, Derby CD. 2004. Localized ablation of olfactory receptor neurons induces both localized regeneration and widespread replacement of neurons in spiny lobsters. J Comp Neurol. 471:72-84.

Leclerc C, Néant I, Moreau M. 2011. Early neural development in vertebrates is also a matter of calcium. Biochimie. 93:2102-2111.

Matthews HR, Reisert J. 2003. Calcium, the two-faced messenger of olfactory transduction and adaptation. Curr Opin Neurobiol. 13:469-475.

Menini A.1999. Calcium signaling and regulation in olfactory neurons. Curr Opin Neurobiol. 9:419-426.

Schild D, Restrepo D. 1998. Transduction mechanisms in vertebrate olfactory receptor cells. Physiol Rev. 78:429-466.

Skeath JB, Carroll SB. 1994. The *achaete-scute* complex: generation of cellular pattern and fate within the *Drosophila* nervous system. FASEB J 8:714-721.

Skeath JB, Doe CQ. 1996. The *achaete-scute* complex proneural genes contribute to neural precursor specification in the *Drosophila* CNS. Curr Biol 6:1146-1152.

Stepanyan R, Hollins B, Brock SE, McClintock TS. 2004. Primary culture of lobster (*Homarus americanus*) olfactory sensory neurons. Chem. Senses. 29:179-187.

Stepanyan R, Day K, Urban J, Hardin DL, Shetty RS, Derby CD, Ache BW, McClintock TS .2005. Gene expression and specificity in the mature zone of the lobster olfactory organ. Physiol Genomics 25: 224-233.

Steullet P, Cate HS, Derby CD. 2000. A spatiotemporal wave of turnover and functional maturation of olfactory receptor neurons in the spiny lobster *Panulirus argus*. J Neurosci 20:3282-3294.

St John JA, Key A. 2001. EphB2 and two of its ligands have dynamic protein expression patterns in the developing olfactory system. Brain Res Dev Brain Res. 126: 43-56.

Toescu EC, Vreugdenhil M. 2010. Calcium and normal brain ageing. Cell Calcium. 47:158-164.

Ukhanov K, Bobkov Y, Ache BW. 2011. Imaging ensemble activity in arthropod olfactory receptor neurons in situ. Cell Calcium. 49:100-107.

Vidovic M, Nighorn A, Koblar S, Maleszka R. 2007. Eph receptor and ephrin signaling in developing and adult brain of the honeybee (*Apis mellifera*). Dev Neurobiol. 67:233-251.

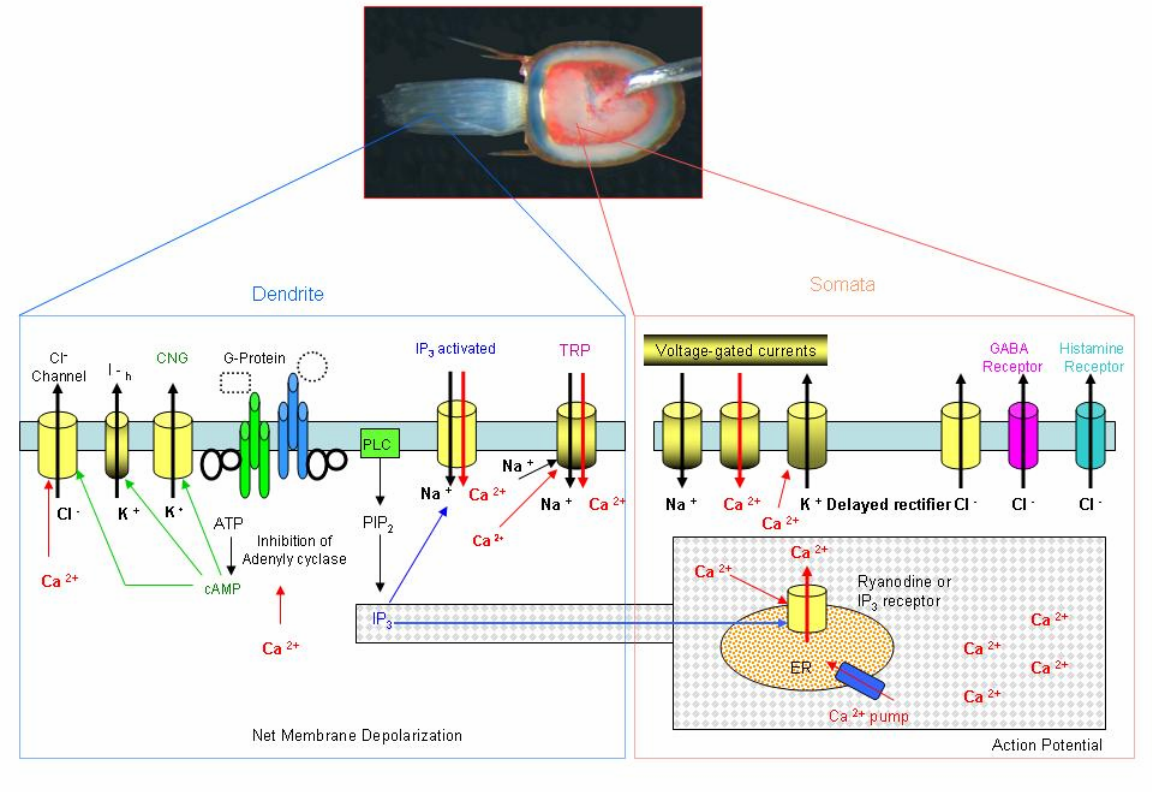

Figure 5-1 A model for odor transduction cascade for ORNs based on the results from *H. americanus* and *P. argus* is shown.

Odors activate G-proteins (Gαq and Gβ) that associate with phospholipase C-β (Xu and McClintock 1999; Xu et al., 1999) to mediate synthesis of the 2nd messenger inositol 1,4,5-triphosphate (IP_3) (Fadool and Ache, 1992; Boekhoff et al., 1994). IP_3 activates cyclic nucleotide gated non-selective cation (CNG) channels and in turn cause an influx of Na^+ and Ca^{2+}. Ca^{2+} activated Cl^- channels depolarize the cell further and activate somatic voltage-gated Na^+ and Ca^{2+} channels, which further depolarize the cell and result in spiking activity in the axon. Odor-activated Ca^{2+} transients arise from influx of extracellular Ca^{2+} and Ca^{2+} from the endoplasmic reticulum.

APPENDICES

Appendix A*: *Gene cloning and immunocytochemical labeling of ionotropic glutamate receptor (GluR1) from the lateral flagellum of P. argus.

INTRODUCTION

ORNs are housed in aesthetasc sensilla on the lateral flagellum (LF) of the paired first antennae, or antennules. Aesthetascs and their ORNs are added in the proximal proliferation zone (PZ) of the LF (Steulletet al., 2000). These ORNs mature (i.e. become responsive to chemical stimuli in the mature zone (MZ). Aesthetasc sensilla and their associated ORNs become old in the senescence zone (SZ) and are gradually shed with each molt (Harrisonet al., 2001, 2003). The rate of addition of ORNs in the PZ is dependent on molt stage. Addition of cells is highest in premolt compared to postmolt or intermolt animals (Harrisonet al., 2001).

Ionotropic glutamate receptor subunit, GluR1, cloned from *H. americanus* (Hollinset al., 2003) and *P. argus* (Tadesse et al., 2011) showed expression in the somata of all mature ORNs (Hollinset al., 2003; Stepanyanet al., 2004, 2006; Tadesse et al., 2011). This study tested the hypothesis that GluR1 is associated with functional maturation of adult-born ORNs. Using immunocytochemical labeling with anti-GluR1 antiserum, S-phase marker following systemic injection with 5-bromo-2-deoxyuridine anti-BrdU, and Hoechst 33258, a nuclear marker, I examined GluR1 expression in the PZ and MZ from premolt and intermolt LF.

MATERIAL AND METHODS

Tissue preparation and ICC

Each piece was hemisectioned and fixed in 4% paraformaldehyde (PFA) overnight, decalcified for 5 days in 0.5 M disodium ethylenedeamine tetraacetate (EDTA), and stored in 0.1 M Sörensen phosphate buffer (SPB) in 4° C. Each hemisectioned tissue was embedded in 15% gelatin 75-100 bloom in 0.1 M SPB and fixed overnight in 4% PFA. 4% PFA was discarded and tissues were rinsed in 0.1 M SPB. Tissues were sectioned at 50 µm using a vibratome. Free floating sections were immersed in 1.4 ml of 0.1 M TSPB (SPB, sodium azide, and 0.3% Triton-X-100), and anti-GluR1 antibody (1:500 dilution) was placed on the sections. The sections remained on the shaker overnight at room temperature. Sections were rinsed 4 times in 0.1 M TSPB for 30 min each. Alexa 488 goat anti-rabbit for GluR1 antibody (1:400 dilution) was then placed on the slides as a secondary antibody, along with phallodin 568 (1:50 dilution). The sections were left on a shaker over night at room temperature. On the last day, the sections were rinsed using 0.1 M SPB twice for 30 min. each. Then 10 µl of Hoechst (1 ml/ml) (a nuclear marker) was added to 1.4 ml of 0.1 M SPB and rinsed for 30 min. Finally, the sections were rinsed in 0.1 M SPB for 30 min, placed on slides, and cover slipped. Images were captured using Leica DC 500 camera attached to an Axioplan 2 microscope.

RESULTS

In the figures below, the annulus number is as follows: annulus ‘1’ represents the most proximal aesthetasc-bearing annulus. Annuli proximal to ‘1’ have progressively larger negative numbers, and annuli distal to ‘1’ have progressively larger positive numbers. According to this numbering scheme, the PZ is represented by annuli -10 to 12, with the proximal PZ being annuli -10 to -5, the middle PZ being annuli -4 to 4, and the distal PZ being annuli 5 to 12. The mature zone is represented by annuli 13 to 52.

REFERENCES

Harrison PJH, Cate HS, Swanson ES, Derby CD. 2001. Postembryonic proliferation in the spiny lobster antennular epithelium: rate of genesis of olfactory receptor neurons is dependent on molt stage. J Neurobiol 47:51-66.

Harrison PJH, Cate HS, Steullet P, Derby CD. 2003. Amputation-induced activity of progenitor cells leads to rapid regeneration of olfactory tissue in lobsters. J Neurobiol 55:97-114.

Hollins B, Hardin D, Gimelbrant AA, McClintock TS. 2003. Olfactory-enriched transcripts are cell-specific markers in the lobster olfactory organ. J Comp Neurol 455:125-138.

Steullet P, Cate HS, Derby CD. 2000a. A spatiotemporal wave of turnover and functional maturation of olfactory receptor neurons in the spiny lobster *Panulirus argus*. J Neurosci 20:3282-3294.

Stepanyan R, Hollins B, Brock SE, McClintock TS. 2004. Primary culture of lobster (*Homarus americanus*) olfactory sensory neurons. Chem Senses 29:179-187.

Stepanyan R, Day K, Urban J, Hardin DL, Shetty RS, Derby CD, Ache BW, McClintock TS. 2006. Gene expression and specificity in the mature zone of the lobster olfactory organ. Physiol Genom 25:224-233.

Tadesse T, Schmidt M, Walthall WW, Tai PC, Derby CD. 2011. Distribution and function of *splash*, an *achaete-scute* homolog in the adult olfactory organ of the Caribbean spiny lobster *Panulirus argus*. Dev Neurobiol.71:316-335.

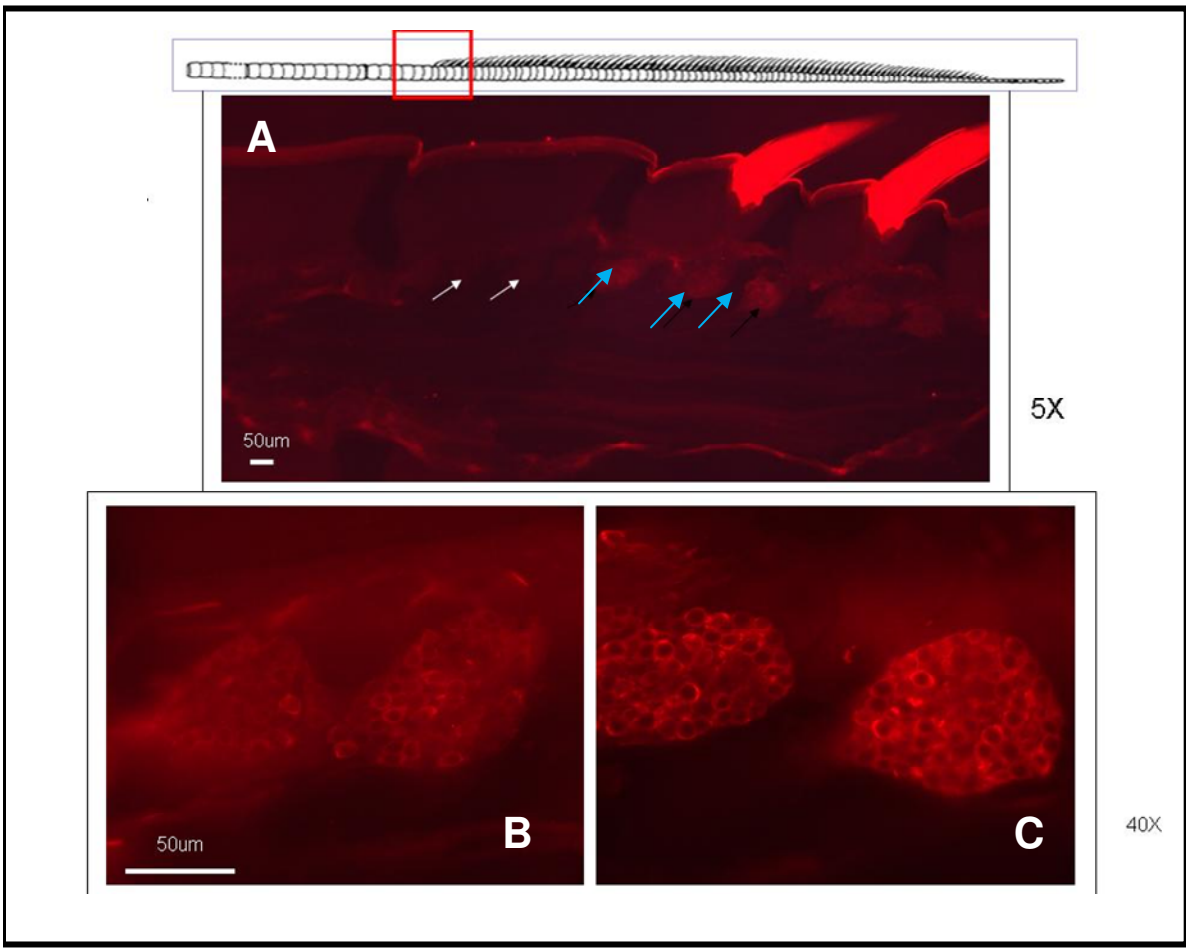

Figure A-1 Immunocytochemical labeling with anti-GluR1 in the proliferation zone

(A) Sagittal section from the proliferation zone shows immature ORN clusters that are not associated with a sensilla (white arrows) and those that are associated (blue arrows). **(B)** There is anti-GluR1 labeling in somata of immature ORNs that are not associated with a sensilla. **(C)** There is more labeling in immature ORNs associated with a sensilla.

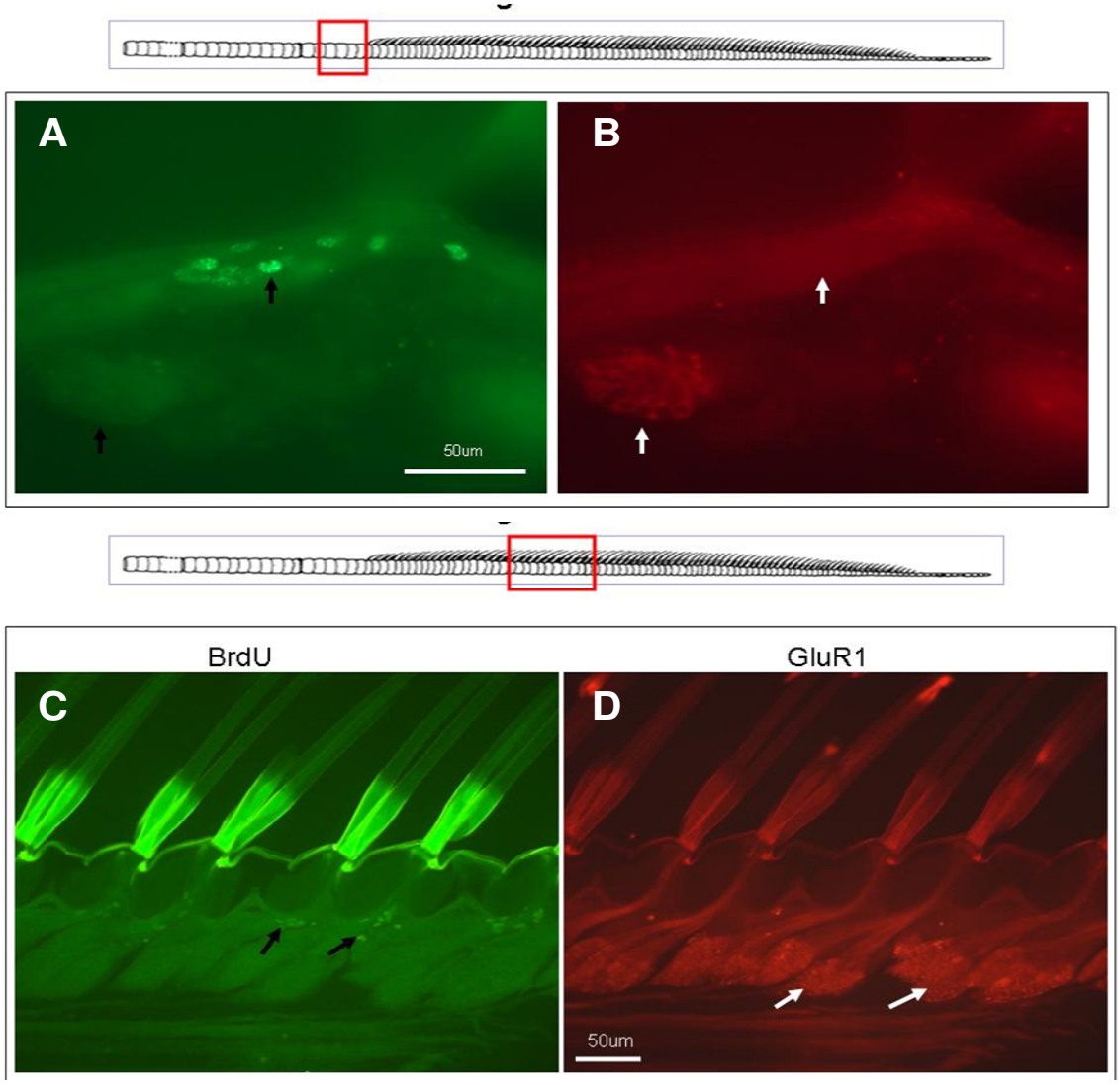

Figure A-2 Double labeling with anti-GluR1 and anti-BrdU in LF.

(A) Anti-BrdU labeling of epithelial cells (black arrow) in proximal PZ and not of ORN clusters. **(B)** Double labeling shows anti-GluR1 labeling of ORN clusters and not of epithelial cells (white arrows). **(C)** Anti-BrdU labeling of epithelial cells (black arrows) in the mature zone. **(D)** Anti-GluR1 labeling of mature ORN clusters (white arrows).

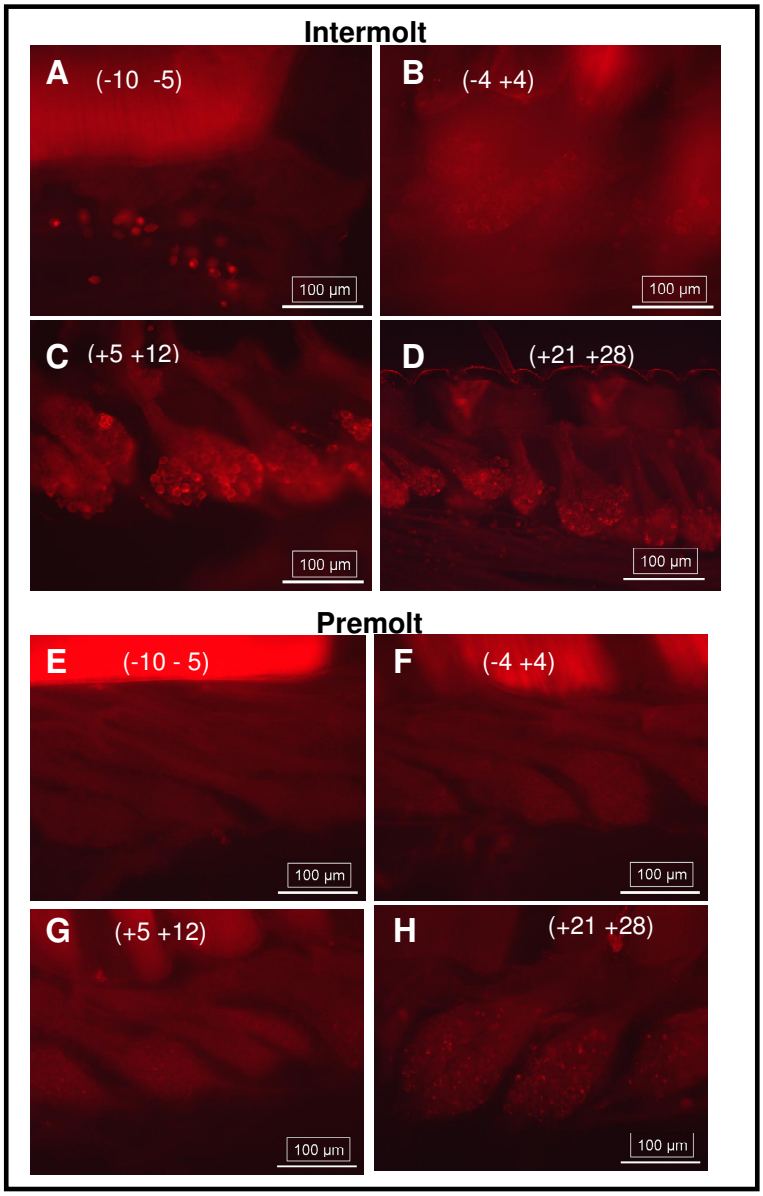

Figure A-3 Immunocytochemistry labeling with anti-GluR1 in LF.
(A) In the -10 -5 region of PZ, ORN clusters have not begun to form. The staining in this figure results from other types of cells that picked up the stain but not neurons. **(B)** In the -4 +4 zone, there is clearly labeling of GluR1 in some but not all cells. **(C-D)** In the +5 and above region, there is abundant labeling of GluR1. **(E)** In premolt -10 -5 region of PZ, there is no GluR1 labeling in the ORN clusters. **(F)** In the -4 +4 region, there are some cells that have GluR1 labeling. **(C-D)** The +5 and above region shows GluR1 labeling but it is less intense.

Figure A-4 Partial sequence of *GluR1* homolog cloned from the antennular LF of spiny lobster. *GluR1* gene sequence cloned from the LF (Accession # GQ252689.1).

Appendix B: *Gene cloning and expression of notch, delta and, ephrin-B from the lateral flagellum of P. argus.*

INTRODUCTION

Notch encodes a 300-kD single-pass transmembrane protein receptor first characterized in *Drosophila melanogaster* (Artavanis-Tsakonas et al., 1983; Johansen et al., 1989), Notch signaling is activated by ligands Delta and Serrate, which are single-pass transmembrane proteins expressed in neighboring cells. Notch signaling is involved in cellular proliferation, differentiation, fate determination, and apoptosis (Artavanis-Tsakonas et al., 1999). For example, activation of the neurogenic receptor gene *Notch* (Baker 2000) and ligand *Delta* induces ectodermal cells to become neuroblasts during early development in *Drosophila* (Appel et al., 2001). Notch signaling also regulates the formation of eyes, wings, antennae, and legs in Drosophila (Kurata et al., 2000). Notch and Delta are also found in a variety of other species, where they also play a role in many developmental processes mediating intercellular communication.

Axonal pathfinding is also an important part of adult neurogenesis as this is the basis for the peripheral sensors to connect to the central nervous system. Newly-born olfactory receptor neurons (ORNs) send their axons and find their target in the brain. In spiny lobsters, axons of sensory neurons of aesthetasc and non-aesthetasc sensilla innervate the olfactory lobes and lateral antennular neuropils, respectively (Schmidt and Ache, 1992; Schmidtet al., 1992). Candidate genes for axonal pathfinding are the Eph receptor and ephrin ligand (Dearborn et al., 2002) that regulate many aspects of development and plasticity such as neurite outgrowth (Zhou et al., 2001), dendritic morphology, and synaptic plasticity (Goldshmit et al., 2006; Liu et al., 2006). Eph/ephrin signaling is involved in adult neurogenesis in rodents. For example, ephrin B ligands are expressed in astrocytes, which are thought to be adult neural stem cells of the subventricular zone (SVZ). Eph receptors are expressed in the SVZ and olfactory bulb. Disrupting this receptor-ligand interaction inhibited the migration of neuroblasts and increased the

number of astrocytes (Conover et al., 2000). A homologue of ephrin B was cloned from the mature zone of the lateral flagellum (LF) in adult lobsters, *Homarus americanus* (Stepanyan et al., 2005).

RESULTS

I cloned a *notch* homologue in the LF of the Caribbean spiny lobster, *Panulirus argus*, using degenerate primers from *Strigamia maritima* (Chipman and Stollewerk, 2006) for PCR amplification (Fig. B-1). I identified a total of five independent *notch* clones from the N' terminal end containing the epidermal growth factor (EGF) repeat. I also identified additional *notch* clones with various lengths; however, further analysis of these sequences is required. The identity of *notch* was determined based on nucleotide and translated amino acid sequences using the NCBI database. I found one clone containing a partial sequence for *delta* homologue in spiny lobsters, which is also within the EGF repeat (Fig. B-5).

Semi-quantitative PCR normalized to GAPDH shows that the LF from intermolt animals has *notch* expression in all zones (Fig. B-2). *notch* expression is highest in premolt LF and some in intermolt but not postmolt LF (Fig. B-3).In intermolt animals, *notch* is also expressed in brain and eye but not muscle tissue. In premolt, *notch* expression is undetectable in the brain and muscle but present in the eye (Fig. B-4).

The aim was to determine whether *ephrin B* signaling is involved in proliferation, differentiation, and/or maturation of ORNs in adults. Using degenerate PCR primers, I cloned an *ephrin* homologue from the LF of adult spiny lobsters (Fig. B-6). A total of ten clones were identified containing the ephrin domain. ICC labeling with anti-ephrin in the brain showed some labeling of unidentified cells (Fig. B-7).

REFERENCES

Appel B, Givan L, Eisen JS.2001.Delta-Notch signaling and lateral inhibition in zebrafish spinal cord development. Dev Biol. 1:13.

Artavanis-Tsakonas S, Muskavitch MA, Yedvobnick B. 1983. Molecular cloning of Notch, a locus affecting neurogenesis in *Drosophila melanogaster*. Proc Natl Acad Sci USA. 80: 1977-1981.

Artavanis-Tsakonas S, Rand MD, LakeRJ. 1999. Notch signaling: cell fate control and signal integration in development. Science. 284: 770-776.

Chipman AD, Stollewerk A. 2006. Specification of neural precursor identity in the geophilomorph centipede *Strigamia maritima*. Dev Biol.290:337-350.

Conover JC, Doetsch F, Garcia-Verdugo JM, Gale NW, Yancopoulos GD, Alvarez-Buylla A. 2000. Disruption of Eph/ephrin signaling affects migration and proliferation in the adult subventricular zone. Nat Neuroscience. 3:1091-1097.

Dearborn R Jr, He Q, Kunes S, Dai Y. 2002. Eph receptor tyrosine kinase-mediated formation of a topographic map in the *Drosophila* visual system. J Neurosci 22: 1338-1349.

Goldshmit Y, McLenachan S, Turnley A. 2006. Roles of Eph receptors and ephrins in the normal and damaged adult CNS. Brain Res Rev. 52:327-345.

Johansen KM, Fehon RG, Artavanis-Tsakonas S. 1989. The notch gene product is a glycoprotein expressed on the cell surface of both epidermal and neuronal precursor cells during *Drosophila* development. J Cell Biol. 2427-2440.

Kurata S, Go MJ, Artavanis-Tsakonas S, Gehring WJ. 2000. Notch signaling and the determination of appendage identity. Proc Natl Acad Sci USA. 97: 2117-2122.

Liu X, Hawkes E, Ishimaru T, Tran T, Sretavan DW. 2006. EphB3: an endogenous mediator of adult axonal plasticity and regrowth after CNS injury. J Neurosci. 26: 3087-3101.

Schmidt, M, Van Ekeris L, Ache BW. 1992. Antennular projections to the midbrain of the spiny lobster. I. Sensory innervation of the lateral and medial antennular neuropils. J Comp Neurol 318:277-290.

Schmidt M, Ache BW. 1992. Antennular projections to the midbrain of the spiny lobster. II Sensory innervation of the olfactory lobe. J Comp Neurol 318:291-303.

Stepanyan R, Day K, Urban J, Hardin DL, Shetty RS, Derby CD, Ache BW, McClintock TS .2005. Gene expression and specificity in the mature zone of the lobster olfactory organ. Physiol Genomics 25: 224-233.

Zhou X, Suh J, Cerretti DP, Zhou R, DiCicco-Bloom E. 2001. Ephrins stimulate neurite outgrowth during early cortical neurogenesis. J Neurosci Res. 66:1054-1063.

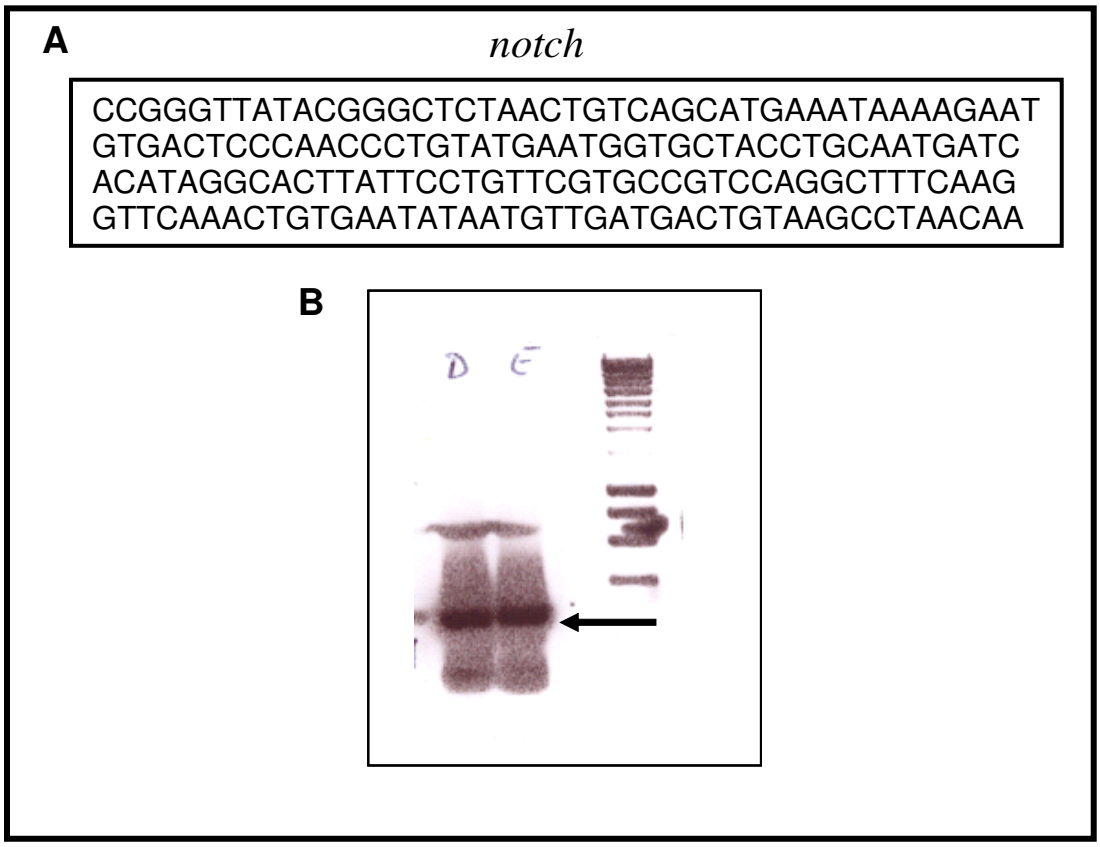

Figure B-1 Partial sequence of *notch* homolog cloned from the antennular LF of spiny lobster.

A *notch* gene sequence cloned from the LF (Accession # GQ252687.1). **B** Agarose gel showing the PCR product from which *notch* was cloned.

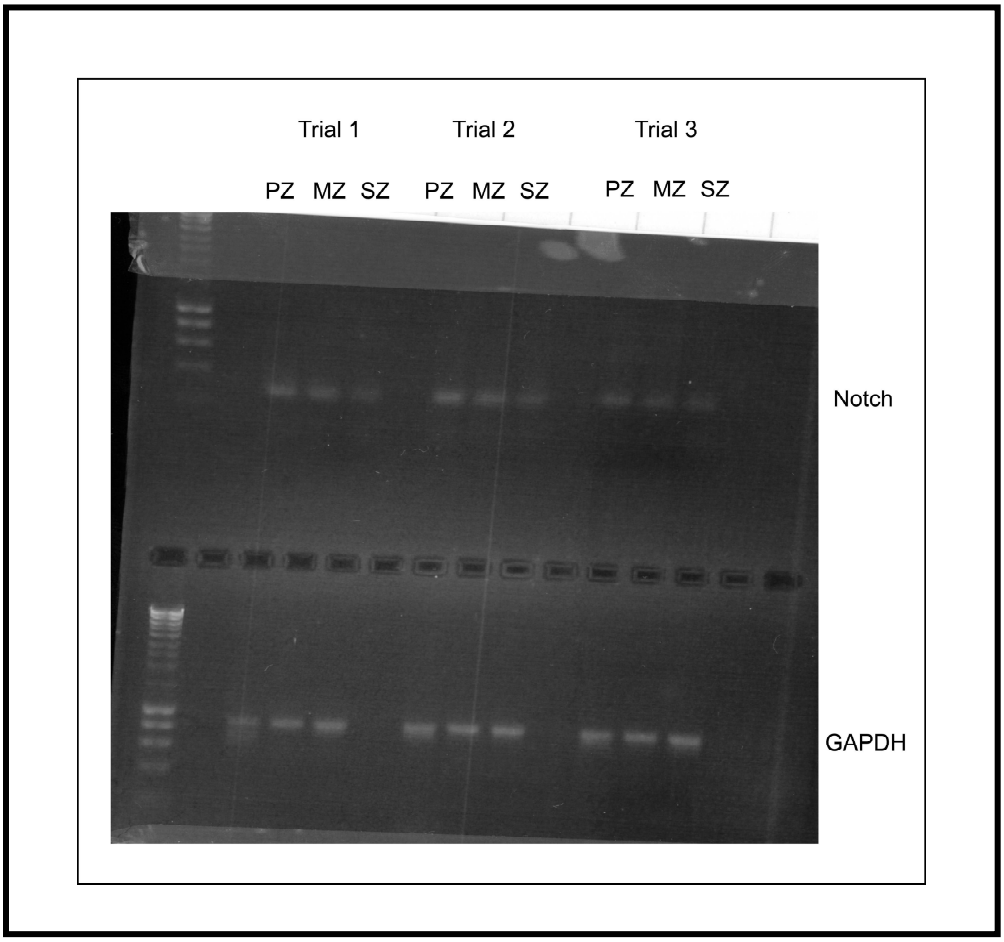

Figure B-2 Semi-quantitative PCR gel showing *notch* expression in intermolt LF.

An agarose gel showing PCR products run in triplicate for *notch* gene expression and *GAPDH* (control) in the proliferation, mature and senescence zones, PZ, MZ and SZ respectively, of intermolt LF.

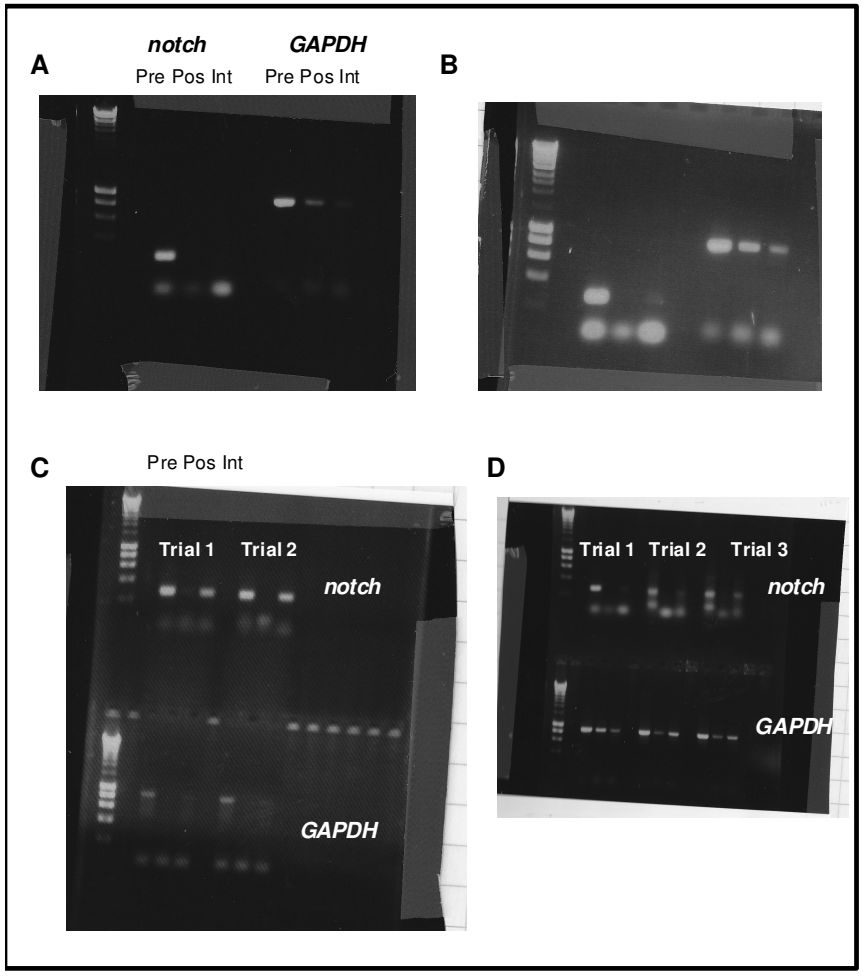

Figure B-3 Molt stage effect on *notch* expression using semi-quantitative PCR.

A *notch* expression is highest in premolt LF. **B** Increased exposure time in capturing image of gel in **A** shows intermolt also has a faint band but not postmolt. **C – D** Repeated experiments confirm the above results.

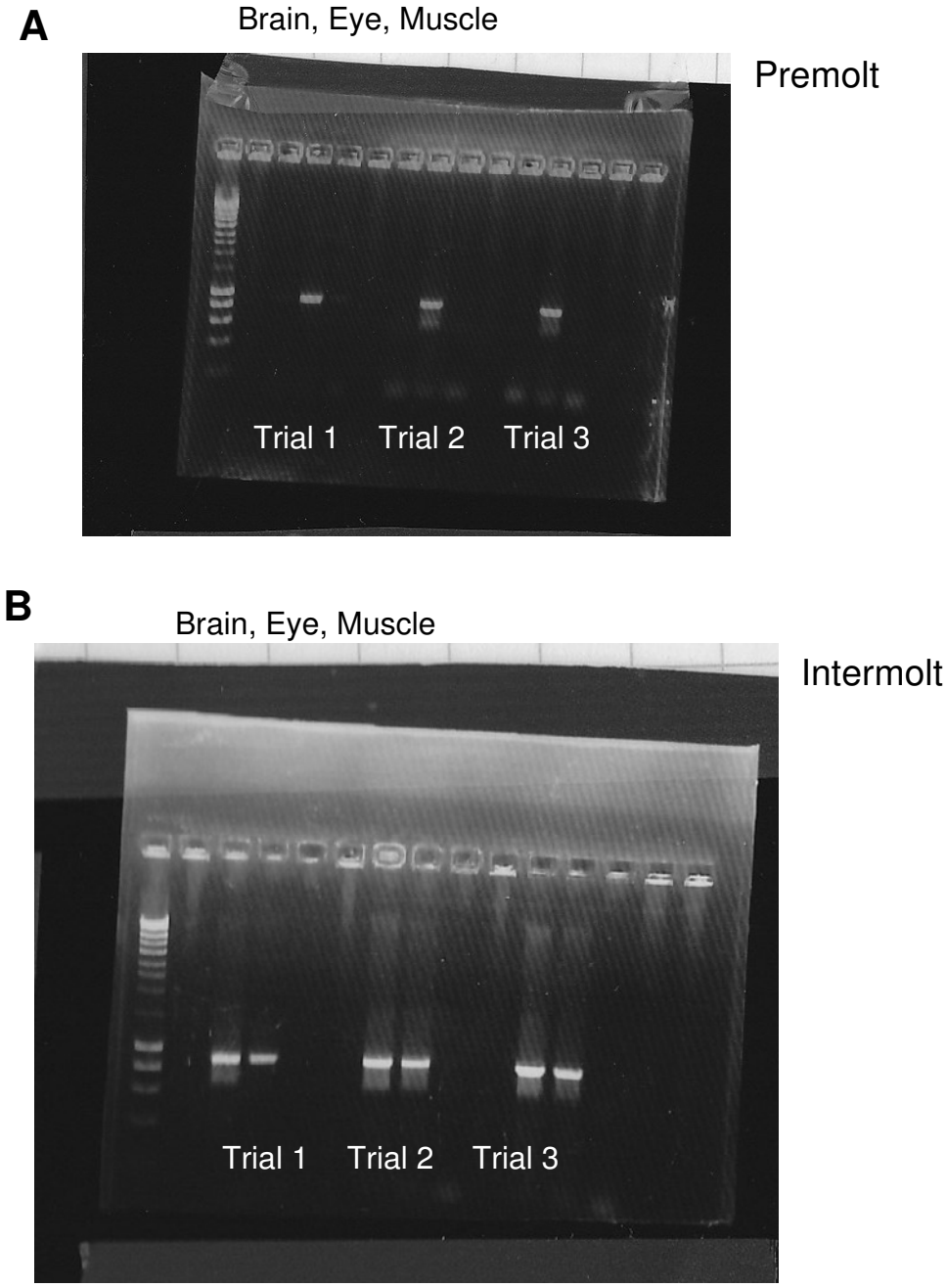

Figure B-4 *notch* expression in premolt and intermolt tissue.
A Semi-quantitative PCR shows *notch* is expressed in the eye in premolt lobsters but not in brain or muscle. **B** *notch* is expressed in brain and eye but not in muscle tissue in intermolt lobsters.

A

delta

CCGGGTTATACCGGTTCCAACTGCGAGGTCATCAACGACACTTGT
GCCACCACGCCGTGTCGTAATGGAGGCACTTGCCTCGATACCGG
GGATGACAACTTCGTGTGCCAGTGCCCCTCTGGCTACACCGGCC
AGTACTGTGAGATATCTGGCCAGTCATGCATCGACCGACCGTGTG
TGAACGGTGCCTCCTGTATTGACACTGCCACGGGCTATCGGTGCG
AGTGTCATGCGGGTTATGAGGGGACCAACTGTGAGCGGCCCGTG
AACGAATGCGAGTCCGACCCGTGTCTCAATGGCGGGTCGTGCGT
GGACGAACACGATGGGTTCCAGTGCGTGTGTCCCGTGGGCTACA
CTGGCCAACGCTGCGAAACCGATATCGACGACTGTGCGCATCGT
CCTTGTCTCAATGGAGGCACCTGCATCGACGGCGTCGACTCTTAC
AAGTGTCGCTGTGTGCCAGGCTTCTTGGGAAGCTTTGTCAGACGA
ACGTGGATGACTGTAGCACTCAACCCTGTGCCAACGGTGGGACTT
GCGTCGATTCCGTCAACGATTTTCGTTGTCAGTGCAAACCGGGTT
GGGGAGGCCGTCACTGTACCGATAAAGTGCCAGTTCCACCATCTC
CTTGTGCCTCTTCGCCCATGTCAAAACGGCGGCACCTG

B

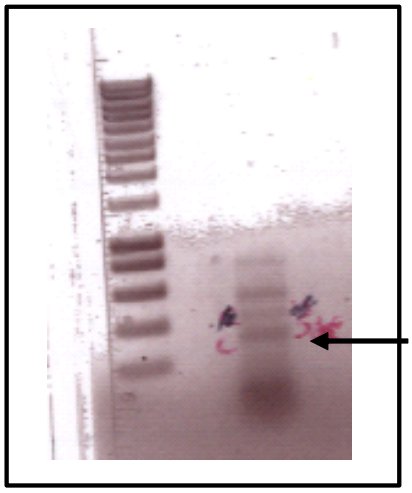

Figure B-5 Partial sequence of *delta* homolog cloned from the antennular LF of spiny lobster. **A** *delta* gene sequence cloned from the LF (Accession # GQ252686.1). **B** Agarose gel showing the PCR product from which *notch* was cloned.

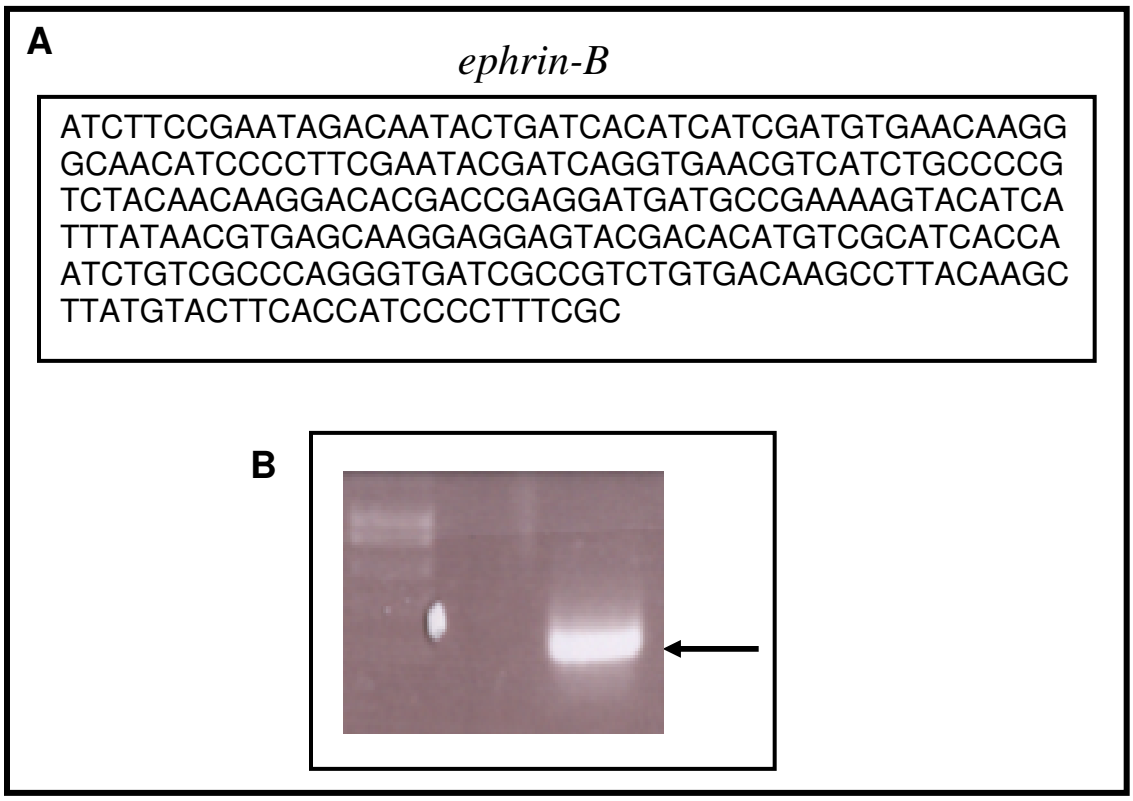

Figure B-6 Partial sequence of *ephrin-B* homolog cloned from the antennular LF of spiny lobster.

A *ephrin-B* gene sequence cloned from the LF (Accession # GQ252685.1). **B** Agarose gel showing the PCR product from which *ephrin-B* was cloned.

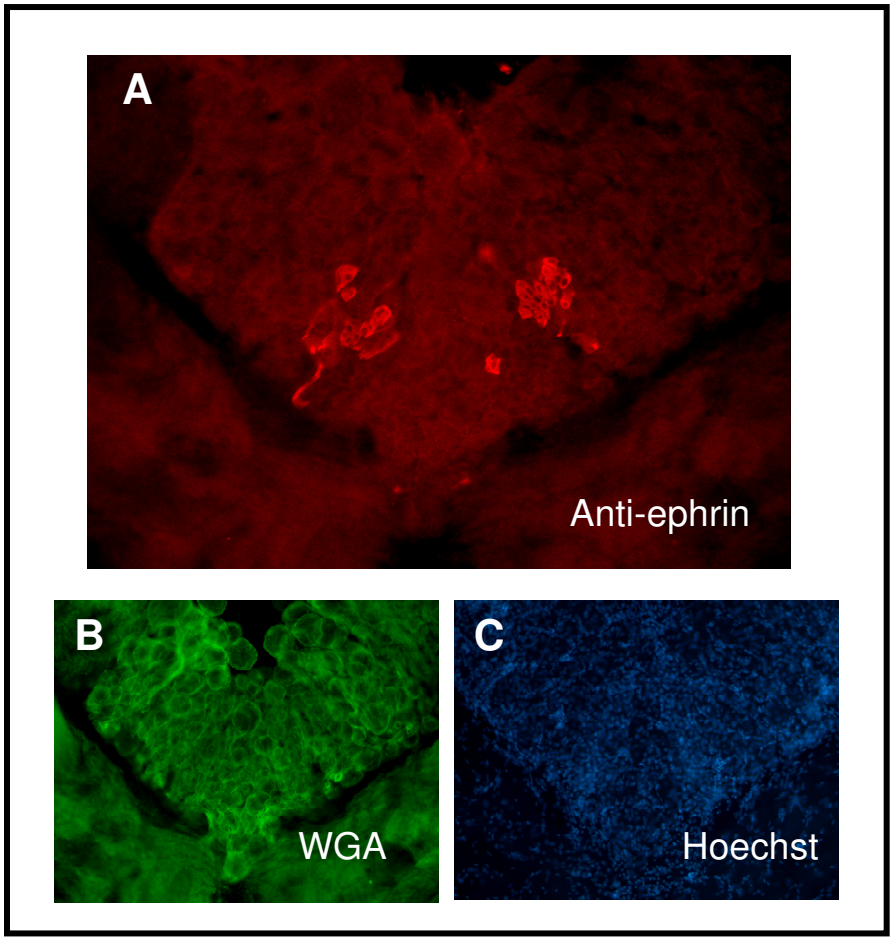

Figure B-7 Immunocytochemistry labeling with anti-ephrin in the brain of spiny lobster.

A Triple labeling with anti-ephrin, **B** Wheat Germ Agglutinin (WGA) and **C** Hoechst is shown. Unidentified cells are labeled with anti-ephrin.